

**Application of Remote Sensing and Geographic Information System
Techniques to Monitoring of Protected Mangrove Forest Change in
Sabah, Malaysia**

2016

NURUL AINI BINTI KAMARUDDIN

Acknowledgement

First and foremost, I would like to give my sincere thanks to my supervisor, Prof. Shigeo Fujii, who has accepted me as his Ph.D. student and offered me so much advice, patiently supervising me and always guiding me in the right direction. I have learned a lot from him. Without his help, I could not have finished my desertion successfully.

Special thanks also go to Assoc. Prof. Shuhei Tanaka. He is the one who offered me the opportunity to study at Kyoto University during his visiting research in Malaysia in 2008. I am thankful to Dr. Binaya Raj Shivakoti for his kindness and sharing his knowledge on remote sensing techniques. He is the one who helps me very much how to use the remote sensing software and analyzed the satellite data. Many thanks are also due Asst. Prof. Hidenori Harada for his advised and suggestions.

I would like to express my gratitude to Prof. Datin Sri Panglima Dr. Hajjah Ann Anton at University Malaysia Sabah (UMS), Malaysia for her valuable support and collaboration during the sampling in Sabah. Also, I would like to thank to all her staff at the Kota Kinabalu Wetlands Centre and UMS students for assisting and supporting me during my internship in Sabah.

I also would like to extend my gratitude to all fellow research colleagues at Prof. Fujii`s laboratory for their support. Also, I would like to give my appreciation to Fukunagasan, Shiozaki-san, and Yasuba-san for their kind supports for their guidance during my stay in Japan.

Last but not least, special appreciation to my parents and family members for their constant support and love that helps me through.

Abstract

Mangroves are vital components of coastal ecosystems worldwide, but they are under threat from expanding human settlement, an explosion of commercial aquaculture, the exploitation of wood fuel and the impact of climate change. Such threats led to increasing demand for detailed mangrove maps for the purpose of measuring the extent of deterioration of the mangrove ecosystem. However, it is difficult to produce a detailed mangrove map mainly because mangrove forest is very difficult to access. Thus, remote sensing technology provides a genuine alternative to the traditional field-based method of mangrove mapping and monitoring. Due to its many advantages, such as being cost-effective, time-saving, and providing access to long-term data, the application of remote sensing technology to mangrove studies is already well established. However, a number of advanced remote sensing applications with the capability of using low-cost satellite data remain unexplored for the purpose of mangrove mapping, change detection, and monitoring. Thus, this study aimed to develop a cost-effective protocol of remote sensing application using low-cost satellite data for mangrove forest monitoring.

Mangrove areas in Sabah, Malaysia, are declining at an alarming rate due to conversion to agricultural, shrimp-pond farming, and urban-development areas, as well as other types of deforestation, even though it has the largest mangrove forest distribution in Malaysia. The use of satellite technology for studying Sabah's mangrove regions remains poorly developed. Therefore, Sabah was selected as the study area for applying remote sensing technology for mapping, change detection, and monitoring of the mangrove forest. The mangrove forest at Mengkabong, located on the west coast of Sabah, was selected as the specific study area due to the problem of mangrove destruction that exists there. To promote cost-effective and long-term monitoring, low-cost satellite data of the Landsat series (TM, ETM+, and OLI_TIRS) were used in this study. Detailed protocols of satellite data acquisition and data processing were developed in this study. Studies have shown that the application of processed Landsat data series using developed protocols and processing procedures has potential for

classifying mangrove forest land cover in the Sabah area. The gap-filling processing used in this study produced good results in terms of the ETM+ SLC-off gap-filled data. The NDVI and maximum likelihood classification techniques that were applied to all processed Landsat data series showed good results of land cover classification. However, there remain several limitations and challenges in the interpretation of mangrove areas when using these conventional methods.

Therefore, due to the potential of recent advances of remote sensing techniques, a decision-tree learning method was determined and applied for classifying and detecting the rapid changes in the Mengkabong mangrove forest area. Multi-temporal Landsat series (TM, ETM+, and OLI_TIRS) data from the years 1990, 2000, 2005, 2010, and 2013 were used in this study. The result of this study showed that the use of the decision-tree learning method on a combined dataset containing multi-temporal Landsat series and GIS (digital elevation model and distance to coastline) data was effective at delineating spatial and temporal changes of the mangrove forest. Various integrated sources of remote sensing data such as greenness, vegetation moisture content, and reflectance band values improved the classification accuracy of mangrove due to the similarity of the spectra of forest and water–vegetation mixed pixels.

Aquaculture activities such as shrimp pond farming have been identified as a major factor of degradation of Mengkabong's mangrove area. Therefore, this study demonstrated the potential of MODIS time-series data for detecting the timing of conversion of mangrove areas to shrimp pond farming in Mengkabong. A simple and robust statistical method of change analysis was developed and applied to MODIS enhanced vegetation index (EVI) time-series data. The findings of this study confirmed that the technique could successfully determine the history of mangrove deforestation and aquaculture development in the Mengkabong area during a 14-year period (2000–2013). With the continuation of satellite data acquisition by the MODIS sensor, this method may also be useful for the monitoring and verification of changes of Sabah's mangroves in the future. Next, a simplified methodology of application of remotely sensed data for mangrove monitoring in Sabah was developed. To promote the advantages of using remote sensing technology, cost-effective and long-term multi-

temporal remotely sensed data, such as Landsat series and MODIS data, were suggested for the application. The schematic procedures began with the detection of nature change problems. Thus, five potential study sites were identified around Sabah. These study sites were facing mangrove destruction due to human activities such as aquaculture and urbanization. Then, standard protocols and processing procedures for the Landsat satellite and MODIS data that were applied in the previous study were proposed as methods. The methodology protocols included remotely sensed data preparation, pre-processing, classification analysis, selection of change detection algorithms, and evaluation of the change detection results. Subsequently, monitoring program procedures for a mangrove conservation management plan in Sabah were suggested.

The effectiveness of the developed protocols for mangrove monitoring in Sabah are evaluated in Chapter 7 of this work. The selection of the satellite data characteristics of Landsat and MODIS for mangrove study were evaluated by comparing with those of high-resolution data. The cost-effectiveness was evaluated by comparing the cost of the data used with the cost of high-resolution data. The price quotations of satellite data were obtained from the Remote Sensing Agency of Malaysia. The limitations of the developed protocols were evaluated, and they are discussed in this same chapter. The findings showed that the selection of Landsat and MODIS data and the cost-effectiveness of these data should promote the effective use of low-cost satellite data for mangrove monitoring and change detection in the Sabah area.

Thus, remote sensing technology offers considerable advantages in mangrove studies and has become a useful tool for monitoring change of the mangrove ecosystem in Sabah. In addition, the availability of schematic procedures for applying remotely sensed Landsat series and MODIS data for mangrove change detection will promote the potential for application of these data for mangrove monitoring in Sabah in the future.

Keywords

Mangrove, remote sensing (RS), geographic information system (GIS), change detection, monitoring, Sabah.

Table of Contents

Chapter	Title	Page
	Title Page	i
	Acknowledgement	ii
	Abstract	iii
	Table of Contents	vi
	List of Tables	xii
	List of Figures	xiv
	List of Abbreviations	xvii
1	Introduction	
	1.1 Research Background	1
	1.2 Significance of Study	3
	1.3 Research Objectives	4
	1.4 Research Outline	4
2	Literature Review	
	2.1 Global Mangrove Distribution	7
	2.2 Mangroves in Malaysia	8
	2.3 Mangroves in Sabah	10
	2.4 Importance of Mangrove Forest	13
	2.5 Threats to the Mangrove Forest	14
	2.5.1 Threats to Sabah Mangrove	17
	2.6 Application of Remote Sensing and Geographic Information System Technology to Mangrove Research	19
	2.6.1 Characteristics for Identifying Mangroves in Remotely Sensed Data	20
	2.6.2 Overview of Low-cost and High-cost Satellite Remote Sensing Data-Based on the Studies and Methods of the Mangrove Ecosystem (Application and Methods)	21

2.6.2.1	Application of Low-cost Satellite Data to Mangrove Study	21
(i)	Mangrove Studies Based on Aerial Photography	23
(ii)	Mangrove Studies Based on Landsat Series	24
(iii)	Mangrove Studies Based on MODIS	27
2.6.2.2	Application of Low-cost Satellite Data to Mangrove Study	29
(i)	Mangrove Studies Based on SPOT	29
(ii)	Mangrove Studies Based on Quickbird	31
(iii)	Mangrove Studies Based on IKONOS	31
2.7	Conventional and Advanced Remote Sensing Technique for Mangrove Land cover Mapping	32
2.7.1	Conventional Approaches of Remote Sensing Technique	32
(i)	Visual Interpretation	32
(ii)	Vegetation Index	33
(iii)	Pixel-based Classification	34
(iv)	Spectral Transformation Technique	35
2.7.2	Recent Advances Approaches of Remote Sensing Techniques	36
(i)	Object-based Image Analysis (OBIA) Classification	36
(ii)	Neural Network (NN) Classification	37
(iii)	Rule-based (Decision-Tree Learning) Classification	37
2.8	Benefits and Limitations of Low-cost and High-Cost Satellite Data in Mangrove Studies	39
3	Classification Protocol for Mangrove Forest Land Cover in Sabah using Landsat Data Series	43
3.1	Introduction	43
3.2	Objectives	45
3.3	Location of Study Area	46
3.4	Materials and Methods	47
3.4.1	Materials of Satellite Images and Reference Data	47

3.4.2 Methodology	49
3.4.2.1 Pre-processing Analysis	50
3.4.2.2 Statistical Analysis	60
3.4.2.3 Classification Analyses	60
(i) Unsupervised Classification	61
a) K-Means	61
(ii) Supervised Classification	61
a) Visual Interpretation and Features Extraction Technique	61
b) Spectral Profile	62
c) Normalize Difference Vegetation Index (NDVI)	63
d) Maximum Likelihood	65
3.4.2.4 Validations	65
3.4.2.5 Accuracy Assessment	69
3.5 Results and Discussion	70
3.5.1 Quality Assessment of Landsat Data Series (TM, ETM+ and OLI_TIRS)	70
3.5.2 Classification of Mengkabong Mangrove Forest Land Cover using Multi-temporal Landsat Data Series	73
(i) Visual Interpretation Classification	73
(ii) Spectral Profile Classification	74
(iii) Normalized Difference Vegetation Index (NDVI) Classification	77
(iv) Maximum Likelihood Classification	81
3.6 Summary	84
4 Machine Learning Approach in Mengkabong Mangrove Forest Land Cover Classification	86
4.1 Introduction	86
4.2 Objectives	88
4.3 Materials and Methods	88

4.3.1	Materials of Satellite Images and Reference Data	88
4.3.2	Methodology	90
4.3.2.1	Data Pre-processing	90
4.3.2.2	Applying the Decision-Tree Learning Method	91
	(i) Feature Extraction and Determining Attributes	92
	a) Tasseled Cap Transformation (TCT)	92
	b) Normalized Difference Vegetation Index	94
	c) Bands Ratio	96
	d) Band 4	97
	e) Bands 5 and 7	97
	(ii) Generating Decision-Tree Learning	97
4.3.2.3	<i>M</i> -statistic	100
4.3.2.4	Assessment of Classification	100
4.4	Results and Discussion	102
4.4.1	Decision-Tree Learning Classification of Mengkabong Mangrove Land Cover	102
4.4.2	Results of Change Detection	107
4.4.3	Assessment of Classification	110
4.5	Summary	110
5	Detection of Regional-scale Conversion of Sabah`s Mangrove to Aquaculture Using Change-point Analysis of MODIS Time-series Data	111
5.1	Introduction	111
5.2	Objectives	114
5.3	Materials and Methods	114
5.3.1	Study Area	114
5.3.2	Acquisition of Remote sensing Data	116
5.3.3	Data Pre-processing	118
5.3.4	Change-point Analysis	119
5.3.5	Validation	122
5.4	Results and Discussion	124

	5.4.1 Change Detection	124
	5.5 Summary	127
6	Satellite Monitoring Procedures for Mangrove Change Detection and Conservation Management Plan in Sabah	128
	6.1 Introduction	128
	6.2 Objectives	130
	6.3 Materials and Methods	130
	6.3.1 The Nature of Change Detection Problems	131
	6.3.2 Preparation and Selection of Remotely Sensed Data	133
	6.3.3 Remotely Sensed Data Processing (Pre-processing and Processing)	135
	6.3.4 Classification Analysis	136
	6.3.5 Classification Accuracy Assessment	136
	6.3.6 Selection of Change Detection Algorithm	137
	6.3.7 Evaluation of Change Detection Result	137
	6.3.8 Monitoring Program	139
	6.4 Results and Discussion	140
	6.4.1 The Nature of Change Detection Problem	140
	6.4.2 Selection of Remotely Sensed Data	141
	6.4.3 Remotely Sensed Data Processing (Pre-processing and Processing)	142
	6.4.4 Classification Analyses and Accuracy Assessment	143
	6.4.5 Selection of Change Detection Algorithm	143
	6.4.6 Evaluation of Change Detection Result	145
	6.4.7 Monitoring Program	145
	6.5 Summary	146
7	Evaluation of Developed Protocols for Monitoring Protected Mangrove Forest in Sabah	147
	7.1 Introduction	147
	7.2 Objectives	148

7.3	Materials and Methods	148
7.3.1	Evaluation of Satellite Data Characteristics	148
7.3.2	Cost Analysis of Low-cost Satellite Data	148
7.3.3	Time Requirement	149
7.3.4	Degree of Expertise	149
7.3.5	Accuracy of Method	149
7.4	Result and Conclusion	149
7.5	Summary	153
8	Conclusions and Recommendations	154
8.1	Conclusions	154
8.2	Recommendations	156
	References	158
	Appendices	177

List of Tables

Table	Title	Page
2.1	Area of mangrove forest in Malaysia during 2006–2010 (ha)	9
2.2	Percentage distribution of mangrove forest area in Peninsular Malaysia in 2010	9
2.3	Mangrove change by region (1980–2005)	15
2.4	Mangrove areas affected by human activities	16
2.5	Summary of selected mangroves studies during the past 20 years	22
2.6	Summary of the types of mangrove forest mapping by aerial-photographs	23
2.7	Summary of applications of low-cost and high-cost satellite data integrated with conventional and advanced methods	39
2.8	Benefits and limitations of low-cost and high-cost satellite data types in mangrove studies	40
2.9	Free-access websites providing Landsat series and MODIS data	41
3.1	Specifications of multi-temporal Landsat data series	49
3.2	Specifications of ETM+ SLC-off data for gap-filling analysis	55
3.3	Classes of NDVI lands cover	65
3.4	Min value of Landsat ETM+ SLC-off and ETM+ SLC-off gap-filled data	70
3.5	Min value of all Landsat data series (TM, ETM+, and OLI_TIRS)	73
3.6	Land cover classes by visual interpretation technique	74
3.7	NDVI classification of Landsat data series of Mengkabong mangrove forest	80
3.8	Error matrix of NDVI classification for 23 years of data	81
3.9	Total area of land cover classes by maximum likelihood classification	82
3.10	Error matrix of maximum likelihood classification for 23 years of data	84
4.1	Specifications of multi-temporal Landsat data series used in this study	89

4.2	Tasseled cap coefficient for Landsat TM and ETM+ at satellite reflectance	93
4.3	Tasseled cap coefficient for Landsat OLI_TIRS at satellite reflectance	93
4.4	Attributes used for the decision tree-learning method	98
4.5	<i>M</i> -statistics value between mangrove area and non-mangrove area	103
4.6	Changes in mangrove forest and other land cover types from 1990 to 2013	108
4.7	Error matrices of decision-tree learning classification for 1990, 1995, 2000, 2005, 2010, and 2013	110
5.1	MODIS data characteristics used in this study	118
6.1	Total Tuaran mangrove area from 1990–2013	145
7.1	Comparison of satellite characteristics between low-cost and high-cost satellite data	150
7.2	Cost comparison of low-cost and high-cost satellite data	151

List of Figures

Figure	Title	Page
1.1	Framework of the study	6
2.1	Mangrove forest distribution around the world	7
2.2	Percentage of world mangrove forest by country in 2005	8
2.3	Mangrove forest distribution in Malaysia	10
2.4	Mangrove zonation in Sabah	12
2.5	Mangrove distribution in Sabah	15
2.6	Mangrove changes in Asia due to human activities	17
2.7	Aquaculture production in Sabah	18
2.8	Population in Sabah	19
3.1	Map of study area	46
3.2	Access protocols of Landsat data series using the Earth Explorer USGS website	48
3.3	Multispectral data with true-color composite (combination of RGB bands)	51
3.4	Subsetting of multispectral data using map coordinates	52
3.5	True-colour composite (RGB) of multispectral subset data	53
3.6	Scan line errors (gaps) in multispectral ETM+ SLC-off data	54
3.7	Illustration of pixel value extraction of ETM+ SLC-off data in MS Excel	56
3.8	Histogram analyses of band 3 for the main and supplementary ETM+ SLC-off data	57
3.9	Workflow of gap-filling analysis of ETM+SLC-off data	58
3.10	Visual comparison between before and after the cloud-masking analysis of Landsat ETM+ SLC-off gap-filled data for 2010	59
3.11	Spectral profiles of vegetation, soil, and water	62
3.12	Ground-truth points and field photographs of selected points	67
3.13	Classification protocols of mangrove forest land cover in Sabah using Landsat data series	68

3.14	Comparison of quality color composite of ETM+ SLC-off data before and after the gap-filling process	72
3.15	Spectral profile of Mengkabong land cover classes	75
3.16	Spectral profile features of each class integrated with satellite data and field photographs with selected points of field survey	76
3.17	Mengkabong land cover classes for NDVI classification	77
3.18	NDVI land cover classes of ETM+ SLC-off and ETM+ SLC-off gap filled data	79
3.19	Land cover classifications in Mengkabong area from 1990–2013	83
4.1	Condition of mangrove and degradation activities in the Mengkabong area	87
4.2	True-color composite (RGB) of Landsat series images (TM, ETM+, and OLI_TIRS) of the study area	89
4.3	Sample of the decision-tree learning method	91
4.4	Tasseled cap transformation indices of brightness, greenness and moisture of the Landsat data	94
4.5	NDVI extracted using bands 3 and 4 of the Landsat data series	96
4.6	Decision-tree learning classification method	99
4.7	Decision-tree learning method classification protocols	101
4.8	Landsat images of 1990 and 2000 (bands 7, 4, and 2 as R, G, and B). (A) Mangrove forest area (mostly in green color). (B) Band ratio of mangrove forest area (dark tone). (C) Built-up area (light red color). (D) Band ratio of built-up area (light tone)	105
4.9	Spectral characteristics of mangrove and non-mangrove land cover types using Landsat data series (TM, ETM+, and OLI_TIRS)	105
4.10	Spectral characteristics of mangrove and non-mangrove land cover types using NDVI value	106
4.11	Changes in mangrove forest and other land cover types from 1990 to 2013	109
5.1	Location of study area. The red line shows the mangrove area and the yellow line shows the aquaculture area	115
5.2	Example of mangrove coverage and schematic sketch of an	116

	integrated shrimp–mangrove pond farming system in Mengkabong area (a) Dense and healthy mangrove species (<i>Rhizophora apiculata sp.</i>). (b) Degraded mangrove area. (c) Inactive shrimp pond with mangrove seedling of the replanting project. (d) Active shrimp pond in mangrove area	
5.3	Access protocols of MODIS data using the ORNL DACC website	117
5.4	Data preparation and pre-processing analysis of the MODIS data	119
5.5	Identification of temporal change in EVI temporal profile using change-point analysis. (a) Example of EVI time series for two scenarios: unchanged mangrove area (top) and unchanged shrimp pond area (bottom). (b) Conversion of mangrove area to shrimp pond area.	120
5.6	Flow diagram of the change-point analysis used in this study	123
5.7	Several significant changes of EVI value from a single MODIS pixel that was assigned as the actual change of mangrove area to shrimp pond area	124
5.8	Total area of shrimp pond in Mengkabong	125
5.9	Temporal distribution of Mengkabong mangrove area for each quarter of each year	126
6.1	Eight major steps of remote sensing-based land cover change detection and monitoring procedures for mangrove studies in Sabah	131
6.2	Current conditions of mangrove forest in Sabah	132
6.3(a)	Mangrove classification and change detection protocols for Landsat data series	138
6.3(b)	Mangrove change detection protocols for MODIS (VI) time series data	139
6.4	Location of study area	140
6.5	Shrimp pond in the Tuaran mangrove area	141
6.6	Landsat ETM+ SLC-off data before and after gap-filling analysis	142
6.7	Temporal distribution of Mengkabong mangrove area for each quarter of year	144
6.8	Mangroves in replanting areas	144

List of Abbreviations

B4	Band 4 (NIR Infrared band)
B5	Band 5 (Short wavelength infrared band)
CASI	Compact airborne spectrographic imager
DEM	Digital elevation model
DN	Digital number
ENVI	Environment for visualizing images
ETM+	Enhance thematic mapper plus
FAO	Food and agriculture organization
GIS	Geographic information system
LAI	Leaf area index
LPDAAC	Land processes distributed active archive centre
MLC	Maximum likelihood classifier
MODIS	Moderate resolution imaging Spectroradiometer
MSS	Multispectral scanner
NASA	National aeronautics and space administration
NDVI	Normalize difference vegetation index
NIR	Near infra-red
NN	Neural network
OBIA	Object based image analysis
OLI_TIRS	Operational land imager thermal infrared sensor
RGB	Red, green, blue
SAR	Synthetic aperture radar
SLC	Scan line corrector
SPOT	Satellite pour observation de la terre
TCT	Tasseled cap transformation
TM	Thematic mapper
Sp.	Species
USGS	United States geological survey
WRS	World Reference System

Chapter 1

Introduction

1.1 Research Background

Mangrove ecosystems dominate the coastal wetlands of tropical and subtropical regions throughout the world. They provide various ecological and economic ecosystem benefits such as coastal erosion protection, water filtration, habitat for marine organisms, sources of building materials, medicinal ingredients, and attraction for tourists (Giri *et al.*, 2008; Zhang *et al.*, 2003). However, mangroves are also facing threats. Currently a vulnerable ecosystem worldwide, they have experienced a dramatic decline during the last half century.

Uncontrolled exploitation of mangrove forest areas has led to degradation of coastal environments. Problems include coastal erosion, loss of wildlife habitat, and climate change (Barua *et al.*, 2010; Giri *et al.*, 2011). The mangroves of Sabah, Malaysia, also have declined at an alarming rate due to deforestation activities. This problem has affected the coastal erosion along Sabah's coastline and has led to the loss of habitat for migratory birds (Sabah Forestry Department, 2010). To overcome these problems, further extensive monitoring should be conducted continuously.

In the last two decades, remote sensing and geographic information system (GIS) technology has demonstrated high potential in mangrove studies, such as for mapping, identification, monitoring, and detecting changes. The applications of this technology are reflected by the large number of scientific papers that have been published. There are many advantages to using remote sensing and GIS technology in mangrove studies, such as the cost-effectiveness of the technique, its ability to provide large-scale monitoring, time savings, and access to long-term data (Aschbacher *et al.*, 1995; Blasco *et al.*, 1998; Green *et al.*, 1998; Hernanderz *et al.*, 2005; Manson *et al.*, 2003; Mironga,

2004; Mumby *et al.*, 1999; Lee & Yeah, 2009; Wang *et al.*, 2003). Such remotely sensed data can be obtained at different spatial resolutions, such as medium-resolution images (e.g., Landsat series, MODIS, SPOT), high-resolution images (e.g., Quickbird, IKONOS), hyperspectral images (e.g., compact airborne spectrographic imager [CASI]), and radar (e.g., synthetic aperture radar [SAR]).

The Landsat data series, including multispectral scanner (MSS), thematic mapper (TM), enhanced thematic mapper plus (ETM+), MODIS, and SPOT data, has been demonstrated to be extremely useful for providing information on various components of the coastal environment. In addition, the available MODIS Aqua satellite data have been established as being useful in environmental monitoring and natural resource management on a wide scale. MODIS Aqua remotely sensed data have been used widely in mangrove studies compared to other satellite data because of their advantages, which include free access, the availability of multi-date data, large-scale coverage, and the availability of low- to medium-resolution datasets (Green *et al.*, 1998; Chander *et al.*, 2011).

Many remote sensing techniques such as visual interpretation, vegetation index, pixel-based classification (supervised and unsupervised), and spectral transformation have been used to detect and delineate mangrove and non-mangrove areas by using different spatial resolutions (low, medium, and high) of remotely sensed data (Kuenzer *et al.*, 2011). All such approaches can provide important information for monitoring the real extent and changes of mangrove areas. However, in the context of mangrove studies, applications of these techniques still face several limitations and challenges, such as limitations on species-level mangrove interpretation and confusion between mangroves and other types of vegetation (Al Habshi *et al.*, 2007; Benfield *et al.*, 2005; Gao *et al.*, 1999).

Recently, there has been rapid development in remote sensing techniques and satellite data that has aided the interpretation of data and the extraction of information from the data (Gillespie *et al.*, 2008; Wooster, 2007), and several new analysis techniques, such as object-based image analysis (OBIA), rule-based (decision-tree

learning) classification, and neural networks, have been employed to classify remotely sensed data about mangroves (Kuenzer *et al.*, 2011). However, few studies have used these techniques in the context of mangrove studies, especially with low-cost remotely sensed data.

To determine the potential of low-cost remotely sensed data in combination with new analysis techniques for mangrove studies, it is important to explore applications of Landsat and MODIS data. Thus, in the first phase of this research, protocols for using Landsat data for mangrove classification in Sabah are developed. Then, in the second phase, new remote sensing techniques are used with Landsat data for mangrove classification and change detection. In the third phase of this research, the major factors that affect mangrove deforestation and determine the history of mangrove deforestation are identified using MODIS data. In the fourth phase, the protocols and methods of using low-cost remotely sensed data for mangrove studies are simplified. Finally, in the last phase of this research, the developed protocols for mangrove forest monitoring in Sabah are evaluated. The major emphasis of this study is to understand the potential of low-cost remotely sensed data in mangrove studies in the Sabah area.

1.2 Significance of Study

An awareness of the importance of the mangrove ecosystem and the effects of its decline on the global ecosystem forms the basis of this study to promote the use of remote sensing and GIS technology with cost-effective methods for mangrove research. The use of remote sensing technology in the study of mangroves will provide a spatiotemporal framework for the current and the past status of mangrove areas. The output of this study will be a baseline for remote sensing studies of Sabah's mangroves. Thus, Sabah's mangroves will be managed extensively using this technology. In addition, it will increase public awareness, especially among local people, of the importance of the mangrove ecosystem.

1.3 Research Objectives

The main objective of this study is the development and application of new remote sensing techniques with low-cost satellite data for monitoring changes of the mangrove areas of Sabah. Several specific objectives of this study, required to achieve the main objective, are listed below:

1. To develop a protocol of low-cost remotely sensed data for classifying and mapping the mangrove forest.
2. To apply and compare the effectiveness of new remote sensing techniques for classifying the mangrove forest.
3. To determine the potential of low-cost satellite data for detecting and monitoring the deforestation of mangrove areas.
4. To propose an effective method of remote sensing technology application for mangrove monitoring in Sabah.
5. To evaluate the effectiveness of the developed protocol for monitoring mangrove forest in Sabah.

1.4 Research Outline

This dissertation consists of eight chapters (**Figure 1.1**). The main contents of this thesis are presented in chapters 3 to 7. These five chapters are the core of the thesis and are accompanied by an introduction (Chapter 1), literature review (Chapter 2), and conclusion (Chapter 8). In Chapter 3, the study demonstrates the classification protocols on the mangrove forest land cover in Sabah using Landsat data series. The details of the protocols include satellite data acquisition, data processing, and mangrove land cover classification. Then, in Chapter 4, the study determines the effectiveness of the new remote sensing technique, decision-tree learning, integrated with low-cost satellite data, on classifying the mangrove land cover in Mengkabong. Chapter 5 demonstrates the potential of satellite MODIS data for detecting and monitoring the deforestation of a specified mangrove area over 10 years. In this study, change-point analysis is used to detect the regional-scale conversion of Mengkabong mangrove area to aquaculture. In

Chapter 6, the study develops a simplified schematic satellite monitoring procedures for the mangrove conservation management plan in Sabah. Chapter 7 evaluates the developed protocols in terms of satellite data characteristics and cost-effectiveness for mangrove forest monitoring in Sabah.

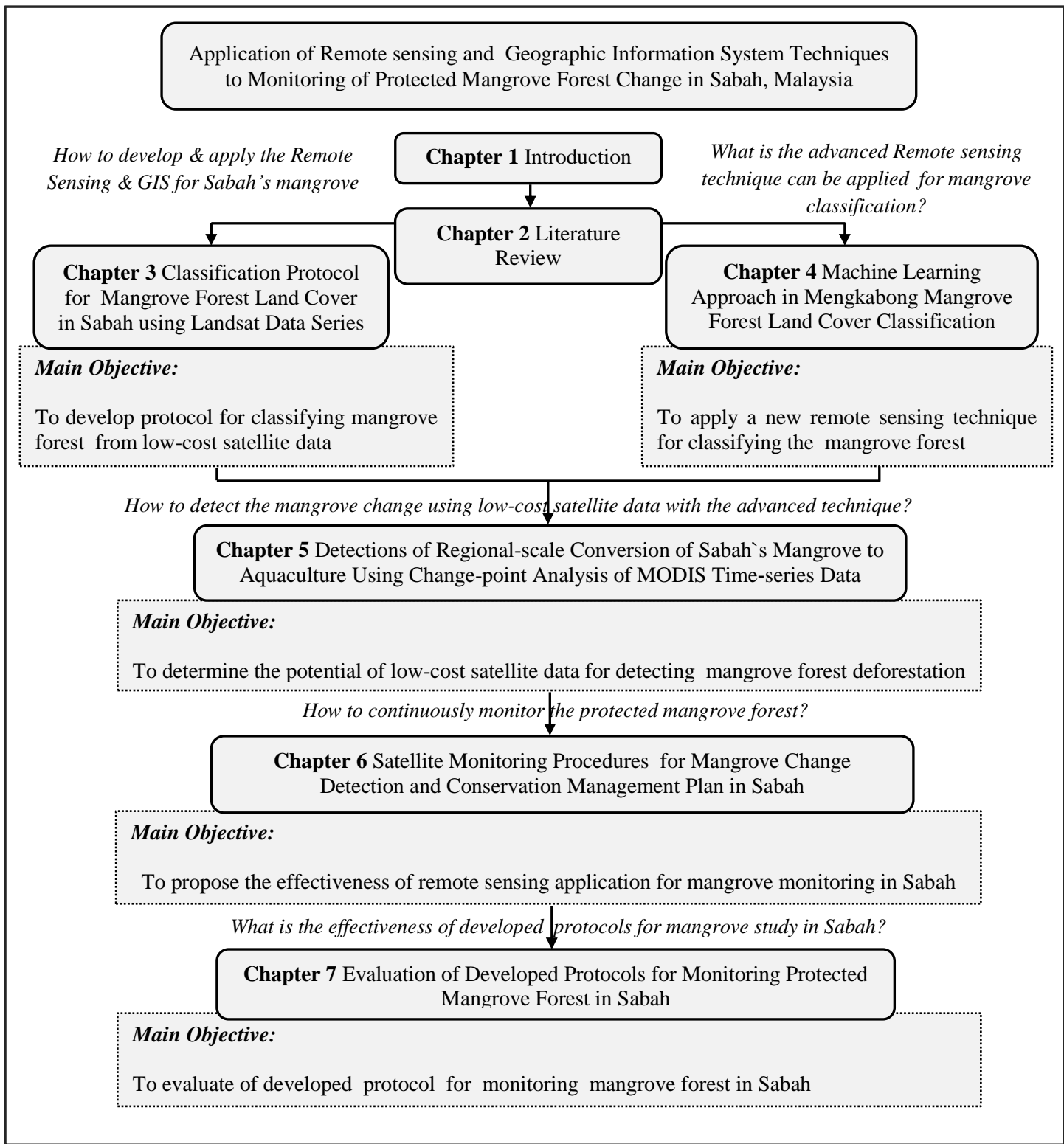


Figure 1.1 Framework of the study

Chapter 2

Literature Review

2.1 Global Mangrove Distribution

Currently, mangrove forest covers an area of about 15 million hectares worldwide and exists in 118 countries (FAO, 2007; Giri *et al.*, 2010; Zhang *et al.*, 2003). Mangrove forest is distributed extensively in the Indo-Pacific region (6.9 million ha), followed by Americas and Caribbean region (4.1 million ha), and Africa (3.5 million ha) (FAO, 2007; Zhang, 2004). **Figure 2.1** shows the distribution of mangrove forest around the world.

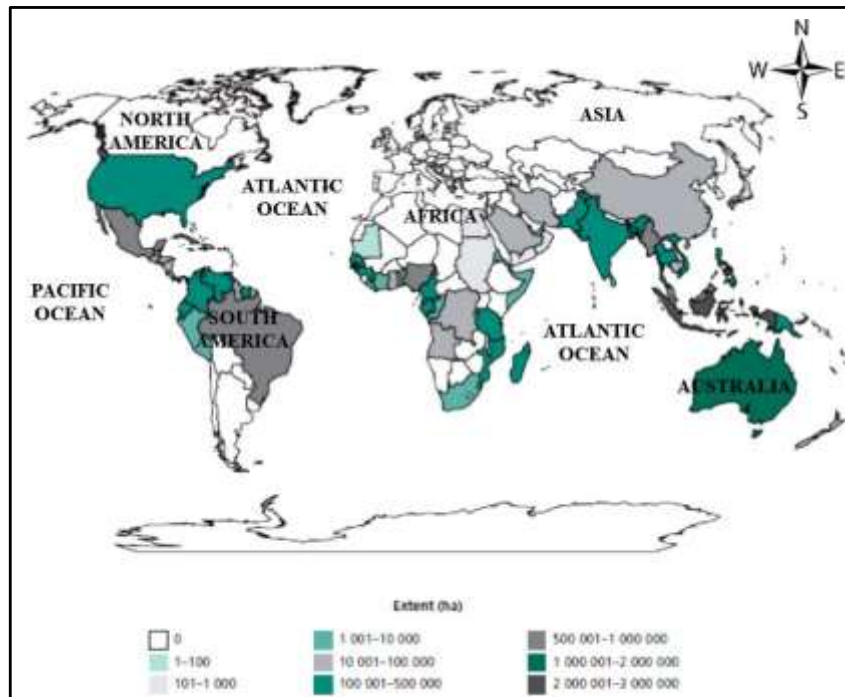


Figure 2.1 Mangrove forest distribution around the world

Source: FAO (2007)

According to FAO (2007), 10 countries have been identified for their extensive mangrove forest distribution (**Figure 2.2**). Among these countries, Indonesia has the most extensive mangrove forest distribution (19%), followed by Australia (10%), Brazil and Nigeria (7%), Mexico (5%), Malaysia and Cuba (4%), and Myanmar, Bangladesh, and India (3%). The total mangrove distribution in these 10 countries represents 65% of the global mangrove area. The remaining 35% is spread among 108 other countries.

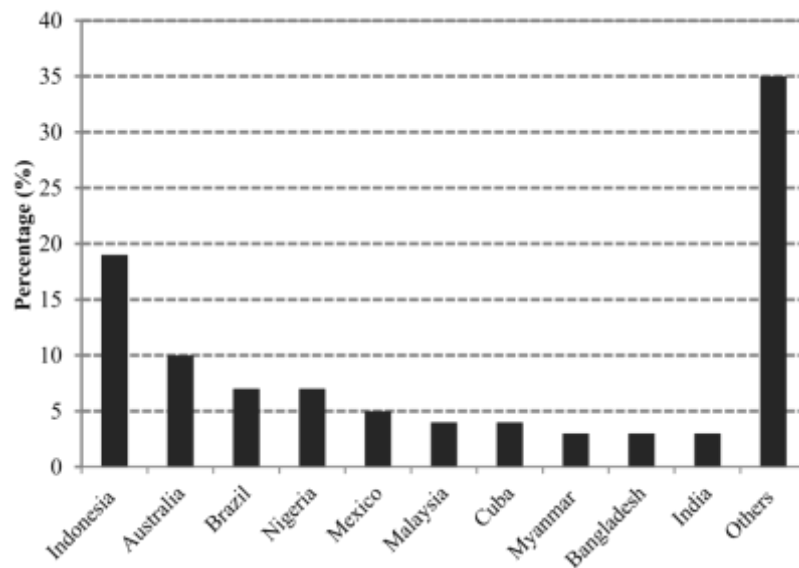


Figure 2.2 Percentage of world mangrove forest by country in 2005

Source: FAO (2007)

2.2 Mangroves in Malaysia

Malaysia has approximately 556,181 ha of mangrove forest, which is the second largest amount, after Indonesia, among Asian countries (Malaysia Department Statistics, 2013). Out of the total mangrove areas in Malaysia, Sabah has the largest mangrove area, 320,000 ha (58%), followed by Sarawak, 132,000 ha (24%), and Peninsular Malaysia, 104,181 ha (18%). **Table 2.1** lists statistics of the total area of mangrove forests in Malaysia from the year 2006–2010 (Malaysia Department Statistics, 2013). In Peninsular Malaysia, Perak has the largest mangrove area, 41,617 ha (42.8%), followed

by Johor, 27,342 ha (20.6%), and Selangor, 18,794 ha (19.1%) (**Table 2.2**) (Malaysia Department Statistics, 2013).

Table 2.1 Area of mangrove forest in Malaysia during 2006–2010 (ha)

Region	Years (ha)				
	2006	2007	2008	2009	2010
Sabah	340,889	340,689	340,448	340,488	320,000
Sarawak	117,000	117,000	117,000	112,570	132,000
Peninsular	100,042	102,334	101,824	101,800	104,181

Source : Malaysia Department Statistics (2013)

Table 2.2 Percentage distribution of mangrove forest area in Peninsular Malaysia in 2010

States	Percentage (%)
Perak	42.4
Johor	27.8
Selangor	19.1
Kedah	6.3
Pahang	2.5
Terengganu	1.3
Penang	0.3
Negeri Sembilan	0.2
Melaka	0.1

Source : Malaysia Department Statistics (2013)

The mangroves in Peninsular Malaysia occur along most of the west coast. The sheltering effect by the island of Sumatra provides a relatively calm sea in the Straits of Malacca compared to the South China Sea, which abuts the east coast of Peninsular

Malaysia. Along the east coast, which faces the South China Sea, mangrove formation is generally small and restricted to river mouths, where it usually extends 0.5–1 km inland (Ibrahim *et al.*, 2000).

In Sabah, mangroves occur largely on the east coast, facing the Sulu and Sulawesi seas, whereas in Sarawak, they occur largely at the mouths of the Sarawak and Rajang rivers. **Figure 2.7** shows the estimated geographic distribution of mangrove forests in Malaysia. The details of Sabah's mangroves are presented in **Section 2.3**.

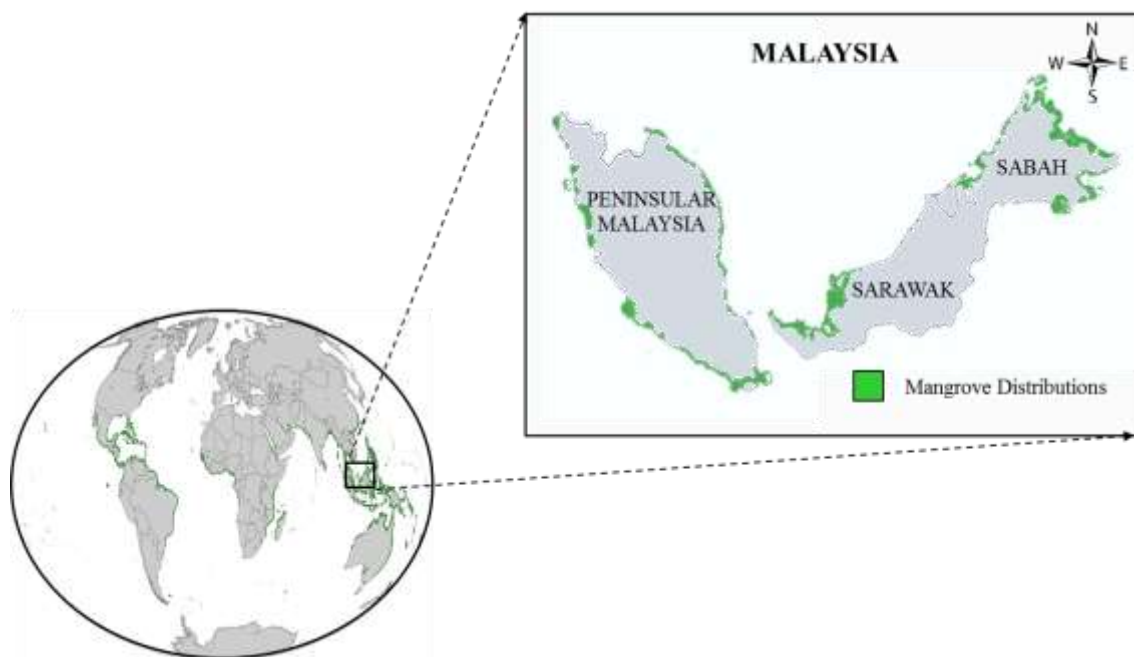


Figure 2.3 Mangrove forest distribution in Malaysia

Source: Malaysia Department Statistics (2013)

2.3 Mangroves in Sabah

Sabah, which is located in the northern part of Borneo at 4°20'–7°20' N latitude and 115°15'–119°15' E longitude, has a landmass of 7.37 million ha. It has an equatorial climate with an annual temperature range of 26–32°C, relative humidity range of 85 to 95%, and total rainfall range of 1500 to 4500 mm. Various types of forest, varying from mangroves at sea level up to sub-alpine vegetation on Mt. Kinabalu (4097 m above sea

level), occur in Sabah. The high heterogeneity of forest types is due to the occurrence of several different soils and latitudinal zones (Sabah Forestry Department, 2012). There are three broad mangrove zones in Sabah (Sabah Forestry Department, 2012), as described below.

(i) Seaward/Front Mangrove Zone

This zone occurs at the forefront of the mangrove zonation and is usually exposed to harsher physical conditions, mainly tidal current and wind. The forest usually has low structure (<10 m tall and small trunk diameter). Mangrove species such as *Avicennia alba* and *Sonneratia alba* commonly grow in this seaward mangrove zone.

(ii) Main Mangrove Zone

This zone is usually in the central parts of the mangrove zonation and is less affected by tidal current and wind. It has higher structure (up to 15 m tall with various medium-sized trunk diameters) and a diversity of mangrove communities and associates. *Rhizophora apiculata* and *Rhizophora mucronata* are the major mangrove species in this zone. Other mangrove species that are commonly distributed randomly in this zone are *Ceriops tagal* and *Bruguiera parviflora*.

(iii) Back Mangrove Zone

The back mangrove zone is often located behind the main mangrove zone, where the duration of tidal influence is short. Three major mangrove associates (Nipah swamp, Nibung stand, and *Bruguiera* stand) have been colonizing and dominating this zone. **Figure 2.4** shows the mangrove zonation in the Sabah.

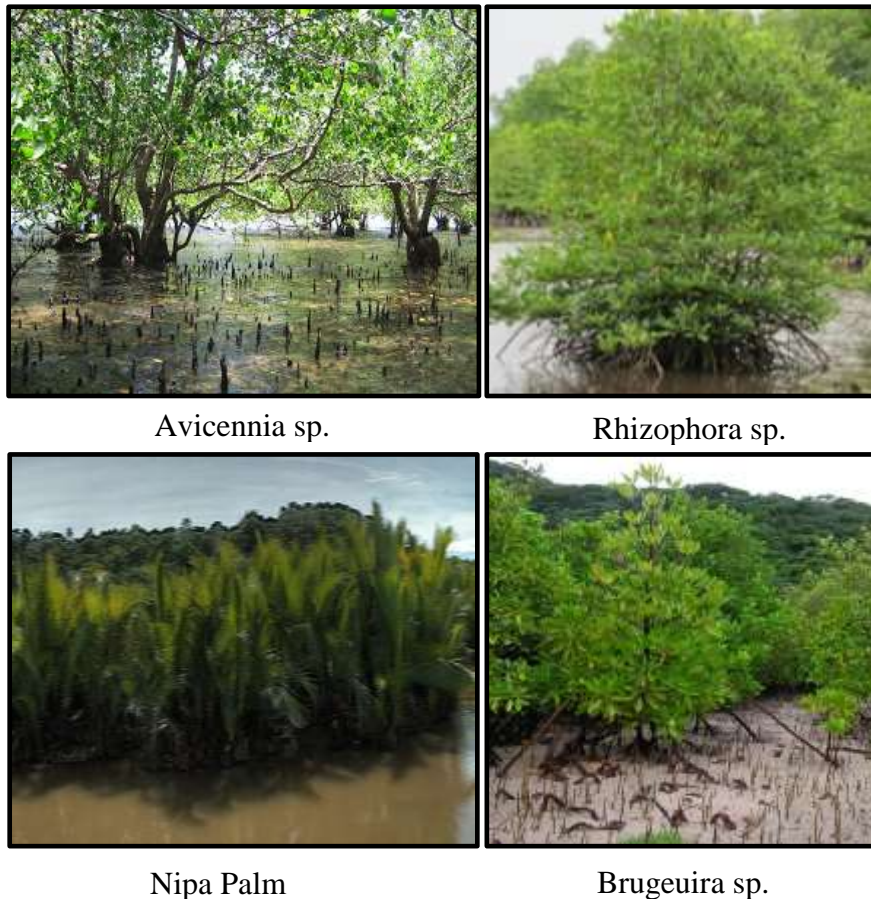


Figure 2.4 Mangrove zonation in Sabah
 Source : Sabah Forestry Department (2010)

Presently, the total mangrove area in Sabah is 320,000 ha (Sabah Forestry Department, 2010) (**Figure 2.5**). From the total, 95.7% (304,000 ha) has been reserved as permanent forest, but the remaining amount is allocated to supply timber and other products (Sabah Forestry Department, 2010). The reservation was conducted under the Forest Enactment, which is administered by the Sabah Forestry Department. The important uses of mangrove resources in Sabah are forestry (timber and charcoal), fishery (prawn, molluscs, crab, and fish), and ecotourism (Sabah Forestry Department, 2012).

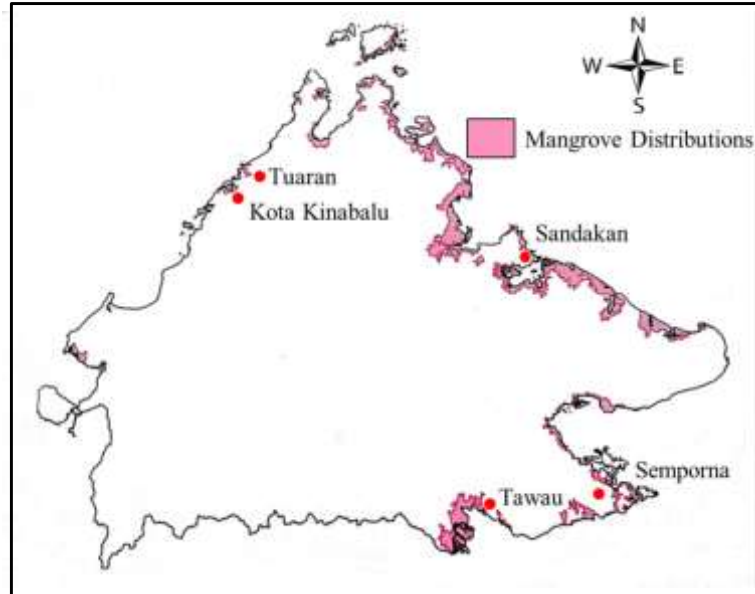


Figure 2.5 Mangrove distribution in Sabah
 Source : Sabah Forestry Department (2010)

2.4 Importance of Mangrove Forest

Mangrove forest has a variety of importances to ecosystem goods and services. Examples of ecosystem goods and services include timber and fuel (Walters *et al.*, 2008), carbon sequestration (Komiyama *et al.*, 2008), nutrient cycling to the marine system (Carlos & Cebrih, 1996), habitat for rare terrestrial fauna (Dvorak *et al.*, 2004), economically important fisheries (Laegdsgaard *et al.*, 2001; Mumby *et al.*, 1999), filtration of pollution (Harbison, 1986), and potential reduction of the impacts of tsunami and storm surge (Giri *et al.*, 2010).

The importance of the mangrove ecosystem in providing ecosystem goods and services is well established (Zhang *et al.*, 2003). Mangrove ecosystems provide important goods and services that can be divided broadly into four categories: supporting, regulating, provisional, and cultural (Corvalan, 2005; Giri *et al.*, 2011; Kathiresan & Bingham, 2001; Manson *et al.*, 2001; Spalding, 1997; Walters, 2008). The ecosystem provides valuable goods and services that support and regulate the climate, biodiversity, and human well-being (Corvalan, 2005). For example, 45 species of

mammals, 45 species of reptiles, 315 species of migratory birds, 177 species of fish, and 31 species of shrimp were found in the mangrove ecosystems of Bangladesh and India (Rashid *et al.*, 1994). The mangrove forests here are the world's largest and contain a diversity of mangrove fauna.

In many countries such as Malaysia, Myanmar, India, and Sri Lanka, mangrove forest is a major source valuable timber and wood fuel (FAO, 2007; Zhang *et al.*, 2003). The timber industry in the Matang mangrove forest, which is located on the west coast of Peninsular Malaysia, employs 2,400 people and generates a revenue of US \$6 million per year, and the associated fishing industry in the area employs about 10,000 people and has an annual revenue of US \$12–30 million (FAO, 2007).

A study by Robertson and Duke (1987) found that mangrove forests dominated by *Rhizophora sp.* can assimilate approximately 219 kg of nitrogen and 20 kg of phosphorus per hectare per year. This benefit may reduce the incidence of eutrophication and possibly red tides. Recent reviews by Costanza *et al.* (1997) and FAO (2007) suggested that the overall average value (based on the value of the US economy) of the physical and ecological services provided by the mangrove ecosystem is around USD 1000/ha.

2.5 Threats to the Mangrove Forest

Mangroves are sensitive to changes of habitat condition, so the forests are vulnerable to destruction. Changes to mangrove habitat may occur due to natural factors or human activities (Giri *et al.*, 2010; Kuenzer *et al.*, 2011; Zhang *et al.*, 2003). Recently, more than 50% of the world's total mangrove forests have been reduced due to both factors (Alongi *et al.*, 2009; Giri *et al.*, 2010). **Table 2.3** shows the changes of mangrove forest according the regions that include the total world's mangrove forests (FAO, 2007).

Table 2.3 Mangrove change by region (1980–2005)

Region	Year/1000ha			
	1980	1990	2000	2005
Asia	7,769	6,741	6,163	5,858
Africa	3,670	3,428	3,218	3,160
North & Central America	2,951	2,592	2,352	2,263
Ocenia	2,181	2,090	2,012	1,972
South America	2,222	2,073	1,996	1,978
World Total	18,793	16,924	15,741	15,231

Source: FAO (2007)

A study by Giri *et al.* (2008) found that some mangrove areas in India and Sri Lanka that were affected by the Indian Ocean tsunami in 2004 suffered severe damage from breaking and uprooting. Another case study by Hussain and Archa (1994) found that 45 million hectares of mangroves areas in Bangladesh had been damaged due to the shortage of freshwater flows. The freshwater shortage may have been caused by the construction of dams and the diversion of water for irrigation.

However, more than 50% of global mangroves have been destroyed by human activities, such as land reclamation, conversion of mangrove forest into areas of aquaculture, agriculture, urban development, and residential settlement (Giri *et al.*, 2008; Kathiresan & Bingham, 2001; Kuenzer *et al.*, 2011; Primavera, 1997), overexploitation of mangrove forest goods such as timber and wood fuel (Giri *et al.*, 2010), domestic and industrial pollution, and waste disposal (Wasserman *et al.*, 2000). **Table 2.4** summarizes mangrove areas affected by human activities.

Table 2.4 Mangrove areas affected by human activities

Activity	Area affected by each activities (10 ³ km ²)					Percentage of World (%)
	Asia	America	Africa	Australia	Word Total	
Shrimp culture	12.00	2.30	None	0.01	14.00	38.0
Forest use	4.60	4.90	None	None	9.50	27.0
Fish culture	4.90	None	None	None	4.90	13.0
Diversion of freshwater	4.00	None	0.09	None	4.10	11.0
Land reclamation	1.90	None	None	None	1.90	5.0
Herbicides	1.00	None	None	None	1.00	3.0
Agriculture	0.8	None	None	None	0.80	3.0
Salt ponds	0.02	None	0.03	None	0.05	None
Coastal development	0.05	None	None	None	0.05	None
Total Area	29.77	7.2	0.12	0.01	36.3	100.0

Note: None represents unavailable data

Source: Ivan *et al.* (2001)

According to Giri *et al.* (2008), the conversion of mangrove areas to areas of aquaculture, especially shrimp farming, has been spreading quickly, especially in Asian countries. A survey by FAO (2007) found that the high economic return of shrimp farming has been promoted to increase its national economic potential as a source of income for local communities, especially in developing countries. This activity has caused a major loss of mangrove forests in parts of Asia, such as in Indonesia, Malaysia, and Myanmar (Giri *et al.*, 2008) (**Figure 2.6**).

A report by FAO (2007) stated that Malaysia lost about 110,000 ha of mangroves between 1980 and 2005. During the first decade (1980–1990) of this time period, mangrove loss was due primarily to the conversion of land to agriculture, shrimp farming, or urban development. However, shrimp farming was spreading quickly in the country, especially in Peninsular Malaysia, and this led to reclamation and conversion

of large areas of mangroves to ponds. The National Mangrove Committee of Malaysia has strongly recommended that strict guidelines be implemented for development of this industry in the future.

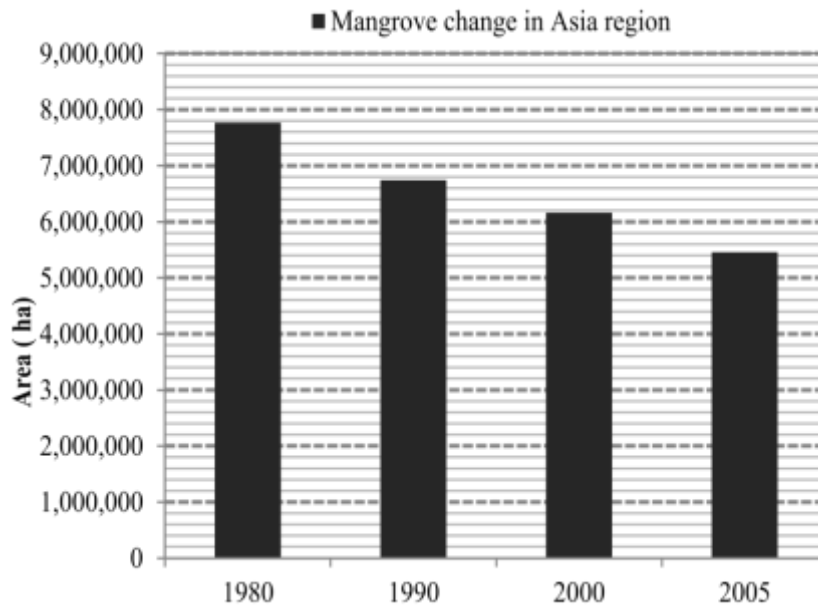


Figure 2.6 Mangrove changes in Asia due to human activities

Source: Giri *et al.* (2008)

2.5.1 Threats to Sabah Mangrove

The pressures of increasing population occurring simultaneously with the expansion of agriculture, aquaculture, and urban development have resulted in the destruction of a significant proportion (6.2% or 21,142 ha) of Sabah’s mangrove forest reserve since the 1990’s (Jakobsen *et al.*, 2007; Sabah Forestry Department, 2011). Aquaculture activities have been conducted on a large scale in the mangrove areas in Sabah (Jakobsen *et al.*, 2007). As a result, production from aquaculture increased rapidly (Sabah Fisheries Department, 2010). **Figure 2.7** shows statistics of aquaculture production in Sabah.

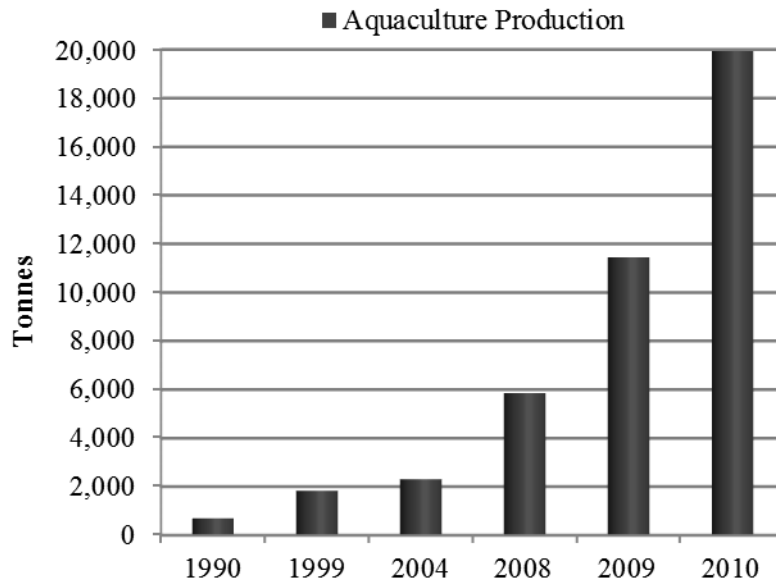


Figure 2.7 Aquaculture production in Sabah
 Source: Sabah Fisheries Department (2010)

Shrimp farming has been considered a major contributor to the aquaculture production, and it plays an important role in meeting the demand for fresh shrimp by the local seafood industry in Sabah (Sabah Fisheries Department, 2012). It also creates economic opportunities for other related supportive activities, such as hatcheries, feed producers, packaging, processing, retailers, exporters, and aquaculture consultants (Norasma, 2007).

Urban development for housing, industry, and tourism has been considered as the second major activity, after aquaculture, affecting the mangrove forest areas in Sabah (Jakobsen *et al.*, 2007). A study by Lo Man *et al.* (2011) reported that the demand for residential development in Sabah has been increasing due to increasing population. **Figure 2.8** shows the population growth in Sabah (Malaysia Department Statistics, 2013).

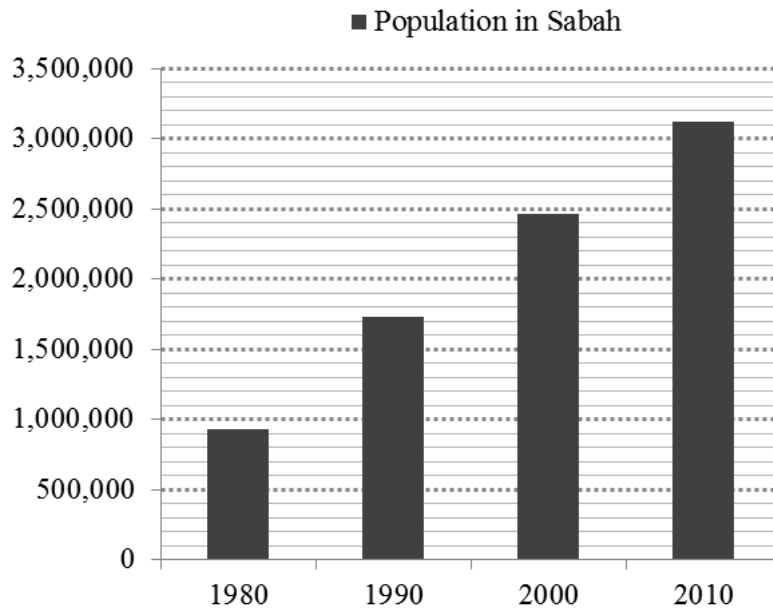


Figure 2.8 Population in Sabah

Source: Malaysia Department Statistics (2011)

According to the Sabah Forestry Department (2012), deforestation of mangrove areas has resulted in some mangrove areas being threatened. These include the areas in Kota Kinabalu, Tuaran, Tawau, Sandakan, and Semporna. Uncontrolled exploitation of mangrove forest areas has led to some degradation of the coastal environment, such as coastal erosion, loss of wildlife habitat, and climate change (Barua *et al.*, 2010).

Sabah's coastline is also facing coastal erosion, as are the areas in Tuaran and Papar where mangrove forests have been degraded. Thus, it is necessary to monitor and assess the mangrove forest structure and dynamics to gain both a better understanding of their basic biology and to help guide the conservation and restoration efforts.

2.6 Application of Remote Sensing and Geographic Information System (GIS) Technology to Mangroves Research

Remote sensing and geographic information system (GIS) technologies have been found to be very valuable application tools for classifying various types of vegetation,

including mangroves. The use of these technologies provides valuable information about land cover, such as the types of habitats and the ecological diversity present in certain areas. Previous studies have also shown that remote sensing is a significant tool for inventorying, mapping, classifying, monitoring, managing, and developing effective strategies for the sustainable utilization of natural resources (Aschbacher *et al.*, 1995; Chauvaud *et al.*, 2001; Karthisen & Birgham, 2001).

2.6.1 Characteristics for Identifying Mangroves in Remotely Sensed Data

Mangroves grow at the land–sea interface. Therefore, the three major features contributing to the pixel composition in remotely sensed imagery are vegetation, soil, and water. However, any mixture of individual surface appearance is influenced by seasonal and diurnal intertidal interactions. According to Blasco & Aizupuru (2002), these circumstances are the major obstacles to rigorous radiometrics and greatly affect spectral characterization.

Additionally, the diversity of mangrove species, especially in Asia, where it is higher than in tropical and subtropical regions, aggravates the difficulties of discrimination because of the high number of spectrally unique species (Kuenzer *et al.*, 2011). In Malaysia, 36 main mangrove species have been recorded in the Peninsular region, and 34 species have been recorded in Sabah and Sarawak (Hamdan *et al.*, 2012; Mohd Lokman *et al.*, 2001; Sabah Forestry Department, 2012). However, the most important species in Malaysia belong to the genera *Rhizophora*, *Avicennia*, *Sonneratia*, and *Laguncularia* (Hamdan *et al.*, 2012).

Kairo *et al.* (2002) suggested that the textural and spectral characteristics of the canopy and leaves are the main features used to distinguish mangrove communities. Their structural appearance, more homogenous or more heterogeneous, depends on several factors such as species composition, distribution pattern, growth form, density of growth, and stand height. The spectral signature of a single species is defined by age, vitality, and physiological characteristics (Blasco *et al.*, 1998).

Kuenzer *et al.* (2011) described that the near-infrared signal from remote sensing reveals different reflections in relation to internal leaf structure, thus facilitating mangrove discrimination. Furthermore, spectral distinctions caused by other leaf components interacting with electromagnetic radiation at longer wavelengths in the near- and mid-infrared regions might work even better (Vaiphasa *et al.*, 2005). A study by Jones *et al.* (2004) confirmed that the different spectral signatures of *Rhizophora* and *Avicennia* species in the near-infrared signal of satellite data is a reflection of their principal biophysical and chemical properties, such as water, cellulose, and chlorophyll pigments.

2.6.2 Overview of Low-cost and High-cost Satellite Remote Sensing Data Based on the Studies and Methods of the Mangrove Ecosystem (Application and Methods)

2.6.2.1 Application of Low-cost Satellite Data to Mangrove Study

For more than two decades, low-cost satellite data have been used extensively to obtain facts and data about the condition of and the extent of the threat to mangrove ecosystems. **Table 2.5** lists several selected mangrove studies that provide a summary of the large variety of mangrove studies that have been conducted over the last 20 years using low-cost satellite data and methodologies.

More than 70 studies that used low-cost satellite data in more than 16 countries have been reviewed. Most of these studies applied the data for mangrove mapping, classification of mangrove and non-mangrove vegetation, mangrove land cover change detection, and monitoring, and several different methods have been used to extract the this information.

Table 2.5 Summary of selected mangrove studies during the past 20 years

Satellite Data	Methods (Years & Study area)					
	Visual Interpretation	Vegetation Indices	Pixel-based classification	Neural Network	Decision-tree learning	Object-based
Aerial Photography	Sulong & Ismail, '90; <i>et al.</i> , '99, '00 (Malaysia) Kairo <i>et al.</i> , '00 (Kenya) Binh <i>et al.</i> , '05 (Vietnam)	None	Manson <i>et al.</i> , '01 (Australia) Everit <i>et al.</i> , '91 (America)	None	None	None
Landsat MSS	Vasconcelos <i>et al.</i> , '02 (Guinea-Bissau)	Giri <i>et al.</i> , '07 (Bengal) Seto <i>et al.</i> , '07 (Vietnam)	Seto <i>et al.</i> , '07 (Vietnam)	None	None	None
Landsat - 5TM	Green <i>et al.</i> , '98 (Turks) Sulong <i>et al.</i> , '00 (Malaysia) Wang <i>et al.</i> , '00 (Tanzania)	Green <i>et al.</i> , '98 (Turks) Seto <i>et al.</i> , '07 (Vietnam) Giri <i>et al.</i> , '07 (Bengal)	Green <i>et al.</i> , '98 (Turks) Alongi <i>et al.</i> , '08 (US) Thu & Populus, '04 (Vietnam)	Seto <i>et al.</i> , '07 (Vietnam) Liu <i>et al.</i> , '08 (China)	None	Green <i>et al.</i> , '98 (Turks)
Landsat 7 ETM+	Mumby <i>et al.</i> , '99 (Turks)	Luo <i>et al.</i> , '12 (China)	Fatayinbo <i>et al.</i> , '08 (Africa) Alongi <i>et al.</i> , '08 (US).	None	None	None
SPOT	Green <i>et al.</i> , '98 (Turks) Fromard <i>et al.</i> , '04 (French)	None	Blasco <i>et al.</i> , '01 (Bangal) Thu & Populus, '04 (Vietnam)	Zhang <i>et al.</i> , '11 (China)	Concheda <i>et al.</i> , '08 (Senegal)	Green <i>et al.</i> , '98 (Turks)
MODIS	Vo <i>et al.</i> , '13 (Vietnam)	Jian <i>et al.</i> , '13 (China) Rahman <i>et al.</i> , '13 (Indonesia)	None	None	Rivera <i>et al.</i> , '12 (American)	None

(i) **Mangrove Studies Based on Aerial Photography**

For several decades, aerial photography has been a dominant remote-sensing technology used to analyze surface events. However, only a few studies on mangroves have been published. Green *et al.* (1996) remarked that the lack of appropriate publications or presentations makes it difficult to obtain an overview of such studies. Based on this review, several such studies have been conducted in locations such as Australia (Manson *et al.*, 2001), Kenya (Kairo *et al.*, 2002), Vietnam (Binh *et al.*, 2005), Texas (Everit *et al.*, 1991), and Malaysia (Sulong & Ismail, 1990; Sulong & Veddin, 1999; Sulong *et al.*, 2002).

Most studies have suggested that aerial photography is suitable for highly detailed mapping in very small and narrow coastal areas (Sulong & Ismail, 1990; Sulong & Veddin, 1999; Sulong *et al.*, 2002). Furthermore, by using different scales of aerial photographs, mangrove forest can be classified into different forest types (Kairo *et al.*, 2002; Sulong & Ismail, 1990; Sulong *et al.*, 2002; Tarmizi *et al.*, 1998). However, large-scale aerial imagery reduces the accuracy of aggregation, but does provide details of individual trees. **Table 2.6** summarizes types of mangrove forest mapping by aerial photo-interpretation.

Table 2.6 Summary of the types of mangrove forest mapping by aerial photographs

Authors	Year	Scale of Arial Photographs	Results
Sulong & Ismail	1990	1:40 000	3 forest types
Tarmizi <i>et al.</i>	1998	1:5000	12 forest types
Sulong <i>et al.</i>	2000	1:20 000	7 forest types
Kairo <i>et al.</i>	2001	1:25 000	9 forest types
Sulong <i>et al.</i>	2002	1:5000	14 forest types

The visual interpretation method, such as by using color, texture, structures, and other image attributes, has been used extensively for species identification (Sulong & Ismail, 1990). The color attribute of aerial photography has potential for the detection of mangrove forest. Manson *et al.* (2001) used the color of aerial photographs to detect changes of mangrove forest in northern Australia. The combination of the color data and the ISODATA clustering algorithm method successfully extracted changes of mangrove in the study area. Verification based on a field survey indicated that mangrove changes were detected with high accuracy.

Furthermore, Binh *et al.* (2005) used 58 aerial photographs taken in the year 1968 and 154 images from the year 1992 and assembled them into a photographic overview mosaic to identify changes in land cover over this long-term period. They identified a rapid increase of shrimp farming from 1997 onward, and the forest area (mainly mangroves) was reduced by about 75%, of which 60% was due to the demand for agricultural land and 40% was due to the development of new shrimp farms.

Based on previous studies, aerial photograph data have been used mostly for mangrove classification and mangrove change detection. Many studies have demonstrated the potential of using satellite data for mangrove studies. However, only a few methods have been used to extract mangrove information from aerial photography.

(ii) Mangrove Studies Based on Landsat Series

The Landsat satellites have been providing multispectral data of the earth environment since the early 1970s. Landsat data have been used in a variety of studies, such as land-water management, land surface change detection, pollution monitoring, and classifying various types of vegetation, including mangroves (Blasco *et al.*, 1998; Giri *et al.*, 2007; Green *et al.*, 1998; Karthisen & Birgham, 2001).

The Landsat data series (MSS, TM, and ETM+) are free data provided by the National Aeronautics and Space Administration (NASA) and the U.S. Geological Survey (USGS). More than 20 studies have applied the Landsat data series and more

than 10 countries have been reviewed. These Landsat data have been used extensively for classifying, mapping, detecting changes, and monitoring mangrove forest (Giri *et al.*, 2007; Green *et al.*, 1998; Sulong *et al.*, 2002) (**Table 2.5**).

Among these data, Landsat TM and ETM+ have been used widely for mangrove studies. The improvements of several additions of infrared bands and better spatial resolution (30 meters) of TM and ETM+ have promoted the application of both data for mangrove monitoring (Green *et al.*, 1998). Additionally, the availability of multi-temporal Landsat data series has helped develop the application of change detection analysis to mangrove ecosystems.

Change detection analysis using satellite data is a powerful tool to visualize, measure, and thus understand better the trends of mangrove ecosystems (Binh *et al.*, 2005; Seto *et al.*, 2007; Thu & Populus, 2004; Wang *et al.*, 2003). It enables the evaluation of subtle changes over a long period of time (trends) as well as the identification of sudden changes due to natural or dramatic anthropogenic impacts (e.g., tsunami destruction or conversion to shrimp farms) (Giri *et al.*, 2008; Sirikulchayon *et al.*, 2008; Thu & Populus, 2004).

Many previous studies have successfully measured, visualized, and monitored changes of mangrove forest using multi-temporal Landsat data. Sirikulchayon *et al.* (2008) examined the impact of the 2004 tsunami on mangrove vegetation in Phang Nga Bay, Thailand, using a Landsat 7 ETM+ dataset. The data were acquired before and after the impact of the tsunami. This study suggested that a mangrove belt of 1,000–1,500 m, parallel to the coast, would be optimal to weaken the destructive impacts of tsunami waves to the hinterland.

A study by Thu and Populus (2004) successfully measured and visualized the changes of mangrove forests in Tra Vinh Province, Mekong Delta, Vietnam, between 1965 and 2001 using Landsat ETM+ data. The mangrove changes in this area were related mostly to the conversion to shrimp farming activities. Furthermore, Seto *et al.* (2007) analysed time series of Landsat MSS and TM data for the Red River Delta in

Vietnam between 1975 and 2002. The study calculated the extent and density of mangrove, the extent of aquaculture, and the landscape fragmentation to assess the land cover condition as a function of time. Their findings indicated that multi-temporal Landsat data series are useful for analyzing the changes of mangrove forest.

Furthermore, various methods have been used to extract mangrove information from Landsat data series. More than five image-processing methods have been used extensively to extract mangrove information. The methods can be applied exclusively or in combination. Visual interpretation, unsupervised classification such as ISODATA, and supervised classification such as maximum likelihood methods are frequently used for mangrove mapping (Giri *et al.*, 2007, 2008; Sulong & Ismail, 1990; Sulong *et al.*, 1990, 2002; Wang *et al.*, 2003).

Other common approaches for the classification of mangroves using multispectral imagery include spectral vegetation indices such as the normalized difference vegetation index (NDVI) and the leaf area index (LAI). Vegetation indices have been used widely in pre-classification steps to separate vegetation from non-vegetation and mangrove (Alongi *et al.*, 2008; Giri *et al.*, 2007; Green *et al.*, 1998; Thu & Populus *et al.*, 2007).

Several studies have been carried out to investigate and compare the suitability of various classification algorithms for spectral separation of mangroves (Green *et al.*, 1998). In general, application of the supervised maximum likelihood classifier (MLC) is the most effective and robust method for classifying mangroves based on traditional satellite remote sensing data (Giri *et al.*, 2007; Green *et al.*, 1998).

Even though applications of these traditional satellite remote sensing data and methods have been used widely, several limitations and challenges remain in mangrove studies. Confusion between mangroves and other vegetation is commonly reported as a source of classification error (Benfield *et al.*, 2005; Green *et al.*, 1998). Another source of classification error is the omission of fringe mangroves that are less than the pixel size, resulting in mixed pixels (Manson *et al.*, 2001).

Therefore, new classification approaches such as the neural network, machine learning, and object-based methods have been developed to improve the accuracy of mapping the extent of mangrove and detecting change over a time (Green *et al.*, 1998; Liu *et al.*, 2008; Seto *et al.*, 2007). Most studies have shown high potential of recent classification approaches compared with common methods.

A study by Liu *et al.* (2008) used the machine learning approach with multi-temporal Landsat TM data and ancillary GIS data to identify mangrove in the Pearl River Estuary. According to these authors, this approach can produce superior mangrove classification results by using only imagery or ancillary data. Furthermore, according to Zhang *et al.* (2011), the machine learning method has significantly improved the separability between mangrove and water–vegetation mixed pixels. The results of this study showed that the kappa coefficient and the commission error of mangrove identification were 0.90 and 7.9%, respectively.

Only a few object-based approaches have been used in mangrove studies. The object-based method allows the use of additional variables such as texture, shape, context, and other cognitive information provided by the image analyst to segment and classify the image features to improve classification (Blaschke, 2010). Vo *et al.* (2013) successfully detected areas with mixed aquaculture–mangrove land cover with high accuracy in Ca Mau Province, Vietnam. However, few mangrove studies have explored the use of these recent approaches.

(iii) Mangrove Studies Based on MODIS

Moderate Resolution Imaging Spectroradiometer (MODIS) data have been used for environmental monitoring and natural resource management at the global, regional, and country-wide scale. MODIS data also have been applied widely in mangrove studies since 2000. The instrument was launched to earth orbit in 1990 and 2000 onboard the Terra and Aqua satellites, respectively. MODIS data are provided by the National Aeronautics and Space Administration (NASA) and the U.S Geological Survey (USGS) and can be accessed freely.

Based on the previous studies (**Table 2.5**), MODIS data have been used widely for the mapping and monitoring of mangrove forest. The advantages of MODIS data, such as providing multispectral data and low spatial resolution (250–1000 m), have stimulated extensive application of these data in a large-scale mapping of mangrove (Vo *et al.*, 2013). Based on this review, more than 10 studies in 10 countries have used MODIS data for mangrove research.

A study by Rahman *et al.* (2013) analyzed MODIS time series (2000–2010) data to monitor changes of mangrove forest in the Mahakam Delta, Indonesia. The results of this study showed that $21,000 \pm 152$ ha of mangrove land on the Mahakam Delta were deforested and converted to shrimp pond areas within 11 years. Furthermore, a study by Duong (2004) analyzed MODIS 500 m 32-day global composite data for mangrove land-cover mapping in Vietnam.

The special characteristic of MODIS data for providing large spatial coverage is its ability to observe an entire region or a whole country at the same time with the same atmospheric conditions, which simplifies data processing and analysis (Duong, 2004; Rahman *et al.*, 2013; Vo *et al.*, 2013). MODIS data are also available in short revisit times (2 to 4 days). This advantage offers the possibility of creating a cloud-free composite, which is essential for the establishment of a multi-temporal dataset, a most important resource for environmental monitoring. Therefore, the availability of continuously acquired MODIS data has promoted application of these data in mangrove monitoring and mapping (Rahman *et al.*, 2013; Vo *et al.*, 2013).

Pixel-based classification, such as maximum likelihood and vegetation indices such as the normalized difference vegetation index (NDVI) and the leaf area index (LAI), methods have been used extensively to extract mangrove from MODIS data (Jiang *et al.*, 2013). Rivera *et al.* (2012) proved that MODIS data are very affordable and effective by identifying and discriminating land use classes at the country level. According to these authors, the accuracy of the map was very high, particularly for classes such as mangrove forest and commercial agriculture and especially in the tropical country of study.

2.6.2.2 Application of High-cost Satellite Data for Mangrove Study

High-cost satellite data, which are high-resolution data, have been used in mangrove studies since the early 1990s. Application of these data began with data from the SPOT-1 satellite, followed by QuickBird and IKONOS data. Due to the advantage of these data of having high spatial resolution, most studies have applied the data to mangrove species mapping. However, due to limitations such as high cost and small coverage area, no more than 20 studies have been conducted using these data. The paragraphs below provide a review of the use of SPOT, IKONOS, and QuickBird data in mangrove studies.

(i) Mangrove Studies Based on SPOT

SPOT data have high resolution, which promoted application of these data to mangrove studies. SPOT data have been used by many studies for mapping, change detection, and monitoring of mangrove (Giri *et al.*, 1996; Rasolofoharinoro *et al.*, 1998; Thu & Populus, 2007; Tong *et al.*, 2004). A study by Tong *et al.* (2004) assessed the ecological status of mangrove with discrimination by age, density, and species in Phangnga Bay, Thailand, using SPOT XS data. In a similar environment, Thu and Populus (2007) assessed the status and change of mangrove forest in Tra Vinh Province, Mekong Delta, Vietnam, between 1965 and 2001.

Rasolofoharinoro *et al.* (1998) produced the first inventory map of a mangrove ecosystem in Mahajamba Bay, Madagascar, based on SPOT data. A study by Blasco *et al.* (2002) conducted mangrove ecosystem mapping on a regional scale using SPOT multispectral data. They analyzed the ecosystems along three major rivers in the tropical Bay of Bengal, along the Irrawaddy, and along the Mekong and included various criteria such as phonology, physiognomy, and density of the mangrove stands. The result of this study found that mangrove density is influenced by both natural factors and human activities such as the presence and density of aquaculture. Tong *et al.* (2004) assessed the impact of shrimp aquaculture on the mangrove ecosystem in the Mekong Delta using SPOT scenes from the years 1995 and 2001. They identified five

ecologically distinct landscape classes but faced difficulty in applying the same method in a second study area a few hundred kilometres away.

As for other satellite data, several common methods have been used to extract mangroves in SPOT data. Fromard *et al.* (2004) successfully used visual interpretation of SPOT XS data to map the extent and the status of mangroves at Mida Creek, Kenya. Rasolofoharinoro *et al.* (1998) used the vegetation index (VI) NDVI on a multispectral-layer stack for supervised classification of SPOT data. The study showed that the NDVI clearly improved discrimination of non-mangrove and mangrove vegetation. Green *et al.* (1998) found that the NDVI data derived from SPOT XS were correlated to a high degree ($r = 0.913$) with the percentage of mangrove canopy closure.

Furthermore, supervised classification such as maximum likelihood and unsupervised classification ISODATA approaches have been used to detect and delineate mangrove in SPOT data (Blasco *et al.*, 2002; Giri *et al.*, 1996; Rasolofoharinoro *et al.*, 1998; Saito *et al.*, 2003; Thu & Populus, 2007; Tong *et al.*, 2004). These processing methods have been shown to be acceptable for the applications of mapping mangrove, habitat management (including mangrove inventory and mapping), change detection (deforestation), and management of aquaculture activities. According to Rasolofoharinoro *et al.* (1998), SPOT images can be used to classify and identify mangrove forest with 81–95% accuracy using maximum likelihood classification.

Recent approaches such as object-based classification also have been used to map and detect changes of mangrove forest. Conchedda *et al.* (2008) mapped the mangrove land cover in Lower Casamance, Senegal, using SPOT XS data and an object-based classification method. A change detection approach was performed by means of a region-growing algorithm on a multi-date composite for the years of 1986 and 2006. The classification results from the SPOT data for 2006 allowed clear separation between the different land cover classes within the research area, as well as separation among the mangrove classes.

(ii) Mangrove Studies Based on QuickBird

QuickBird satellite data have been used in mangrove studies from 2001 until present. Fewer than 10 studies have been conducted for mapping, change detection, and monitoring of mangrove. However, many studies have applied these satellite data for mangrove species mapping. Several data interpretation methods and processing techniques, including conventional methods (vegetation index, supervised and unsupervised classification) and recent techniques (object-based, neural network), have been used.

QuickBird satellite data have been suggested to be the best high-resolution data for mangrove species identification (Everet *et al.* 2008; Lee & Yeah, 2009). Everet *et al.* (2008) successfully discriminated black mangrove communities in the Texas Gulf Coastal region by integrating conventional and advanced classification techniques. A study by Lee and Yeah (2009) showed high accuracy (97%) mangrove species classification using QuickBird satellite data. However, mangrove monitoring at a broad scale with integrated QuickBird satellite data has not been well applied due to the limitation of high cost.

(iii) Mangrove Studies Based on IKONOS

IKONOS satellite data have been used in mangrove studies since the early 2000s. As discussed in the previous section (2.6.2), most studies have used these data for mangrove species discrimination. IKONOS satellite data have more detailed spectral reflectance (Wang *et al.*, 2004). The application of conventional and recent advanced classification techniques has promoted high accuracy in mangrove discrimination studies (Kovacs *et al.*, 2004; Wang *et al.*, 2004). As for other high-resolution data, high cost and small coverage have limited the use of these data for mangrove monitoring studies.

2.7. Conventional and Advanced Remote Sensing Techniques for Mangrove Land Cover Mapping

2.7.1 Conventional Approaches of Remote Sensing Techniques

Most studies have used conventional approaches of remote sensing techniques to detect and delineate mangrove and non-mangrove areas to the species level. Conventional remote sensing approaches can provide the important information required to monitor the areal extent and changes of mangrove. Several conventional techniques, such as visual interpretation, vegetation index, pixel-based classification (supervised and unsupervised), and spectral transformation, have been used in previous studies. The details of conventional approaches of remote sensing techniques that have been used in mangrove studies are provided below.

(i) Visual Interpretation

The visual interpretation technique is highly dependent on the interpreter's ability to recognize and analyze various characters of the study area. For example, shape, size, and patterns with respect to the spectral bands and the brightness values from field data or aerial photographs indicate that decisions about different mangrove structures can be achieved without further computations or statistical processes (Green *et al.*, 1998; Sivakumar, 2002). However, to facilitate visual comprehension of imagery information, radiometric enhancement (contrast or pseudo-color) needs to be applied.

Sulong *et al.* (2002) classified nine classes of mangrove forest in Kemaman District based on the texture and tone of aerial photograph and Landsat TM data. For example, a light tone with a coarse texture and a dark tone with a medium texture could be classified as *Avecennia–Sonneratia* and *Bruguiera* mangroves, respectively. Green *et al.* (1998) also reported that the visual interpretation technique can be up to 50% accurate. This technique has been used extensively to map complex ecosystems (Blasco *et al.*, 1998; Gang & Agatsiva, 1992; Selvam *et al.*, 2003; Wang *et al.*, 2003).

(ii) Vegetation Index

A vegetation index is a number that is generated by some combination of remote sensing bands and may have some relationship with the amount of vegetation in a given image pixel (Ray, 1994). Many different vegetation indices are available to transform multispectral information into a single index. They may be broadly categorized into three types: ratio indices (e.g., normalized difference vegetation index (NDVI); Jensen, 1986), orthogonal indices (e.g., tasseled cap transformation; Crist & Cicone, 1984), and others (Logan & Strahler, 1983; Perry & Lautenschlager, 1984). Of these, ratio indices have been applied most frequently to mangrove data.

The NDVI technique has been used widely in pre-classification steps to separate vegetation from non-vegetation (Almeida, 2002; Binh *et al.*, 2005; Green *et al.*, 1998; Tong *et al.*, 2004; Thu & Populus, 2007). The NDVI is calculated based on the following equation:

$$\text{NDVI} = \frac{(IR + Red)}{(IR - Red)},$$

where *Red* and *IR* refer to the spectral reflectance measurement acquired at red and infrared wavelength, respectively. For mangrove studies, this index can be calculated by comparing the spectral reflectance from Landsat TM bands 3 and 4 and from SPOT XS bands 2 and 3 (Green *et al.*, 1998). A study by Jensen *et al.* (1991) found that NDVI data derived from SPOT XS were correlated to a high degree ($r = 0.913$) with the percentage of mangrove canopy closure.

Canopy closure charts or density maps provide additional information on the dynamics of mangrove vegetation and their its status (Giri *et al.*, 2007; Ramsey & Jensen, 1996; Ruiz-Luna *et al.*, 1999; Seto & Fragkias *et al.*, 2007). The degree of canopy closure can be used for estimations of canopy structure, which can be described in terms of LAI, defined as the total leaf surface area per unit ground surface (Araoujo *et al.*, 1997; Green *et al.*, 1997). In mangrove studies, LAI cannot be measured directly from satellite imagery. However, Ramsey and Jensen (1996) have identified a strong

relationship ($R^2 = 0.84$) between LAI data derived from in situ mean values of canopy closure and the estimated NDVI for numerous satellite platforms, which was confirmed by the work of Green *et al.* (1997).

(iii) Pixel-based Classification

There are two common techniques of pixel-based classification (supervised and unsupervised) that have been used in mangrove studies. In supervised classification, the spectral features of some areas of known land cover types are extracted from the image. These areas are known as training areas. Every pixel in the whole image is then classified to one of the classes, depending on how similar its spectral signature is to the training areas.

In unsupervised classification, the computer program automatically groups the pixels in the image into separate clusters, depending on their spectral features. Each cluster is then assigned a land cover type by the analyst (Liew, 2001). An advantage of unsupervised classification is that no prior knowledge of the scene is required. However, without further information from ground investigation or published sources, the result cannot be attributed directly to a particular area (Gibson & Power, 2000).

Both of these techniques are frequently used for mangrove mapping (Berlanga & Luna, 2002; Giri *et al.*, 1996, 2007, 2008; Sirikulchayanon *et al.*, 2008; Tong *et al.*, 2004; Vasconcelos *et al.*, 2002). Additionally, several studies have been carried out to investigate and compare the suitability of various classification algorithms for spectral separation of mangroves (Gao, 1999; Green *et al.*, 1998; Saito *et al.*, 2003).

In general, according to previous studies, application of the supervised maximum likelihood classifier (MLC) is the most effective and robust method to classify mangroves based on traditional satellite remote sensing data (Aschbacher *et al.*, 1995; Gao, 1999; Green *et al.*, 1998; Rasolofoharinoro *et al.*, 1998; Tong *et al.*, 2008).

(iv) Spectral Transformation Technique

Spectral transformation techniques have been used to improve mangrove classification results (Beland *et al.*, 2006; Binh *et al.*, 2005; Green *et al.*, 1997, 1998; Keunzer *et al.*, 2011; Kovacs *et al.*, 2001). There are two common spectral transformation techniques that have been used in mangrove studies, principle component analysis (PCA) and tasseled cap transformation (TCT). Both techniques use a measuring pixel intensity of each band in multispectral images to reduce the number of band data. In PCA analysis, scatter plots of pixel intensity in the bands for two different times are used to detect changes of mangrove area.

Unchanged pixels are highly correlated over time and lie in a narrow, elongated cluster along the principle axis, whereas changed pixels are scattered some distance away from it. A study by Green *et al.* (1997) dramatically improved the classification accuracy between mangrove and other vegetation using the Landsat TM bands and bands derived from TCT analysis. Other studies by Binh *et al.* (2005), Green *et al.* (1998), and Kovacs *et al.* (2001) reported that when PCA incorporated with the tasseled cap transformation technique is applied, highly accurate results are produced for mangrove classification and change detection analysis.

Hueman *et al.* (2011) reported that by using conventional techniques, the classification accuracies of mangrove classes ranged from 75% to 90%. Despite the wide application of these conventional remote sensing techniques, several limitations and challenges to using traditional approaches of mangrove study remain. Confusion between mangrove and other vegetation is commonly reported as a source of classification error (Al Habshi *et al.*, 2007; Benfield *et al.*, 2005; Gao *et al.*, 1999). Another source of classification error is the omission of fringe mangroves that are less than the pixel size (Al Habshi *et al.*, 2007; Green *et al.*, 1998) and detection of individual species or estimation of canopy structures (Hermann *et al.*, 2011).

2.7.2 Recent Advanced Approaches of Remote Sensing Techniques

Many image processing and new analysis techniques have been developed to aid the interpretation of remote sensing images and extract information to the greatest extent possible from the images. According to Kuenzer *et al.* (2011), several new analysis techniques, such as object-based image analysis (OBIA), rule-based (decision-tree learning) classification, and neural networks, can be employed to classify remotely sensed data of mangroves. However, all the techniques except for decision-tree learning classification have been explored extensively for mangrove study. Detail explanations of recent advanced techniques that have been applied in mangroves studies are listed below.

(i) Object-based Image Analysis (OBIA) Classification

Object-based image analysis (OBIA) is a technique used to analyze digital images in object space rather than in pixel space. The objects can be used, rather than pixel value, as the primitives for image classification, and the technique was developed relatively recently compared to traditional pixel-based image analysis (Blaschke & Burnett, 2004). The process of detecting objects in an image by applying the object-based approach consists of sequences of image segmentation and classification procedures, which together develop the rule sets.

Only a few studies using the OBIA technique for mangrove research have been conducted due to preference for the pixel-based technique, which is easier to implement (Kamal & Phinn, 2011; Kuenzer *et al.*, 2011). However, previous studies have reported that the classification results of OBIA techniques are more accurate compared to the maximum likelihood classifier technique (Herman *et al.*, 2011; Kamal & Phinn, 2011; Kuenzer *et al.*, 2011; Moskal *et al.*, 2011; Wang *et al.*, 2004). For the most part, previous studies have preferred to use high-resolution satellite data such as QuickBird and IKONOS data, rather than medium-resolution satellite data, for OBIA analysis (Kamal & Phinn, 2011; Kuenzer *et al.*, 2011).

(ii) Neural Network (NN) Classification

Neural network classification is a statistical analysis procedure that relies on parametric and non-parametric multivariate analysis, such as discriminant analysis and cluster analysis (Figueredo *et al.*, 1992; Terhune *et al.*, 1993). According to Gopal and Woodcock (1994), neural network classification provides more flexible solutions to discriminate different classes because no assumption concerning the probability distribution of the classes has to be made. Yet, the neural network technique has seldom been applied to mangrove studies (Kuenzer *et al.*, 2011).

Xiang *et al.* (2010) used this technique to classify a mangrove landscape, and the results showed that the neural network had high classification accuracy (86.86%) compared to maximum likelihood (50.79%). Other studies have also proved that neural network classification has high accuracy in mangrove studies compared to the maximum likelihood method (Paola & Schowengerd, 1997; Wang *et al.*, 2010). Neural network classification has the characteristics of large-scale handling and of distributing information storage (Xiang *et al.*, 2010).

However, the technique also has disadvantages, such as being time consuming, having operation flows that are difficult to understand, and having a parameter that is adjusted empirically instead of using a contingent (Wang *et al.*, 2010; Paola & Schowengerd, 1997; Xiang *et al.*, 2010). Because GIS is based on the yield survey and original maps, it is effective at assisting neural network classification and also can improve the classification accuracy by geographical orientation.

(iii) Rule-based (Decision-Tree Learning) Classification

A decision tree is a classification procedure that repeatedly partitions a dataset into smaller subsets based on a test defined at each branch (or node) of the tree. The tree is composed of a starting node (root), a set of internal nodes (splits), and a set of terminal nodes (leaves). Except for the root, each node has one parent node and, except for the leaves, each node has two or more descendant nodes (Friedl & Brodley, 1997). The

observations are sequentially divided as they pass through the tree, and each observation is finally assigned a class label according to the leaf node that it reaches (Bremen *et al.*, 1984, Quinlan, 1993).

Recent studies have demonstrated that the decision tree is one of the most popular machine learning approaches and that it is accurate and efficient in land cover classification based on remotely sensed data (Defries *et al.*, 1998; Friedl & Brodley, 1997; Friedl *et al.*, 1999; Hansen *et al.*, 1996; Swain & Hauska, 1977). The decision-tree learning algorithm can create classification rules directly from the training data without human intervention.

In addition, unlike many other statistical analysis approaches, such as maximum likelihood classification, the decision tree does not depend on assumptions about value distribution or the independence of variables (Quinlan, 1993). Several studies (Fatoyinbo *et al.*, 2008; Islam *et al.*, 2008; Liu *et al.*, 2008; Shafri & Ramli, 2009) have attempted to apply the decision-tree learning technique, integrated with high-resolution satellite data, to mangrove research. The results of the previous studies showed that decision-tree techniques can produce superior mangrove classification results compared to conventional classification techniques.

However, no study has yet applied the decision-tree learning technique intergrated with low-cost satellite data. Therefore, this study applies decision-tree learning integrated with low-cost satellite data to mangrove classification in the Sabah area. A summary of previous studies on the uses of low-cost and high-cost satellite data integrated with conventional and advanced methods in mangrove studies is presented in **Table 2.7**.

Table 2.7 Summary of applications of low-cost and high-cost satellite data integrated with conventional and advanced methods

Satellite data		Year study	Applications (No. of study)			Methods	
			Mapping		Change-detection & Monitoring	Conventional	Advance
			Spatial/Temporal distributions	Species discrimination		Vegetation index, visual interpretation, supervised & unsupervised	Machine-learning, neural network (NN), Object-based
Medium-resolution (low-cost)	Landsat MSS	1974-2000	(<10)	None	(<10)	√	None
	Landsat TM	1993-2012	(>30)	(<10)	(>30)	√	None
	Landsat ETM+	2000-2013	(<10)	(<10)	(<10)	√	None
	Landsat OLI_TIRS	2013-present	None	None	None	None	None
	MODIS	2000-2013	(>20)	None	(>20)	√	None
High-resolution (high-cost)	SPOT 1-4	1990-2012	(>20)	(<10)	(>20)	√	Object-based
	Quickbird	2001-2012	(<10)	(<10)	(<10)	√	Object-based
	IKONOS	2000-2012	(<10)	(<10)	(<10)	√	Object-based & NN

Note: (√) represent applications of the methods

2.8 Benefits and Limitations of Low-cost and High-Cost Satellite Data in Mangrove Studies

Numerous studies of remote sensing-based mangrove mapping and monitoring have been published over the last two decades. However, most of these studies have used low-cost satellite data such as Landsat and MODIS data. Therefore, this study focuses on the benefits and limitations of low-cost and high-cost satellite data in mangrove studies. **Table 2.8** shows the benefits and limitations in mangrove studies of all these data types.

Table 2.8 Benefits and limitations of low-cost and high-cost satellite data types in mangrove studies

Satellite Data Characteristics	High-resolution Data (Aerial photography, SPOT, IKONOS & Quickbird)		Medium-Resolution Data (Landsat, MODIS)	
	Benefits	Limitations	Benefits	Limitations
Spectral resolution	Red-NIR spectral information with red-edge slope	None at all or very low (R, G, B, NIR)	Several multispectral bands (R, G, B, NIR mid-NIR & thermal bands)	Skilled, trained personnel are required
Spatial resolution	Very high (centimetre to meter)	Only a small area is covered	Ideal for mapping on a large regional scale	Too coarse for local observations requiring in-depth species differentiation
Temporal resolution	Always available on demand	Complex acquisition of equipment	Frequent mapping (e.g. Rainy season and dry season within 1 year)	Repetition rate may be too low to record the impact of extreme events (e.g. Floods)& very weather dependent (clouds)
Costs	Low costs for small areas	Increasing costs with increasing spatial coverage	Depending on sensor, freely available (e.g. Landsat, MODIS), costly (e.g. SPOT) but all are cost efficient compared with field surveys	Software for image processing needed (common software, such as Erdas, ENVI, and ArcGIS, have high license fees)
Long-term monitoring	Available only for short-term monitoring	-	Data availability over three decades	Depending on the future duration of the systems and subsequent comparable sensors
Purpose	Local maps of mangrove ecosystems, parameterization, change detection	Only local-scale studies	Inventory and status maps; change detection, assessment of impact damages & deforestation	For some species-oriented botany-focused studies, resolution may already be too coarse

Many benefits of Landsat and MODIS data have been reviewed. The Landsat and MODIS data have benefits on the multispectral bands compared with the high-resolutions satellite data. The availability of this benefit have promoted the usefulness of Landsat and MODIS for vegetation studies especially for the mangrove. In addition, the large-scale coverage of Landsat series has promoted the usefulness for studying the

mangrove in large area. The details multispectral bands and satellite data characteristics of Landsat and MODIS data are presented in the appendix of this dissertation.

The availability of long-term satellite data has promoted the use of Landsat, and MODIS data for long-term mangrove monitoring. Furthermore, free access to Landsat and MODIS data has contributed to the capability of these satellite data. The USGS (2013) announced on April 21, 2008, that the agency will provide all Landsat and MODIS data archives for free, and it is possible to download these data from several websites (**Table 2.9**). The websites provide thousands of free Landsat and MODIS satellite data for any study area of interest.

Table 2.9 Free-access websites providing Landsat series and MODIS data

Satellites Data	
Landsat series (TM, ETM+& OLI_TIRS)	MODIS
Websites Provided	Websites Provided
Global Visualization Viewer (http://glovis.usgs.gov/)	The Land Processes Distributed Active Archive Center (LP DAAC) (https://lpdaac.usgs.gov/)
EarthExplorer (http://earthexplorer.usgs.gov/)	Global Land Cover Facility (http://glcf.umd.edu/)
Landsat.org. (http://www.landsat.org)	Reverb (http://reverb.echo.nasa.gov/reverb)
Global Land Cover Facility (http://glcf.umd.edu/)	Data Pool (https://lpdaac.usgs.gov/datapool/datapool.asp)

The Landsat data that are provided have standard processing algorithms and terrain correction applied, making them very easy to use. There are three types of Landsat data level corrections: standard terrain correction (Level 1T), systematic terrain correction (Level 1GT), and systematic correction (Level 1G) (USGS, 2013). The selection of the data type depends on the study to which the data are to be applied. However, all of these types of Landsat data are very compatible for mapping,

monitoring, and detecting change in mangrove ecosystems (Churches *et al.*, 2014; Fatoyinbo *et al.*, 2008; Liu *et al.*, 2008).

There are several types of MODIS land data products that can be useful for mangrove studies, such as land cover type (MCD 12C1), leaf area index (MCD15A2), surface reflectance bands (MD09A1), gross and net primary production (MOD 17A), and vegetation indices (MQ13) (Vo *et al.*, 2013). The MODIS vegetation index (MQ13) product is particular for vegetation genealogy research. It consists of the normalized vegetation index (NDVI) and the enhanced vegetation index (EVI) (USGS, 2013).

There are several limitations and challenges of using low-cost satellite data. The too-coarse spatial resolution of Landsat data is required in deep-species differentiation and parameterization (Kuenzer *et al.*, 2011), and the high-resolution spatial data of aerial photography is compatible for only studies of a small area (Kairo *et al.*, 2001; Kuenzer *et al.*, 2011; Sulong *et al.*, 2002; Tarmizi *et al.*, 1998). These limitations could present a challenge for mapping the diverse mangrove species in Malaysia.

Therefore, a combination application of satellite data, such as aerial photography, Landsat, and MODIS data, could be an option for mangrove mapping in tropical countries, especially Malaysia. According to Kuenzer *et al.* (2011), the selection of satellite data in mangrove studies depends on the particular circumstances of the user's study. Furthermore, recent advanced approaches of mangrove classification can be applied to these low-cost satellite data.

Data with cloud cover are the utmost limitation in using temporal low-cost satellite data (Kuenzer *et al.*, 2011; Nezry *et al.*, 1993). The limited review of the sources of free satellite data access could be one reason for insufficient cloud cover-free data (Kuenzer *et al.*, 2011). As discussed above, several websites provide thousands of free satellite data, which could options for selecting the best low-cost satellite data.

Chapter 3

Classification Protocol for Mangrove Forest Land Cover in Sabah using Landsat Data Series

3.1 Introduction

Sabah has the largest mangrove forest area in Malaysia, constituting 58% (341,000 hectares) of the country's total area in 1990. Facing the Sulu and Sulawesi seas, Sabah's mangroves are largely along the east coast. However, according to the Sabah Forestry Department (2012), the area of mangrove forest had decreased to 320,000 hectares in 2010. An increase of population simultaneous with expansion of agricultural land, aquaculture activities, industrial areas, and urban development have caused a significant proportion of Sabah's mangrove forest area to be destroyed (Jakobsen *et al.*, 2007; Polpanisch, 2008; Sabah Forestry Department, 2010).

According to a report by the Sabah Forestry Department (2010), the total of Sabah mangrove cover has decreased by about 6% (20,460 hectares) due to shrimp pond farming, agriculture, and urbanization since the 1990s. Uncontrolled exploitation of Sabah's mangrove forest has led to degradation of the coastal environment, such as by coastal erosion and the loss of wildlife habitat (Barua *et al.*, 2010; Sabah Forestry Department, 2010). Coastal erosion has affected the areas of Tuaran and Papar, where the largest area of mangrove forest has been degraded. In order to cope with this problem, further extensive monitoring of mangrove forest land cover should be conducted continuously.

The same types of application of remote sensing technology for producing and monitoring land cover that are used in any research field have been used widely in mangrove studies. Remote sensing technology has been used in mangrove studies since 1974, with remotely sensed data from the Landsat satellite. The Landsat satellites have

provided multispectral data of the earth environment since the early 1970s. These data have been used in a variety of studies, such as studies on water management, land surface change detection, pollution monitoring, and classifying various types of vegetation, including mangroves (Blasco *et al.*, 1998; Giri *et al.*, 2007; Green *et al.*, 1998; Karthisen & Birgham, 2001). Due to its inaccessibility for conducting a field survey, the indispensable tool of remote sensing has been used extensively to assess and monitor mangrove forest (Lee & Yeh, 2009).

The Landsat data series (MSS, TM, ETM+, and OLI/TIRS) are free data series provided by the National Aeronautics and Space Administration (NASA) and the U.S. Geological Survey (USGS). These Landsat data have been used extensively for classifying, mapping, and monitoring mangrove forest land cover. The Operation Land Imager Thermal Infrared Sensor (OLI/TIRS) onboard Landsat 8 has provided new data that was released by NASA in 2013. However, applications of OLI/TIRS data in mangrove study remain limited. Furthermore, several issues regarding previous Landsat data series (MSS, TM, and ETM+) may discourage their use in contemporary mangrove mapping and monitoring studies (Wijedasa *et al.*, 2012).

One of these issues is the failure of the hardware Scan Line Corrector (SLC-off) of Landsat 7 ETM+ in 2003. This technical problem produced a data gap in Landsat ETM+ that has affected 22% of data (USGS, 2004). The anomaly of the Landsat 7 ETM+ SLC-off remained significant and had an obvious negative impact on the usability of the data for some applications. A study by Singh and Sharma (2010) indicated that there were 14% significant differences in land cover classification between SLC-off and SLC-off gap-filled data of Landsat ETM+.

Another issue is the unavailability of a standard protocol for Landsat data acquisitions and analysis processing (Kuenzer *et al.*, 2011; Mohammady *et al.*, 2013). Due to limitations on obtaining high-quality data free of cloud cover, several websites have been established by many international organizations. The different websites have promoted different qualities and types of remotely sensed data. However, few previous studies have presented detailed protocols on how to access the free data using various

sources of available websites. This issue has limited the usage of Landsat satellite data. In addition, few studies have presented the processing procedures for the Landsat ETM+ SLC-off data. However, many users prefer these data over costlier alternatives. According to Wijedasa *et al.* (2012), Landsat data, especially ETM+ SLC-off data, still have appreciable utility for classification and monitoring of tropical forests.

Thus, a standard method for the selection of appropriate data and processing protocols of the Landsat satellite series, especially to recover the missing data of ETM+ SLC-off, is proposed. The classification protocol of mangrove study is also explored in detail to optimize this application of the Landsat data. The application of Landsat 8 data to mangrove research will provide a new perspective on the application of Landsat data series. These approaches are used to maximize the application of the Landsat data series for classifying mangrove forest in Sabah, Malaysia.

3.2 Objectives

The main objective of this chapter is to develop a classification protocol for the mangrove forest in Sabah using the Landsat data series. The specific objectives of this study follow:

1. To present a detailed protocol for data selection and processing procedures of Landsat data series (TM, ETM+, and OLI_TIRS).
2. To assess the quality of Landsat data series (TM, ETM+, and OLI/TIRS).
3. To determine the potential of Landsat data series (TM, ETM+, and OLI/TIRS) for classifying the mangrove forest in Sabah

3.3 Location of Study Area

The study area is located in the Mengkabong mangrove forest (west coast of Sabah), which is 40 km from Kota Kinabalu city. The total study area extends from 6°8'24" N to 6°11'24" N latitude and from 116°08'6" E to 116°12'54" E longitude (Google Earth, 2012) (**Figure 3.1**). The Mengkabong mangrove forest is dominated by *Rhizophora apiculata*, which is a healthy and dense mangrove species (Sabah Forestry Department, 2010). This area has been used extensively by local villagers for fishing, and some mangrove wood collection for firewood and fishing poles has been carried out. Increased development pressure in this area has led to the depletion of mangrove forest and changes in the coastal environment.

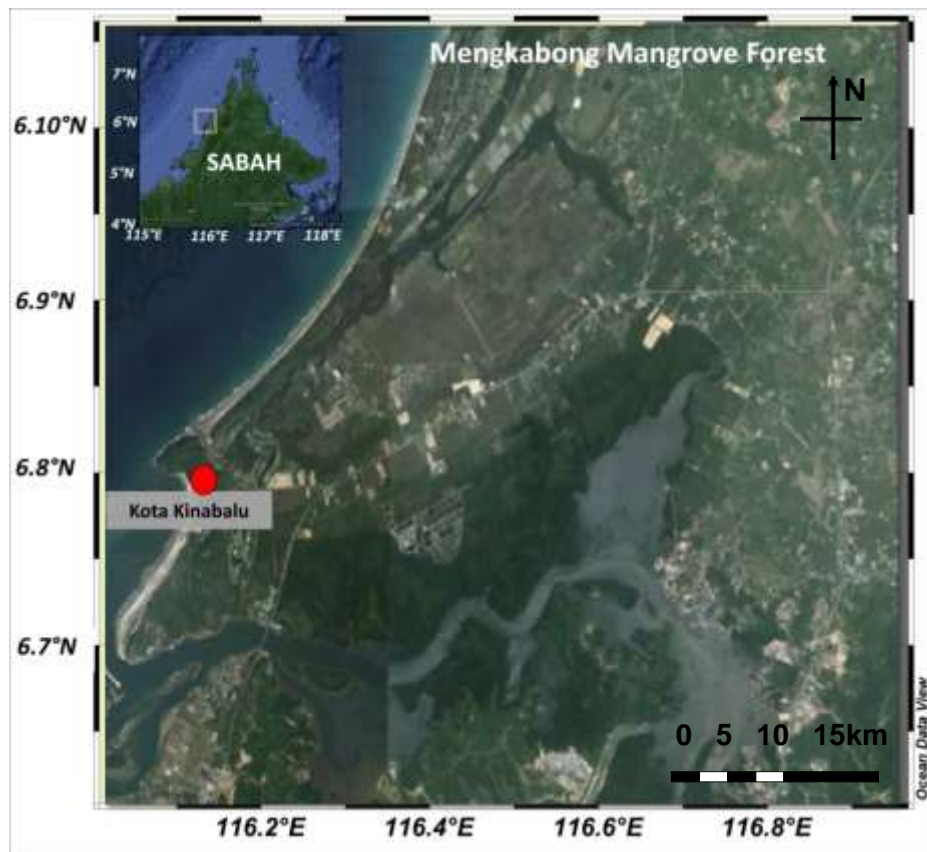


Figure 3.1 Map of study area

3.4 Materials and Methods

3.4.1 Materials of Satellite Images and Reference Data

(i) Acquisition and Selection of Landsat Data Series

Landsat data series (TM, ETM+, and OLI/TRS) were used in this study and were downloaded free of charge from the Earth Explorer US Geological Survey (USGS) website (<http://earthexplorer.usgs.gov/>). The USGS website provides *search data criteria tools*, such as the World Reference System (WRS), data range, data type, and dataset selection to help access the needed Landsat data series.

For example, by using the WRS tool, an image of the Mengkabong area was acquired at the path and row of 118 and 056, respectively. The multi-temporal Landsat data range used in this study covered the years of 1990 to 2010, with a five-year interval period (i.e., 1990, 1995, 2000, 2005, 2010), along with the year 2013 as a new Landsat series of OLI_TIRS data.

The purpose of selecting the five-year interval data was to detect the mangrove land cover change for that period and the use of the 2013 data was to identify the potential of Landsat OLI_TIRS for mangrove study. The final Landsat dataset archived covered all of the scene bands and metadata of each Landsat series and metadata file containing information from the Landsat data series was used.

The details of data accessing protocols using the USGS website for this study area are shown in **Figure 3.2**. The sample of Landsat data set archived and metadata are shown in the **Appendix I (A, B & C)**. The simplify of Landsat satellite data acquisition protocol are presented in this study.

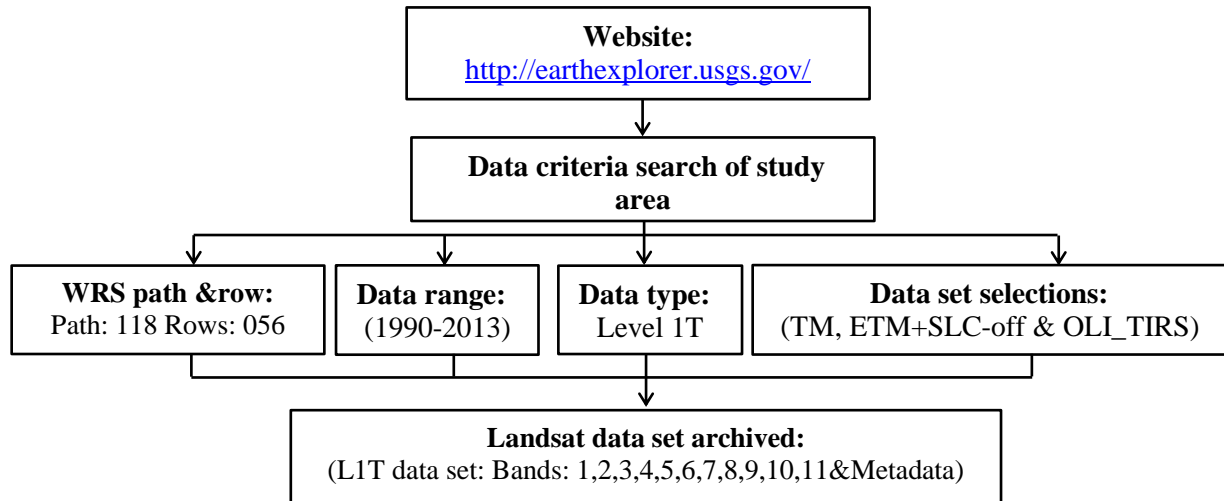


Figure 3.2 Access protocols of Landsat data series using the Earth Explorer USGS website

The data characteristics that were selected for this study were only multispectral bands with same spatial resolution (30 m), data with less cloud cover, and data accurately co-registered with Level 1 Terrain correction (L1T). The details characteristics of multispectral bands of Landsat data series are shown in the **Appendix I (D)** of this dissertation. Panchromatic and thermal bands were not selected for analysis to avoid the complexities of dealing with data at different spatial resolution.

Due to the failure of the Scan Line Corrector (SLC) in the ETM+ sensor, there were line errors in the year 2005 and year 2010 Landsat ETM+ SLC-off data. Therefore, supplementary data for both years were needed to correct the scan-line error in the image. The sample of Landsat ETM+ SLC-off showed details of the gap-filling analysis, as described in **section 3.4.2.1 (iv)**. The specifications of multi-temporal Landsat data that were used in this study are summarized in **Table 3.1**.

Table 3.1 Specifications of multi-temporal Landsat data series

Landsat series	Year	Date acquired	Date of supplementary data for interpolation	Cloud cover (%)	Multispectral bands
L4 TM	1990	19.06.1990	None	20	
L5 TM	1995	01.02.1995	None	5.25	1-5, 7
	2000	07.12.2000		13.46	
L7 ETM+ SLC-off	2005	20.02.2005	02.10.2005*	6.18 & 32.15*	
	2010	06.03.2010	13.08.2010*	9.00 & 15.86*	
L8 OLI_TIRS	2013	23.04.2013	None	11.57	2 - 7

Note: (*) represents supplementary data

(ii) Field Data and Reference Data

The reference data included mainly field data, topographic data, and vegetation maps that were used to validate the results of this study. The field survey was conducted in the study area in November 2011 and September 2013. The identified sample location was measured using GPS. A detailed topographic map and vegetation map at the scale of 1:50,000 were obtained from the Sabah Survey and Mapping Department and the Sabah Forestry Department (SFD), respectively. Secondary data of mangrove distributions in Sabah were obtained from the Sabah Forestry Department (SFD).

3.4.2 Methodology

All multi-temporal Landsat series (TM, ETM+, and OLI_TIRS) were analyzed for the data analysis. The analysis protocols involved (1) pre-processing, (2) statistical analyses, (3) classification, (4) validation, and (5) accuracy assessment. The Environment for Visualizing Images (ENVI) 4.7, 5.1 software and MS Excel 2010 were used to analyze the data. The ENVI software is an image processing system designed for multispectral and hyperspectral data analysis and information extraction.

3.4.2.1 Pre-processing Analysis

All multi-temporal Landsat data were analyzed for the pre-processing analysis. The analyses included radiometric calibration, the creation of multispectral data, subsetting analysis, gap-filling analysis, and cloud masking. The purpose of the preprocessing analysis was to normalize the data, to allow intercomparison between data, to correct the atmospheric effects, and to reduce noise. The protocols of the pre-processing analysis that were used in this study are explained below.

(i) Radiometric Calibration Analysis

The multispectral bands of TM, ETM+ SLC-off, and OLI_TIRS data were processed for the calibration analysis using ENVI software. Due to the limitations of the image processing tools in ENVI 4.7, the multispectral bands of OLI_TIRS were analyzed using the latest version of the software, ENVI 5.1. The sun elevation and acquisition date parameters from the metadata were used in this analysis.

The multispectral bands of the Landsat series were calibrated by converting the digital numbers (DN) (0–255) to absolute reflectance values (0.1–1.0). Therefore, the true reflectance value and the physical characteristics of the earth's surface could be determined and retrieved (Thomas *et al.*, 2008). The reflectance value in ENVI software was calculated using Equation 3.1:

$$\rho\lambda = \pi * L\lambda d^2 / ESUN\lambda * COS\theta_s, \quad (3.1)$$

where $\rho\lambda$ = unitless planetary reflectance

$L\lambda$ = spectral radiance

d = Earth–sun distance in astronomical units

$ESUN\lambda$ = mean solar exoatmospheric irradiance

θ_s = solar zenith angle (sun elevation angle in metadata)

(ii) Creating Multispectral Data from L1T Data

Then, the multispectral data were created by combining the single bands (1–5, 7) of the L1T datasets (**Figure 3.3**). The data were created based on the same spatial resolution (30 m) and the wavelength of the bands. However, the multispectral data of OLI_TIRS were created by combining bands 2–7, which have the same 30 m spatial resolution. The purpose of creating the multispectral data was to produce a true color composite image for visual interpretation. Therefore, the image can be used for detecting certain objects in further analysis. This analysis was performed using ENVI 4.7 software. The multispectral data of all Landsat data used in this study are shown in the **Appendix I (C)**.

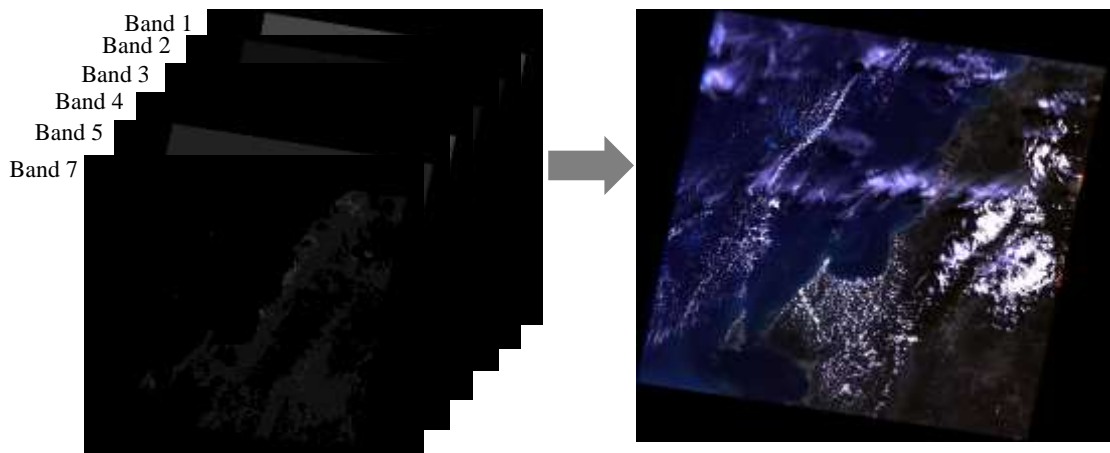


Figure 3.3 Multispectral data with true-color composite (combination of RGB bands)

(iii) Subsetting Data Analysis

The subsetting analysis was performed on all the full scene of the multi-temporal Landsat series. The purpose of this analysis was to select only the data of interest within the study area. The subsetting of data was performed using ENVI software. The study area was selected as the subset using the map coordinate system by referring to the topographic map and Google Earth (**Figure 3.4**).

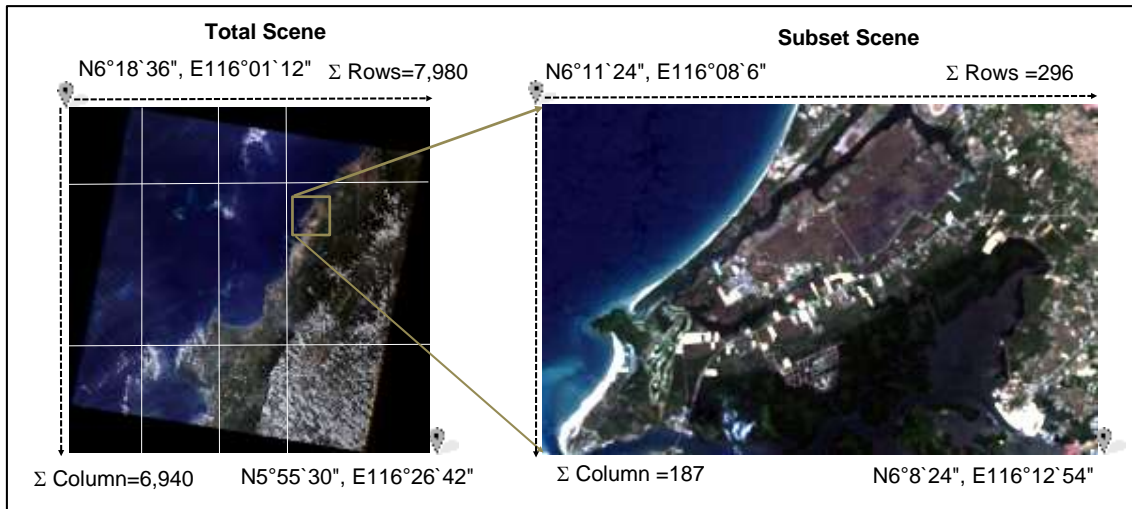


Figure 3.4 Subsetting of multispectral data using map coordinates

The total pixels of full image of Landsat series is 55,381,200. Then, after the subset analysis the total pixels of interested area is 55,352. Using this technique, we considered that all the multi-temporal data were accurately subset to the study area with the same total pixels of rows and columns. **Figure 3.5** shows the true color composite (RGB) of the multispectral subset of all multi-temporal data used in this study. Then, all the subset data were used for the further analyses.

Subset Image

1. L4 TM 19.06.1990



2. L5 TM 01.02.1995



3. L5 TM 07.12.2000



4. L7 ETM+ SLC-off 20.02.2005



5. L7 ETM+SLC-off 02.10.2005*



6. L7 ETM+SLC-off 06.03.2010



7. L7 ETM+SLC-off 13.08.2010*



8. L8 OLI_TIRS 23.08.2013



Note: (*) represents supplementary data

Figure 3.5 True-color composite (RGB) of multispectral subset data

(iv) Gap-filling Analysis of Landsat ETM+ SLC-off Data

The gap-filling analyses were processed for only the multispectral subset of ETM+ SLC-off data. As explained before, all Landsat ETM+ SLC-off data have a scan line error in the scene due to a sensor malfunction (**Figure 3.6**). Therefore, gap-filling analysis was needed to correct line errors (gaps) in the data.

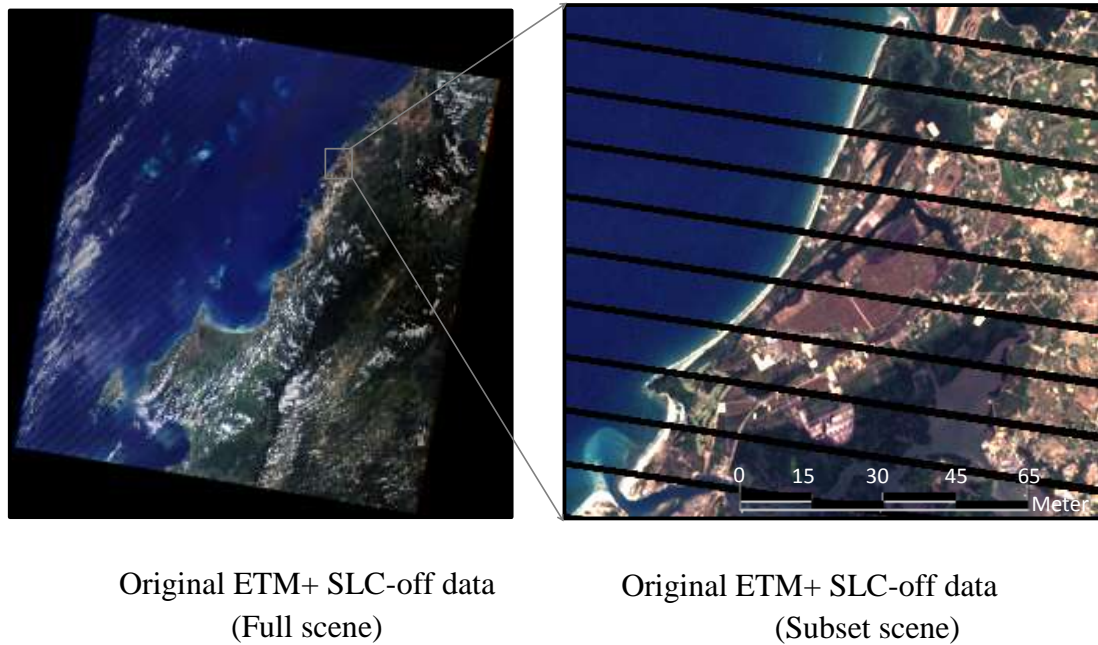
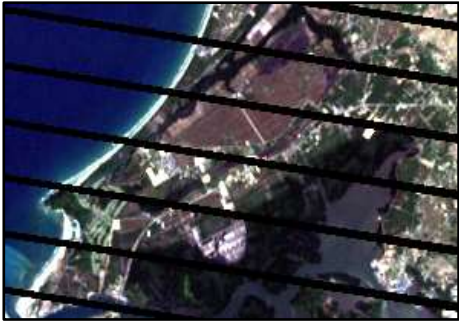





Figure 3.6 Scan line errors (gaps) in multispectral ETM+ SLC-off data

The gap-filling analysis used two forms of original data from ETM+ SLC-off. One was for the main data and the other was for the supplementary data. The main data are the data to be filled, and the supplementary data are the data used to fill. A local linear histogram method was used to fill the gaps in the SLC-off data (USGS, 2004). The criteria of the main and supplementary data were selected based on the suggestion from the USGS, which is less cloud cover and the same spatial resolution (**Table 3.2**).

Table 3.2 Specifications of ETM+ SLC-off data for gap-filling analysis

Data Specifications	Main data (Data to be filled)	Supplementary Data (Data to be fill in)
Date	20.02.2005	02.10.2005
Cloud cover (%)	6.18	32.15
		
Date	06.03.2010	13.08.2010
Cloud cover (%)	9.00	15.86
		

Gap-filling analysis was performed using Microsoft Excel 2010 and the Frame & Fill tool in ENVI 4.7 software. The output of the gap-filing analysis produced the final data of the SLC-off gap-filled data. The protocol for the gap-filling analysis included several steps, which are described below.

(a) Extraction Windows Pixel of the Main and Supplementary Data

An $n \times n$ window pixel of the main and the supplementary SLC-off data was extracted into MS Excel 2010 (**Figure 3.7**). This technique was used to scan the gap value in both

data. The 0 values represent the gap pixels of SLC-off data. Then, the gap pixels in the lines and rows of the main and supplementary data could be defined clearly. Once a gap was identified, the histogram analysis was attempted to test the quality and normality and determine a linear transformation between the two data.

0.097	0.097	0.098	0.099	0.010	0.011	0.012	0.010	0.010
0.098	0.099	0.097	0.010	0.011	0.011	0.010	0.011	0.011
0.097	0.099	0	0	0	0	0	0.010	0.010
0	0	0	0	0	0	0	0	0
0	0	0	0	0	0	0	0	0
0	0	0	0	0	0	0	0	0
0.096	0.098	0	0	0	0	0	0.099	0.098
0.095	0.011	0.010	0.010	0.011	0.099	0.099	0.098	0.090

Figure 3.7 Illustration of pixel value extraction of ETM+ SLC-off data in MS Excel

(b) Testing the Quality and Normality of ETM+ SLC-off Data

The histogram analysis was conducted on the main and supplementary data using MS Excel 2010. The purpose of the analysis was to analyze the quality of the brightness and the normality of the selected two data. An example of the histogram analysis of the main and supplementary data is presented in **Figure 3.8**. The figure shows the histogram of band 3 (red band) for both data, which indicates that there is a significant difference in brightness between the main and supplementary data. The data with high brightness value contain less cloud cover (Zhu & Woodcock, 2014). Thus, the main data that were selected in this study are good data for the gap-filling analysis. Such an analysis may be useful for testing the quality of the selected main and supplementary data .

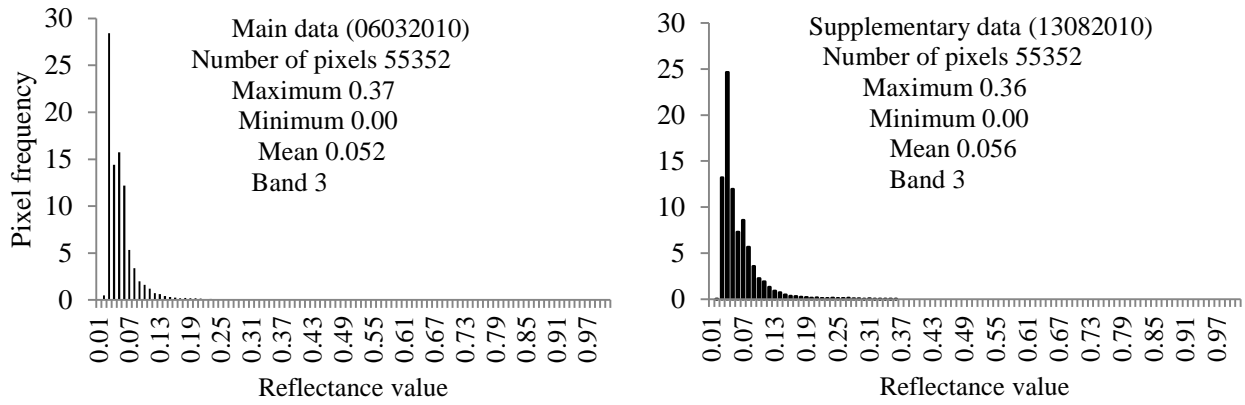


Figure 3.8 Histogram analyses of band 3 for the main and supplementary ETM+ SLC-off data

(c) Calculating the Gain and Bias of Target Pixels

Finally, the local linear histogram method was applied to predict the value of the main data pixels (USGS, 2004). A linear transformation between the main and supplementary data was performed by calculating the gain and the bias of the data. The gain and bias were calculated using the mean and standard deviation of the input and target data (Equations 3.2 and 3.3), respectively.

$$gain = \frac{\sigma_p}{\sigma_F} \tag{3.2}$$

$$bias = \mu_p - \mu_F * gain , \tag{3.3}$$

where μ_p and μ_F are the mean value of the non-gap pixels in the main and supplementary data, and σ_p and σ_F are the standard deviation of the non-gap pixels in the main and supplementary data, respectively. The result of the values was used to fill the missing pixels in the main data.

Qualitative and quantitative analyses were used to evaluate the algorithm’s performance. Using qualitative analysis, visual interpretation was applied to check the

individual bands and the color composite of the main data. The purpose of this analysis was to determine of the remaining gaps (Chen *et al.*, 2011). For the quantitative evaluation, the data were readied for classification analysis. **Figure 3.9** shows the workflow of the gap-filling analysis of ETM+ SLC-off data used in this study.

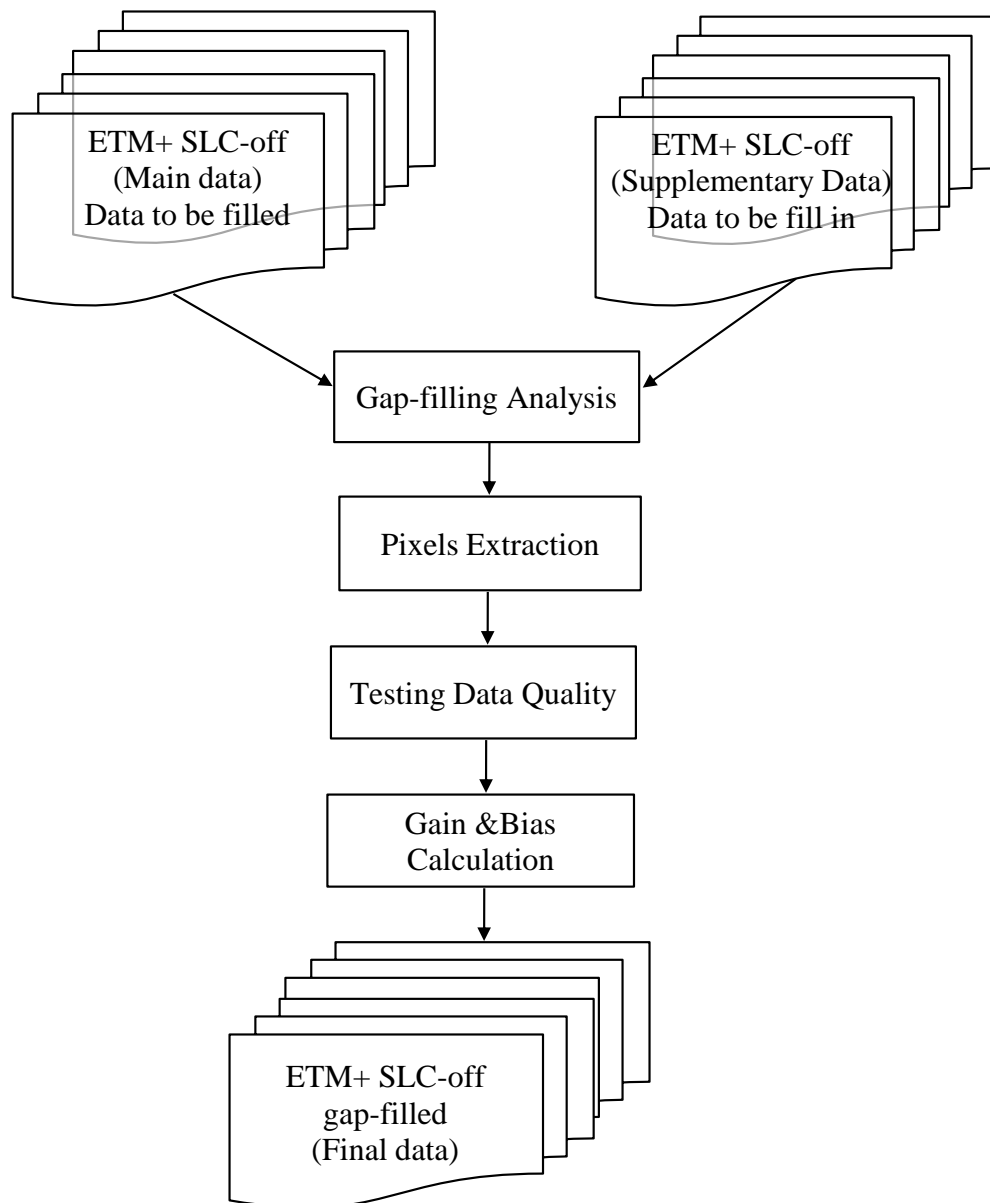


Figure 3.9 Workflow of gap-filling analysis of ETM+ SLC-off data

(v) Cloud-masking Analysis

Cloud-masking analysis was performed on all subset Landsat data using the ENVI 4.7 software. The purpose of this analysis was to confine and remove the remaining cloud cover area in the image. The remaining cloud cover was identified using the image interpretation, Google Earth tools and multi-temporal Landsat image comparisons. Firstly, the image was interpreted by true color image using band combination red, blue and green (RGB). As such, the cloud area and non-cloud area could be identified by color. For the areas in white were initially assumed to be cloud area. Next, the clear image from Google Earth was used to verify the white color features using overlay tool. The comparison of white area in the Google Earth and Landsat images verify the features either to be cloud or non-cloud area. In addition, further clarification has been done by comparing with other multi-temporal Landsat images.

Then, cloud masking technique was applied to identify white area in the images. Using the cloud-masking technique, the image consisted of two of values 1 and 0. The pixel areas covered with clouds represented in uniform area of 0 values. In addition, total pixels of cloud area were extracted using MS Excel 2010. For example, in the 2010 data, the numbers of pixels with 0 values were 150. Therefore, the remaining cloud area of interest is 0.27%. Then, the masked pixels were removed using region of interest (ROIs) tools. Detail procedures are shown in the appendix of dissertation. **Figure 3.10** shows a visual comparison of the Landsat image before and after the cloud masking and ROIs tool analysis.



(i) Before cloud-masking and ROIs (ii) After cloud-masking and ROIs

Note: Red circle with white area in (i) shows a cloud cover area of 2010 Landsat data

Figure 3.10 Visual comparisons between before and after the cloud-masking analysis of Landsat ETM+ SLC-off gap-filled data for 2010

3.4.2.2 Statistical Analysis

The multispectral subset of the Landsat data series (TM, ETM+ SLC-off, SLC-off gap-filled, and OLI_TIRS) was analyzed for statistical analysis using MS Excel 2010. The purpose of this analysis was to assess the quality of the Landsat data that were used in this study before proceeding to the classification analysis. According to Maselli (2002), it is useful to initially assess the quality of satellite data by performing statistical analysis. Thus, the data were analyzed using univariate descriptive statistics and histogram analysis.

Univariate descriptive statistics can measure unusual anomalies in satellite data, whereas histogram analysis can show the frequency of occurrence of data brightness values (Maselli, 2002). Therefore, both analyses are useful for checking the quality of the Landsat data series after pre-processing analysis. First, analyses were performed to analyze the Landsat ETM+ SLC-off and SLC-off gap-filled data. These analyses analyzed the quality of the ETM+ SLC-off data before and after the gap-filling analysis. Then, analyses were performed on the TM and OLI_TIRS data, respectively.

3.4.2.3 Classification Analyses

The multispectral subset data of the multi-temporal Landsat series (TM, ETM+ SLC-off, SLC-off gap-filled, and OLI_TIRS) were then analyzed for classification analysis. Both unsupervised and supervised classification techniques were applied in this study. The unsupervised classification technique classified the land cover classes randomly, without knowing the properties of the pixels, using the software. The K-Means unsupervised classification in the ENVI 4.7 software was applied in this study.

The supervised classification technique classified the land cover classes by forming groupings based on the properties of the pixels. Several supervised classification techniques including visual interpretation, features extraction, spectral profile, maximum likelihood, and normalized difference vegetation index (NDVI) were applied in this study. The classification analysis was performed on the data using ENVI

4.7, 5.1, and MS Excel 2010. The protocols of the unsupervised and supervised classification analyses are explained in the details below.

(i) Unsupervised Classification

a) K-Means

First, all of the multi-temporal Landsat data series were classified using K-Means unsupervised classification. In this technique, the ENVI software program automatically groups the pixels in the image into separate clusters, depending on their spectral features. Each cluster is then assigned a land cover type by the analyst (Liew, 2001).

(ii) Supervised Classification

a) Visual Interpretation and Features Extraction Technique

In the supervised classification, the analysis was started with the visual interpretation technique. The technique identifies and extracts ground features based on their tone, color, and spectral characteristics of the data. To interpret the data, a true-color image (natural color) was produced by combining of the visible bands (red, green, and blue). Then, the data could be interpreted clearly. Syed *et al.* (2001) suggested that this technique is useful as a first step in land cover classification protocols.

The elements of tone and texture were used to identify different land cover classes. Tone refers to the relative brightness or color of objects in satellite data, and it can be classified into three conditions: light, medium, or dark. Texture is the frequency of tonal change in the photographic image and can be classified as coarse, medium, or fine (Sulong *et al.*, 2002). Green color normally represents areas of vegetation, and different tones of greenness indicate different levels of vegetation types (Sulong *et al.*, 2002). The purpose of this analysis was to qualitatively classify the land cover classes into vegetation and non-vegetation areas.

b) Spectral Profile

Then, the spectral profile classification technique was used on the data. The technique quantitatively classified land cover features into vegetation and non-vegetation areas. The basic features of vegetation, soil, and water are shown via different shapes and values of reflectance spectral profile (**Fig. 3.11**). The features were collected using the collecting endmember spectra tool and were identified using the spectral library in the ENVI 4.7 software.

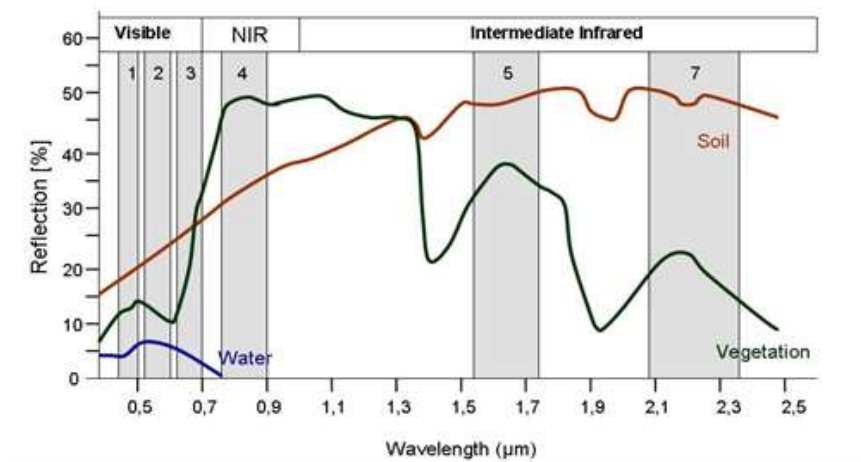


Figure 3.11 Spectral profiles of vegetation, soil, and water

The vegetation profile has low reflectance in the blue and red regions (0.45–0.60 µm) of the spectrum due to absorption by chlorophyll for photosynthesis. It has a peak in the green region (0.60–0.70 µm), in which it rises to the green color of vegetation. In the near-infrared (NIR) region, the reflectance value is much higher than in the visible band due to the cellular structures in the leaves. Therefore, the vegetation can be identified by high NIR and low visible band reflectance. The shape of this reflectance spectrum can be used for identification of vegetation types (USGS, 2004). Various shades of vegetation occur based on the types, leaf structure, moisture content, and health of the plants (Ozesmi *et al.*, 2002).

Bodies of water are generally highly reflective in the invisible spectrum. In the near-infrared and mid-infrared regions, increasing light absorption makes water darker.

However, clearer water has lower reflectance than turbid water. This characteristic depends on water depth and wavelength. Soil reflectance in satellite data is influenced by mineral composition, soil moisture, organic matter content, and soil texture (surface). Increasing soil reflectance occurs from the visible to the short-infrared bands (1.4 μm and 1.9 μm) and is related to the amount of soil moisture (USGS, 2004).

In the Landsat data, the visible spectrums of band 1 (0.45–0.52 μm), band 2 (0.45–0.60 μm), and band 3 (0.63–0.69 μm) were used to extract the water spectral signature features in the study area. Then, a combination of band 3 (0.63–0.69 μm), band 4 (0.76–0.90 μm), and band 5 (1.55–1.75 μm) was used to extract vegetation spectral reflectance. The band 3 region has a tendency for strong chlorophyll absorption, band 4 operates in the best spectral region for distinguishing varieties of vegetation, and band 5 is sensitive to the amount of water in the plants. Based on this concept, we were able to extract a variety of spectral reflectances for vegetation in the study area.

c) **Normalize Difference Vegetation Index (NDVI)**

Instead of the aforementioned classification techniques, the normalized difference vegetation index (NDVI) was applied to the data to classify vegetation and non-vegetation areas quantitatively. This technique was applied to all of the multi-temporal subset data. In addition, the technique was also applied to the SCL-off and SLC-off gap-filled data of Landsat ETM+. The purpose of this analysis was to compare the classification results between both data and determined the percentage of gap in the SLC-off data. The NDVI is a simple numerical indicator that can be used to analyze remote sensing measurements whether the target object being observed contains or does not contain live green vegetation. The NDVI was calculated based on the equation:

$$\text{NDVI} = \frac{(\text{NIR} + \text{Red})}{(\text{NIR} - \text{Red})} . \quad (3.4)$$

In the equation, *Red* and *NIR* refer to the spectral reflectance measurement acquired in the red and near-infrared wavelength, respectively. The wavelength range of

the NIR band is (750–1300 nm), whereas that of the red band is (600–700 nm). In this study, we used the spectral reflectances of bands 3 and 4 of the TM and ETM+ and those of bands 4 and 5 of OLI_TIRS, which are closely related to the wavelengths of the red and NIR bands, respectively. The range of NDVI values is from -1 to 1.

A very low value of NDVI (0.1 and below) corresponds to barren areas of rock or soil or snow. Moderate values (0.25–0.3) represent shrub and grassland areas, and high-value indices (0.5–1) indicate temperate and tropical rainforest. Bare soil is represented by NDVI values close to 0, and bodies of water are represented by negative NDVI values (Chouhan & Rao, 2011; Karaburun, 2010; Ramachandra, 2004; Xie *et al.*, 2010). Other materials, such as man-made materials, are represented by values ranging from 0.1 to 0.2. The NDVI values vary due to the absorption of red light by plant chlorophyll and the reflection of infrared radiation from water-filled leaf cells.

The NDVI analysis was performed using different NDVI threshold values (**Table 3.3**). Several threshold values were developed by using the range of NDVI values (-1 to 1) to classify the land cover classes in the study area. The analysis was performed using the conditional formatting in MS Excel 2010. Then, the spectral profile technique was re-applied to confirm the spectral reflectance of each class. The mean spectral signature of each class was examined to assess the relevancy of the classification. After completing the classification procedure, the results were assessed for accuracy.

Table 3.3 Classes of NDVI land cover

No.	Threshold value			Classes
(i)	Min value	\leq NDVI <	0	Class 1
(ii)	0	\leq NDVI <	0.1	Class 2
(iii)	0.1	\leq NDVI <	0.25	Class 3
(iv)	0.25	\leq NDVI <	0.35	Class 4
(v)	0.35	\leq NDVI <	0.5	Class 5
(vi)	0.5	\leq NDVI <	Max value	Class 6

d) Maximum Likelihood

The supervised classification maximum likelihood technique was performed on the data. The maximum likelihood classification technique assumes that the statistics for each class in each band are normally distributed and calculates the probability of a given pixel that belongs to a specific class (Richard, 1999). The analysis was performed using the ENVI software. However, the numbers of classes were identified according to the visual interpretations, spectral profile analysis, and region of interest (ROI) techniques that were utilized before. The ROI was applied to extract the statistics for the classification.

3.4.2.4 Validations

Validations were performed on the classification results of the satellite data using the field survey data, topographic map, vegetation map, and Google Earth.

(i) Field Survey

Field surveying was conducted to validate the classification analysis performed by using the satellite data and remote sensing techniques. The surveys were conducted in November 2011 and September 2013. The first survey was conducted from November

4–December 25, 2011 (52 days). In the first field survey, a site visit was conducted to survey the real condition of the study area.

During the site visit, the preliminary classification results of the satellite data were used for validation of the land cover classes. Fifteen points were selected to “ground-truth” the preliminary classification results (**Figure 3.12**). The coordinates of each point were recorded using GPS (Garmin GPSMAP 60CSX). At each point, a quadrat within a 30 m × 30 m area, six transects were placed parallel to each other and 5 m apart.

In addition, a field photo was acquired at each point using a digital camera (Canon Power Shoot SX710 HS). The second field survey was conducted from September 13–30, 2013 (18 days). The second field survey was conducted in order to validate the classification result of Landsat OLI_TIRS 2013 (new satellite data). The same field survey procedures used in the first sampling were performed in this survey.

The quadrat survey, transects, and photo transect were re-applied in the second field survey. Unconfirmed classification results such as shrimp pond area, built-up area, and grassland were confirmed using the field survey data. During the second field survey, we also visited and joined the mangrove replanting project conducted by the Kota Kinabalu Wetland Centre. The replanting project was conducted in degraded mangrove areas, such as in-active shrimp pond areas. The details of the field survey activities and photographs are shown in **Appendix IV (A & B)**.



Figure 3.12 Ground-truth points and field photographs of selected points

(ii) Topographic and Vegetation Maps

A detailed topographic map and vegetation map at the scale of 1:50,000 (published in 1990 and 2009) were obtained from the Sabah Survey and Mapping Department and the Sabah Forestry Department (SFD), respectively. Both of these data were used to validate and confirm the land cover classes in the classification map of satellite data. A sample of the topographic map of the study area is shown in **Appendix IV (C)**.

(iii) Google Earth

Google Earth validation was applied during the conducting of the classification analysis in order to confirm roughly any unclear land cover classes. The details of the classification protocols used in this study are presented in **Figure 3.13**.

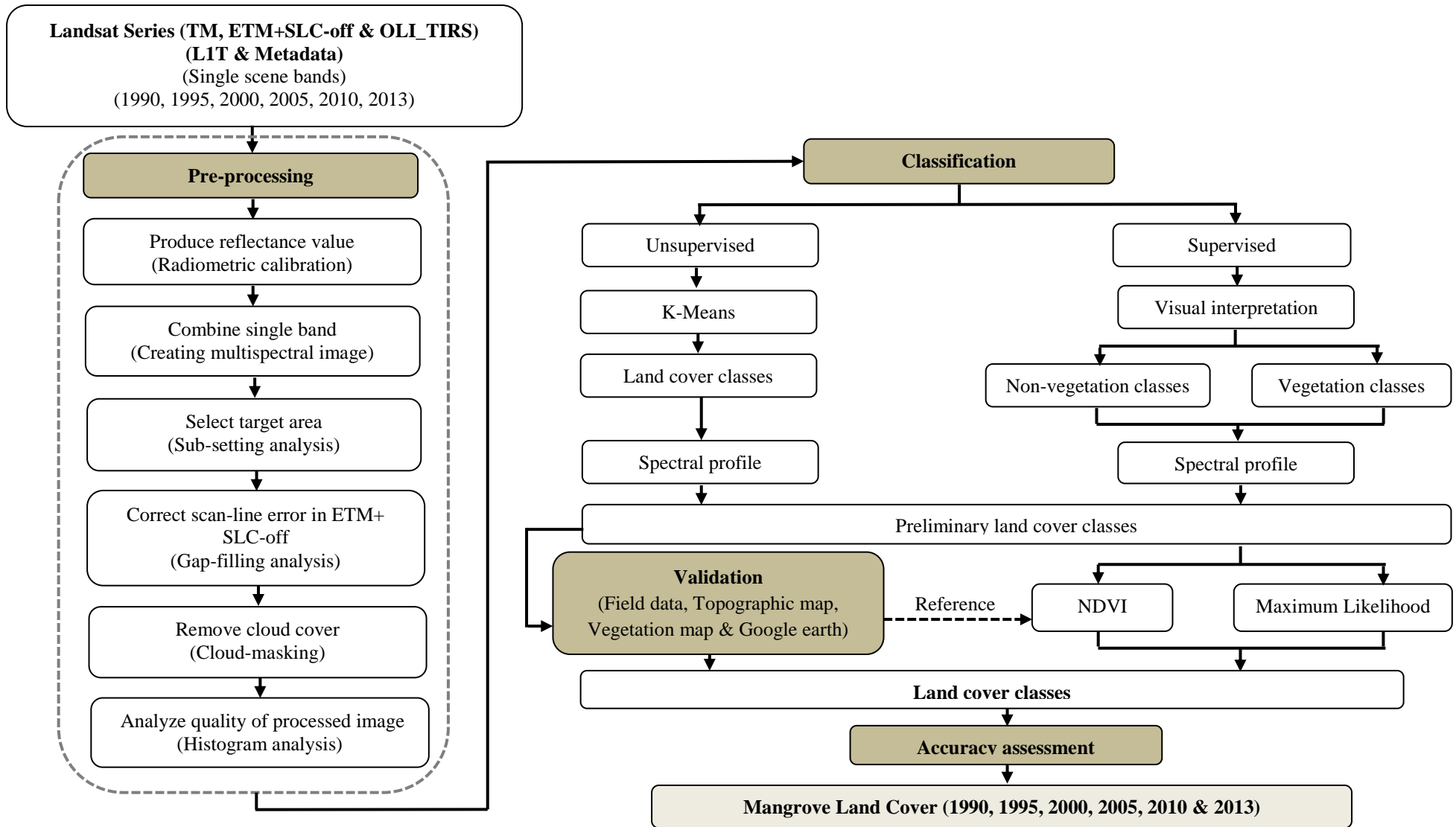


Figure 3.13 Classification protocols of mangrove forest land cover in Sabah using Landsat data series

3.4.2.5 Accuracy Assessment

The land cover classification maps from the satellite data were further subjected to accuracy assessment. The analysis was performed using ENVI 4.7 software. The purpose of the analysis was to demonstrate the accuracy of a classification result by comparing the classification result with ground-truth information. In this study, the confusion matrix method integrated with ground-truth data that were obtained from the field survey, a topographic map, Google Earth and region of interest (ROIs) tools were used for the accuracy analysis.

The confusion matrix is calculated by comparing the location and class of each ground-truth pixel with the corresponding location and class in the classification image. Each column of the confusion matrix represents a ground-truth class and, the values in the column correspond to the classification image's labeling of the ground-truth pixels.

The confusion matrix was performed with the NDVI and maximum likelihood classification results. Then, the total accuracy of each classification can be derived from the confusion matrix table by counting how many pixels were classified the same in the satellite data and on the ground and dividing this by the total number of pixels. In addition, the kappa coefficient also measured the agreement between classification and ground-truth pixels. The kappa (k) coefficient was calculated based on the equation:

$$k = \frac{N \sum_{i=1}^n m_{i,i} - \sum_{i=1}^n (G_i C_i)}{N^2 - \sum_{i=1}^n (G_i C_i)}$$

Where,

i is the class number

N is the total number of classified pixel that are being compared to ground truth

$m_{i,i}$ is the number of pixels belonging to the ground truth class i

C_i is the total number of classified pixels belonging to class i

G_i is the total number of ground truth pixels belonging to class i

3.5 Results and Discussion

The first section of this part of the dissertation (**Section 3.5.1**) discusses the quality assessment of the processed Landsat series that were produced using the developed protocol of this study. The discussion focuses on the results of the correction of the scan-line error in the ETM+ SLC-off data. Then, the following section (**Section 3.5.2**), discusses the classification result of the Mengkabong mangrove from the multi-temporal Landsat series used.

3.5.1 Quality Assessment of Processed Landsat Data Series (TM, ETM+, and OLI_TIRS)

An assessment of the quality of the processed Landsat data series can be defined clearly based on the values of univariate descriptive statistics (min, max, mean, and standard deviation) (Masselli, 2002). The quality of the Landsat ETM+ SLC-off data before and after the gap-filling analysis showed a significant difference in Min values. **Table 3.4** presents the Min values of all bands of Landsat ETM+ SLC-off before and after the gap-filling analysis.

Table 3.4 Min value of Landsat data ETM+ SLC-off and ETM+ SLC-off gap-filled data

Band	Min value					
Date	Blue	Green	Red	NIR	SWIR1	SWIR2
20.02.2005 ETM+ SLC-off Original (main)	0.00	0.00	0.00	0.00	0.00	0.00
02.10.2005 ETM+ SLC-off Original (supplementary)	0.00	0.00	0.00	0.00	0.00	0.00
20.02.2005 ETM+ SLC-off Final (gap-filled)	0.07	0.05	0.04	0.02	0.02	0.03
13.08.2010 ETM+ SLC-off Original (main)	0.00	0.00	0.00	0.00	0.00	0.00
06.03.2010 ETM+ SLC-off Original (supplementary)	0.00	0.00	0.00	0.00	0.00	0.00
13.08.2010 ETM+ SLC-off Final (gap-filled)	0.07	0.03	0.02	0.03	0.03	0.02

The values before and after the analysis were recorded at (0.00) and (0.05–0.09), respectively. The 0.00 value in the original ETM+ SLC-off data represents the gap-data value. This result could confirm the efficiency of the gap-filling method that was applied in this study. A study by Singh and Sherman (2010) suggested that the original data of ETM+ SLC-off need to be analyzed by gap-filling analysis before proceeding to classification analysis. The selection of an appropriate gap-filling analysis should produce a good spatial result of ETM+ SLC-off data (Singh & Sherman, 2010).

Figure 3.14 shows images of the main and supplementary data before the gap filling and the final data after the gap-filling analysis. The final data show that the gaps in the main data of ETM+ SLC-off were filled very well. Despite the SLC failure in Landsat 7, ETM+ is very applicable for many applications (Biro *et al.*, 2013; Chander *et al.*, 2010; Roy *et al.*, 2010), especially in natural resources.

Therefore, it is very important to apply and evaluate different methods to fill in the gaps of these data (Zhang *et al.*, 2013). The strengths of the gap-fill algorithm are that it is able to improve the spatial continuity of the filled results and that it is easy to use (Mohammady *et al.*, 2013; Pringle *et al.*, 2009; USGS, 2004).

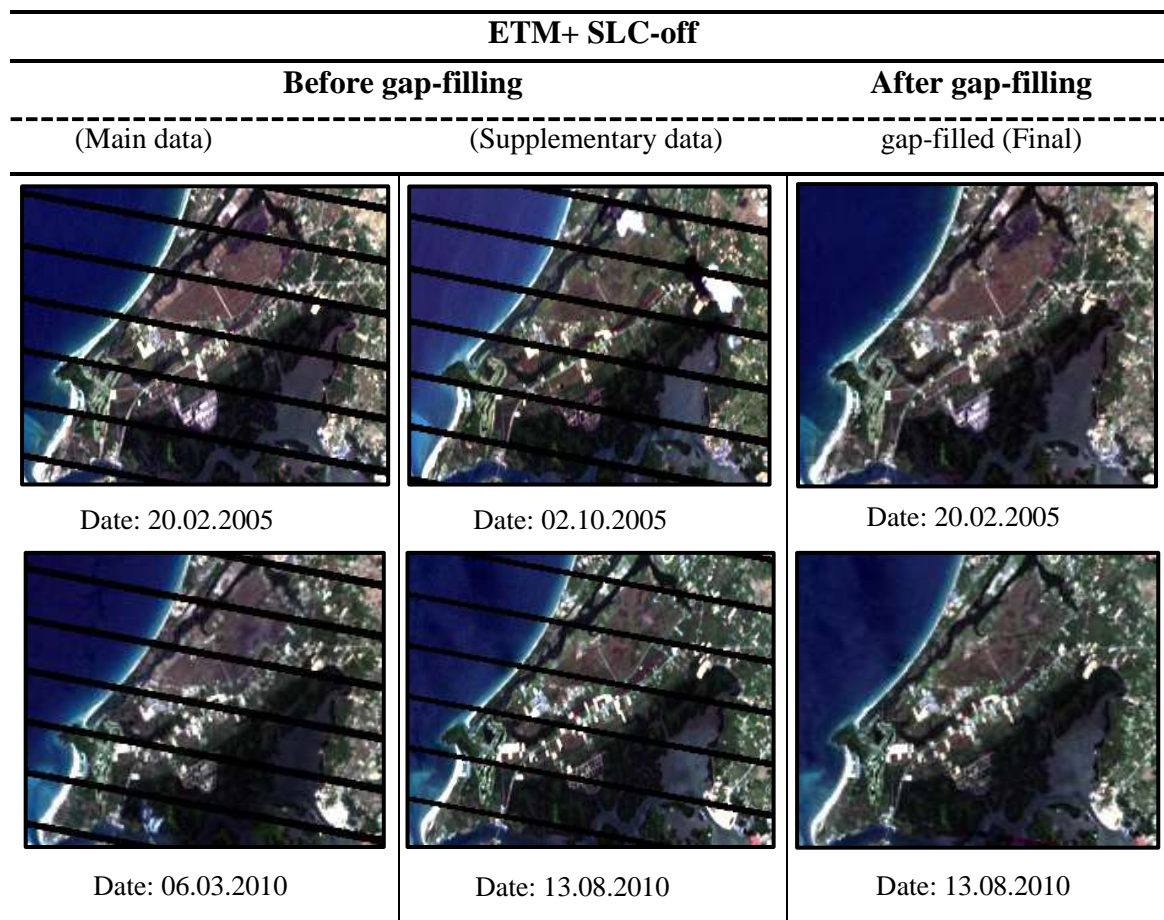


Figure 3.14 Comparison quality color composite of ETM+ SLC-off data before and after the gap-filling process

For further quantitative evaluation, the Landsat ETM+ SLC-off gap-filled data with the classification analyses were compared to the other Landsat data series. In addition, according to Maselli (2002), it may be useful to initially assess the quality of satellite data by performing a statistical analysis. The Min values of all Landsat data series (TM, ETM+, and OLI_TIRS) are presented in the **Table 3.5**. Based on these results, the Min values of all data (TM, ETM+ SLC-off gap-filled, and OLI_TIRS) were not very different. This result reconfirms that the ETM+ SLC-off gap-filling produced good ETM+ SLC-off data.

Table 3.5 Min value of all Landsat data series (TM, ETM+, and OLI_TIRS)

Band	Min value					
Date	Blue	Green	Red	NIR	SWIR1	SWIR2
19.06.1990 TM	0.07	0.05	0.03	0.02	0.02	0.02
01.02.1995 TM	0.07	0.05	0.03	0.02	0.02	0.02
07.12.2000 TM	0.09	0.07	0.04	0.02	0.03	0.03
20.02.2005 ETM+ SLC-off gap-filled	0.07	0.05	0.04	0.02	0.03	0.03
13.08.2010 ETM+ SLC-off gap-filled	0.07	0.05	0.02	0.03	0.00	0.02
23.04.2013 OLI_TIRS	0.07	0.05	0.04	0.02	0.01	0.01

3.5.2 Classification of Mengkabong Mangrove Forest Land Cover using Multi-temporal Landsat Data Series

This study utilized ground-truth data to evaluate the classified mangrove forest obtained from the Landsat data series (TM, ETM+ SLC-off, and OLI_TIRS). Field validation, the topographic map, and visual assessment through Google Earth were used as references to check the accuracy of the classified data. The classification results revealed six land cover classes in the Mengkabong area. The classes were open water area, bare soil, grassland, secondary forest, built-up area, and mangrove area. The details of the classification results are explained in the following.

(i) Visual Interpretation Classification

The visual interpretation technique was able to classify six land cover classes in the Landsat satellite data. This technique extracted the ground features in the satellite data based on tone, color, and spectral characteristics. Initially, this technique classified the Mengkabong land cover into two classes, vegetation area and non-vegetation area. Then, the differences of green color tone (dark green, medium green, and light green) and different textures represented the three different types of vegetation in the study area. The non-vegetation class areas were represented by color difference, such as dark blue,

dark brown, and light yellow. **Table 3.6** shows the land cover class results acquired by using the visual interpretation technique.

The result of this study is supported by the findings of previous studies. A study by Sulong *et al.* (2002) confirmed that the green color normally represents vegetated areas and that the different tones of greenness show different levels of vegetation types. Dark-blue color and fine texture normally represent water area, and dark-brown color and coarse texture normally represent different types of soil area. Light-yellow color normally represents degraded area or built-up area (USGS, 2004). However, the detailed feature extractions of the land cover classes were identified and confirmed based on the spectral profile technique.

Table 3.6 Land cover classes by visual interpretation technique

Vegetation Area	Data characteristics of vegetation area	Non-Vegetation Area	Data characteristics of non-vegetation area
Vegetation 1	Dark green & coarse texture	Non-Vegetation 1	Dark blue & fine texture
Vegetation 2	Medium green & coarse texture	Non-Vegetation 2	Dark brown & coarse texture
Vegetation 3	Light green & medium texture	Non-Vegetation 3	Light yellow & coarse texture

(ii) Spectral Profile Classification

The spectral profile technique is useful for identifying specific features in satellite data. **Figure 3.15** shows the spectral profile classification result of the Mengkabong area. The different spectral profiles of the vegetation cover in this study area presented three different classes of vegetation type. The different spectral profiles of vegetation were defined clearly based on the different reflectance values in band 3 and band 4. The band 3 region is sensitive to strong chlorophyll absorption, and the band 4 region shows different cellular structures.

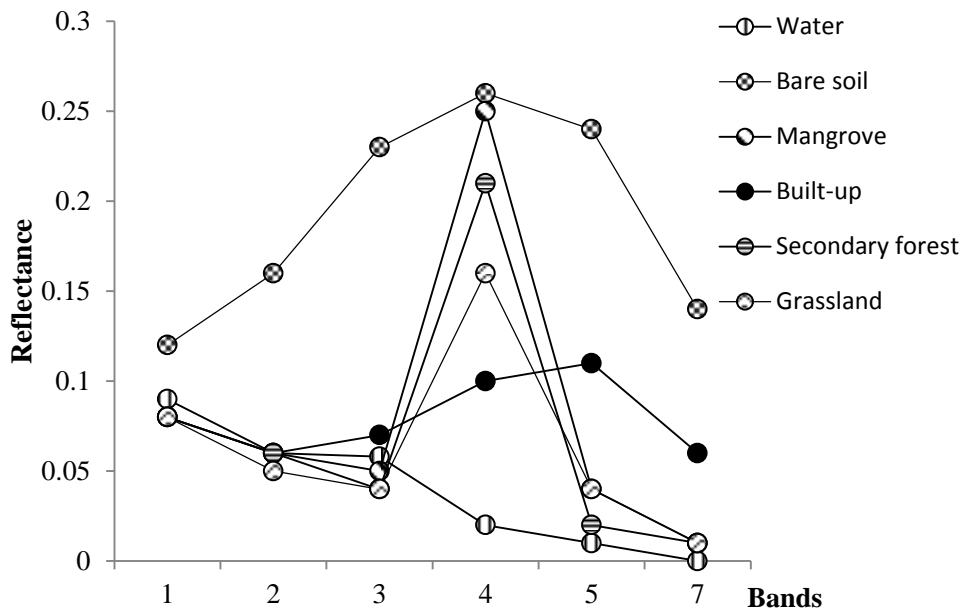


Figure 3.15 Spectral profile of Mengkabong land cover classes

The mangrove and secondary forest showed high reflectance value in band 4 with values of 0.26 and 0.21, respectively, while the grassland showed a low reflectance value of only 0.16. This may be an effect of the water moisture contents in the vegetation. The mangrove has high water moisture content compared to the other classes of vegetation. According to Rahman *et al.* (2013), the different water contents in the vegetation are revealed in the different spectral profiles of the vegetation covers.

The non-vegetation classes such as water, bare soil, and built-up areas also showed clearly different spectral profiles. Water area showed a high reflectance value of 0.09 in band 1 (blue band). According to the USGS (2004), bodies of water generally have high reflectance in the visible spectrum and low reflectance in the near-infrared spectrum. Bare soil and built-up areas could be defined clearly based on the differences in their reflectance values in the visible and near-infrared bands. The different spectral profiles of both classes were supported by previous studies (USGS, 2004). The field photographs shown in **Figure 3.16** clearly show the correlation between the spectral profile in the satellite data and the same coordinate of the point field survey

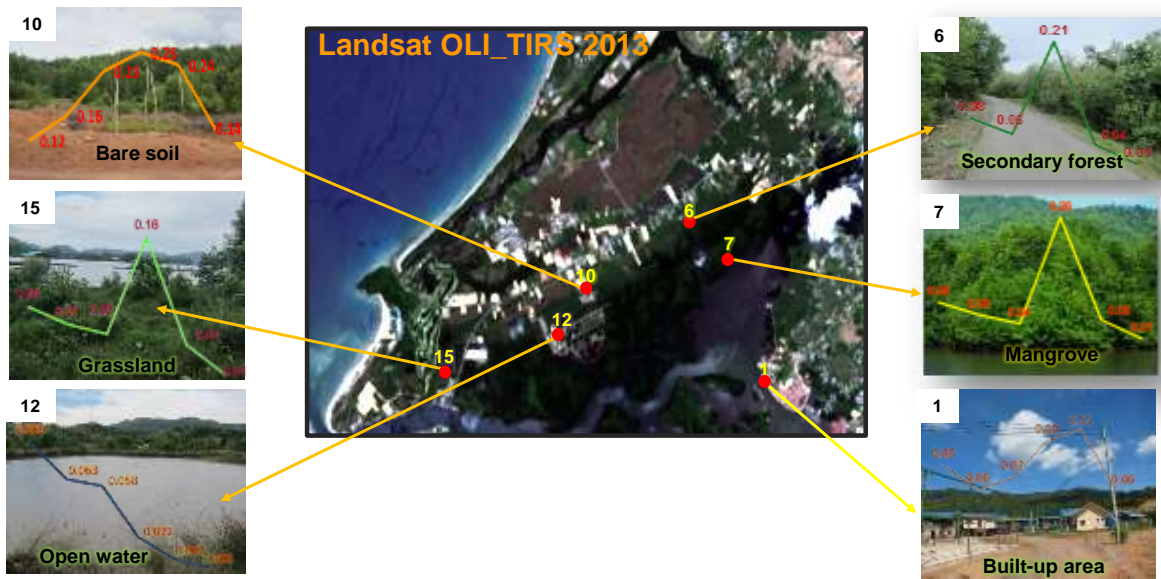


Figure 3.16 Spectral profile features of each class integrated with satellite data and field photographs with selected points of field survey

(iii) Normalized Difference Vegetation Index (NDVI) Classification

Figure 3.17 shows the result of the NDVI classification in the Mengkabong area quantitatively. Six land cover classes were classified significantly with an accuracy of 89.2%.

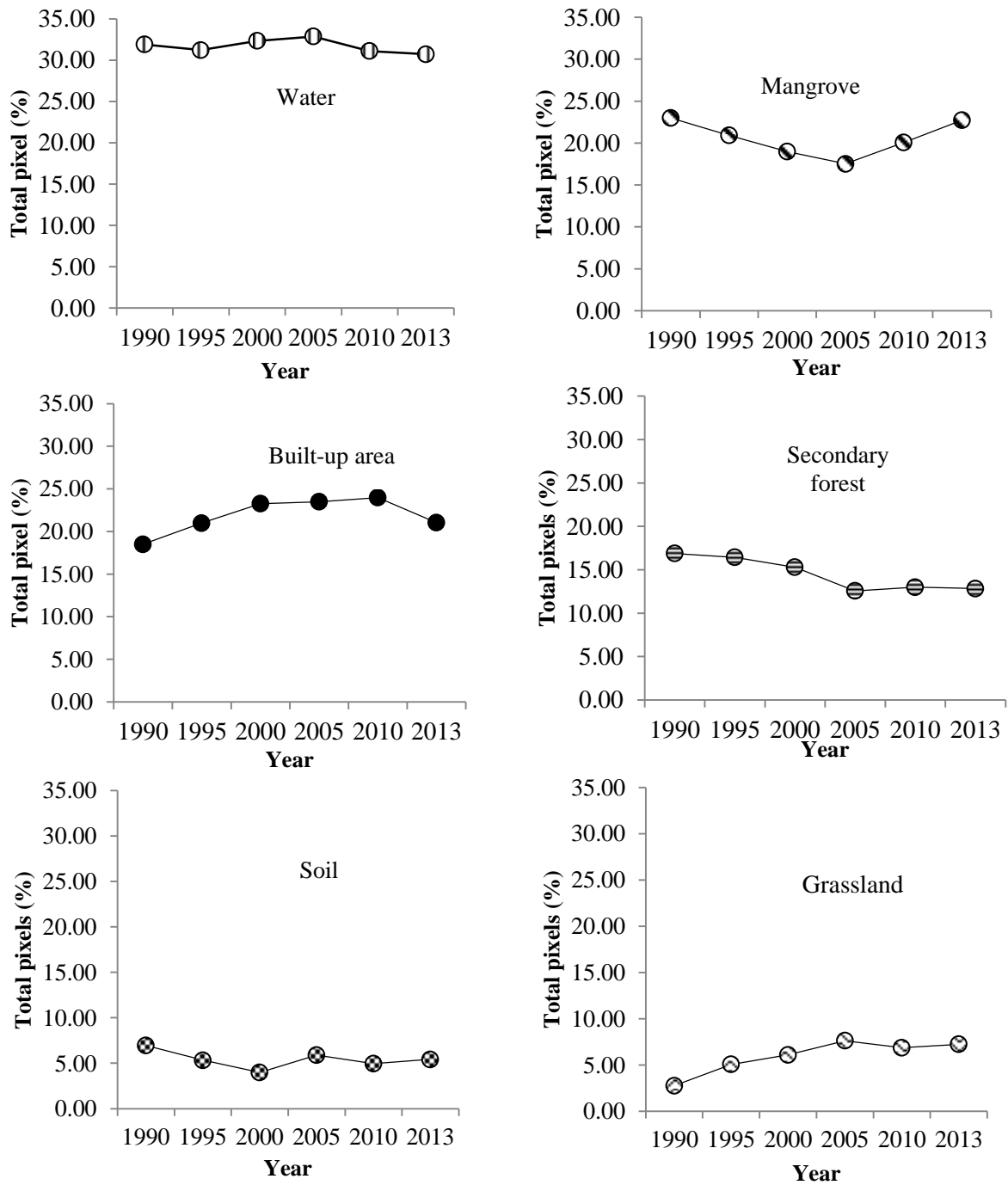


Figure 3.17 Mengkabong land cover classes for NDVI classification

The water area showed the highest total pixel distribution, almost 35%, compared to the other classes. The mangrove area showed the second highest total pixel distribution in 1990 and 2013, with 23% and 20%, respectively. However, it showed a significant decrease from 2000 to 2005 of 15% to 12%. This may be an effect of deforestation activities in the Mengkabong area. The result of this study is supported by the report of the Sabah Forestry Department released in 2010. According to this report, the decreasing mangrove forest in this area was affected by aquaculture and house settlement activities. Aquaculture activities, such as shrimp pond farming, had been conducted extensively since the year 2000.

The NDVI classification technique classified the Mengkabong area based on the differences of NDVI value. A negative NDVI value (<0) represented water areas, whereas a value from 0 to 0.1 represented bare soil area. A value from 0.1–0.24 represented built-up areas. This NDVI value threshold of non-vegetation areas is supported by the results of previous studies (Chouhan & Rao, 2004; Karaburun, 2010; Ramachandra & Kumar, 2004; Xie *et al.*, 2010).

The vegetation areas of grassland, secondary forest, and mangrove were classified using the values ($0.25 \leq \text{NDVI} < 0.35$), ($0.35 \leq \text{NDVI} < 0.5$), and ($0.5 \leq \text{NDVI} < 1.0$), respectively. The grassland in this study area was classified based on its sparse vegetation or medium vegetation value (Chouhan & Rao, 2004), whereas the secondary forest and mangrove area were classified based on the density of the vegetation value (Chouhan & Rao, 2004; Karaburun, 2010; Ramachandra & Kumar, 2004).

The mangrove in the Mengkabong area showed high NDVI values from 0.5 to 0.85. This result is also supported by previous studies. A study by John and David (1999) found that the standard of high NDVI value is 0.4 to 1 and that it corresponds to the density of vegetated area. According to the Sabah Forestry Department (2010), the Mengkabong mangrove forest is dominated by *Rhizophora apiculata*, which is a healthy and dense mangrove species. The NDVI threshold for vegetated area in this study is almost similar to the results of previously conducted studies (Karaburun, 2010; Ramachandra, 2004; Xie *et al.*, 2010).

The NDVI classification result is useful for determining the production of green vegetation as well as for detecting vegetation changes. The results of the NDVI classification were supported by the topographic map and by Google Earth, which showed significant improvement. Furthermore, the use of OLI_TIRS data with a combination of multispectral bands (2–7) produced good land cover classes. The NDVI classification result of the OLI_TIRS data showed almost the same percentages of land cover classifications as the ETM+ and TM data result.

The selection of same spectral wavelength as the TM and ETM+ data produced a significant classification result. OLI_TIRS is new data that has the additional band numbers of 1, 8, 9, 10, and 11, which is a bit different in band order compared to ETM+ and TM data (USGS, 2013). However, the selection of the same spectral wavelength as used for TM and ETM+ is suggested to be the best option for using OLI_TIRS data for mangrove forest land cover classification. In addition, the results of the NDVI classification of the Landsat ETM+ SLC-off and the SLC-off gap-filled data showed a significant difference between both data (**Figure 3.18**).

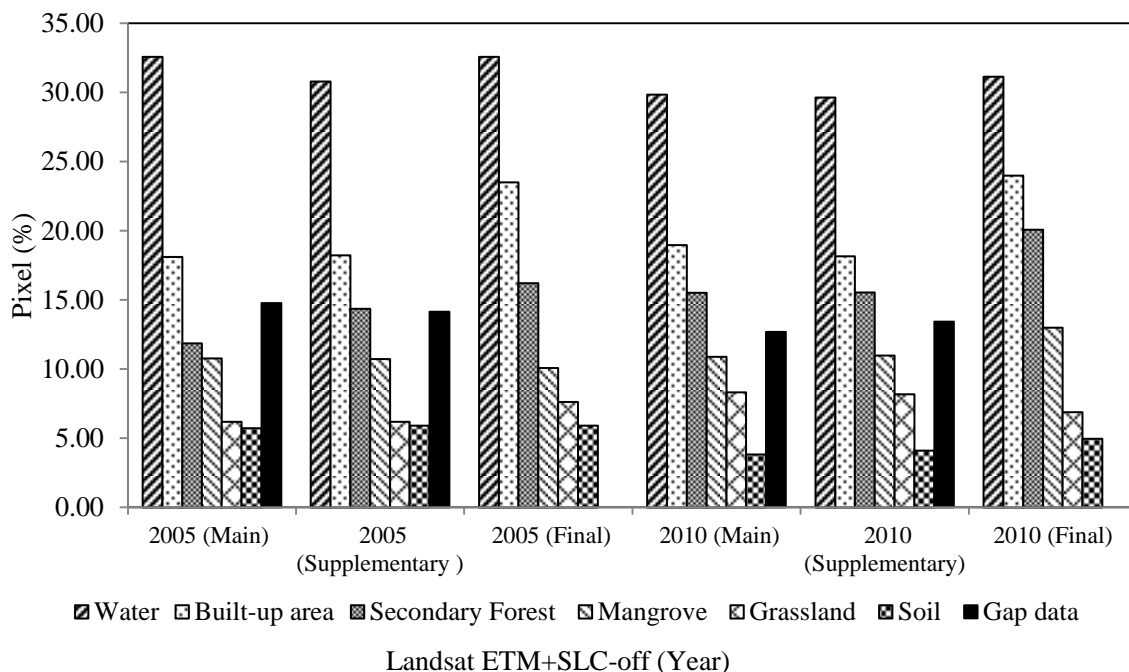


Figure 3.18 NDVI land cover classes of ETM+ SLC-off and ETM+SLC-off gap filled data

The result showed that the percentages of land cover areas in the SLC-off and SLC-off gap-filled data were very comparable. The gap values in the SLC-off data were identified clearly by MS Excel 2010. About 15% of the gap data of all SLC-off data were missing. The results of the NDVI classification in this study provide a quantitative evaluation of the potential of both data for classifying in the Mengkabong area. The results of this study are supported by the previous study of Singh and Sherman (2010), which indicated that there are significant differences in land cover classification between SLC-off and SLC-off gap-filled data.

Table 3.7 shows the total area of Mengkabong land cover classes according to the NDVI classification. Based on the result, the mangrove area decreased significantly from 1990 to 2005, from 1145.16 ha to 827.73 ha. The mangrove area also decreased significantly from 2000 to 2005, from 945.63 ha to 827.73 ha. As discussed above, the decrease of mangrove area in the Mengkabong area was affected by deforestation activities such shrimp pond farming and house construction. Furthermore, the increase of water area from the year 2000 to the year 2005, from 1611.81 ha to 1638.09 ha, may be an effect of the increased opening of shrimp pond areas.

Table 3.7 NDVI classification of Landsat data series of Mengkabong mangrove forest area

Multi-Temporal Landsat Data	Land cover classes (ha)					
	Water	Mangrove	Built-up area	Secondary Forest	Soil	Grassland
1990	1589.94	1145.16	921.33	840.87	346.41	137.97
1995	1556.10	1042.11	1045.53	818.82	266.13	252.99
2000	1611.81	945.63	1159.11	762.12	198.81	304.20
2005	1638.09	827.73	1170.45	626.40	293.85	380.16
2010	1550.34	999.72	1194.21	647.64	247.23	342.54
2013	1530.90	1131.93	1048.41	639.09	270.45	360.90

However, the mangrove area was significantly larger in 2013 at 1131.93 ha. The increased mangrove area may be an effect of mangrove replanting and restoration projects. Such a project has been conducted extensively by the Sabah Forestry Department and the Kota Kinabalu Sabah Wetland Centre since 2010. **Table 3.8** shows the error matrices of the accuracy assessment of the NDVI classification for the 13 years of data and their corresponding kappa values.

Table 3.8 Error matrix of NDVI classification for 23 years of data

Classified Data		Reference Data		Total Accuracy (%)	Kappa Coefficient
		Non-Mangrove	Mangrove		
TM 1990	Non-Mangrove	218	32	81	0.62
	Mangrove	63	187		
TM 1995	Non-Mangrove	215	35	84.4	0.69
	Mangrove	43	207		
TM 2000	Non-Mangrove	224	26	87.2	0.74
	Mangrove	38	212		
ETM+ 2005	Non-Mangrove	228	22	89.2	0.78
	Mangrove	32	218		
ETM+ 2010	Non-Mangrove	230	20	88.8	0.77
	Mangrove	36	214		
OLI- TIRS 2013	Non-Mangrove	238	12	87.6	0.75
	Mangrove	50	200		

Note: Total accuracy and kappa coefficient calculations can be referred to the accuracy assessment analysis in the **Section 3.4.2.5**

(iv) Maximum Likelihood Classification

Similar to the NDVI and spectral profile classification results, the maximum likelihood method also produced six land cover classes in the Mengkabong area. The six land cover classes were open water, bare soil, grassland, secondary forest, built-up, and mangrove areas. In the maximum likelihood classification, the land covers were classified based on the normally distributed statistics of each class in each band and calculated by the probability of a given pixel belonging to a specific class (Richard, 1999). Initially, the numbers of classes were identified using the visual interpretation

technique, spectral profile analysis, and the region of interest (ROI). The ROI was applied to extract the statistics for each class of land cover. This classification protocol was promoted to obtain a high accuracy of classification results in the Mengkabong area, almost 90% accuracy in this study.

Table 3.9 shows the total area of Mengkabong land cover classes from the maximum likelihood classification. The mangrove land cover area also showed significant change from 1990 to 2005, decreasing from 1145.16 ha to 872.82 ha. As discussed in the previous sections, aquaculture activities such as shrimp pond farming led to the decrease of mangrove forest in the Mengkabong area. In addition, an increase of water pixels from 2000 to 2005, 1611.81 ha to 1638.45 ha, supported the conversion of mangrove area to shrimp pond farming. However, mangrove forest cover increased by almost 19% from 2010 to 2013. Within these four years, the mangrove forest area in Mengkabong increased continuously due to mangrove replanting project activity.

Table 3.9 Total area of land cover classes by maximum likelihood classification

Multi-Temporal Landsat Data	Land cover classes (ha)					
	Water	Mangrove	Built-up area	Secondary Forest	Soil	Grassland
1990	1584.45	1145.16	921.42	846.90	346.50	137.25
1995	1555.74	1042.20	1037.34	826.20	267.30	252.9
2000	1611.81	945.72	1142.19	780.12	198.72	303.12
2005	1638.45	872.82	1186.83	627.21	275.85	380.52
2010	1549.80	997.20	1327.41	518.40	246.33	342.54
2013	1536.84	1185.12	1048.50	499.14	270.54	441.54

According to the SFD (2012), this project was implemented due to the decreasing mangrove area around Sabah. The data at five-year intervals clearly showed

that the land cover in the Mengkabong area had changed (**Figure 3.19**). The multi-temporal Landsat data series used in this study were useful for detecting the land cover changes, especially in the mangrove forest area. The studies by Zhang *et al.* (2003) and Green *et al.* (1999) also suggested the usefulness of multi-temporal Landsat data for mangrove studies.

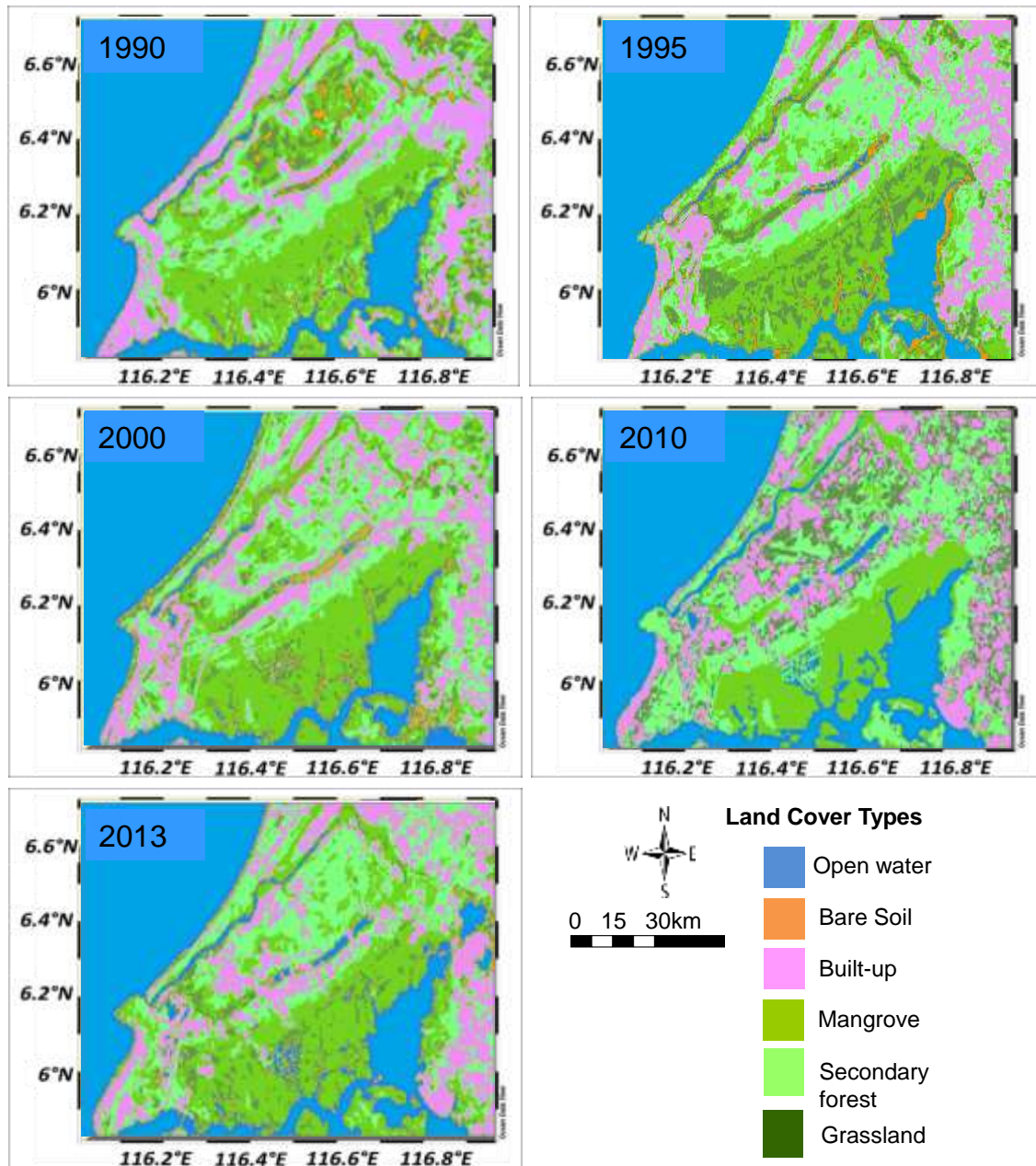


Figure 3.19 Land cover classifications in Mengkabong area from 1990–2013

Table 3.10 shows the classification accuracy of the maximum likelihood classification for the 13 years of data. The error matrix result shows the high accuracy (>80%) of all the data used for mangrove classification using the maximum likelihood method with low-cost satellite data.

Table 3.10 Error matrix of maximum likelihood classification for 23 years of data

Classified Data		Reference Data		Total Accuracy (%)	Kappa Coefficient
		Non-Mangrove	Mangrove		
TM	Non-Mangrove	220	30	79.6	0.59
1990	Mangrove	72	178		
TM	Non-Mangrove	218	32	80	0.60
1995	Mangrove	68	182		
TM	Non-Mangrove	224	26	77.6	0.55
2000	Mangrove	86	164		
ETM+	Non-Mangrove	216	34	80.4	0.61
2005	Mangrove	64	186		
ETM+	Non-Mangrove	228	22	89.2	0.78
2010	Mangrove	32	218		
OLI-	Non-Mangrove	208	42	80.4	0.61
TIRS	Mangrove	56	194		
2013					

Note: Total accuracy and kappa coefficient calculations can be referred to the accuracy assessment analysis in the **Section 3.4.2.5**

3.6 Summary

This study successfully developed and applied processed Landsat data series (TM, ETM+, and OLI_TIRS) using the proposed standard protocol. The processed Landsat data series have great potential for classifying the mangrove forest land cover in the Mengkabong area. The gap-filling processing used in this study produced good results for ETM+ gap-filled data. The NDVI and maximum likelihood classification techniques that were applied to all the processed Landsat data series (TM, ETM+, and OLI_TIRS) showed a good result of land cover classification. However, there are still several limitations and challenges in the interpretation of mangrove when using any of these conventional methods. Thus, recent advanced classification techniques should be

applied to the processed Landsat data series for further validation. These recommendations are applied in the next chapter of this thesis.

Chapter 4

Machine Learning Approach in Mengkabong Mangrove Forest Land Cover Classification

4.1 Introduction

Machine learning techniques have been used widely in remote sensing applications related to wetlands research (Colstoun *et al.*, 2003; Horssen *et al.*, 2002; Huang & Jensen, 1997). Recent research has demonstrated that decision-tree learning, one of the most popular machine learning approaches, may be accurate and efficient for land cover classification based on remotely sensed data (Li *et al.*, 2010).

A decision-tree learning algorithm is able to create classification rules directly from the training data without human intervention. In addition, unlike many other statistical analysis approaches, such as maximum likelihood classification, the decision-tree technique does not depend on assumptions of value distribution or the independence of variables (Quinlan, 1993). This is important for incorporating ancillary GIS data because these data usually have various value distributions and may be highly correlated (Jensen, 2005).

Rule sets may be applied to the classification of multi-temporal images after they have been acquired from the decision-tree learning. Using identical rule sets can ensure that the classification results are comparable between different temporal images, which should be more advantageous than using traditional methods for monitoring the changes of mangrove forest from time series of remote sensing data (Colstoun *et al.*, 2003; Horssen *et al.*, 2002; Li *et al.*, 2010).

The Mengkabong mangrove forest is a major mangrove forest area in the Tuaran District. The forest is dominated by the species *Rhizophora apiculata*, which is a healthy and dense mangrove (Sabah Forestry Department, 2010). The Mengkabong

lagoon plays an important role in Tuaran's coastal ecology and in the socioeconomic development of the local people. The entire area is used extensively by local villagers for fishing, and some mangrove wood collection is carried out for firewood and fishing poles.

Increasing development pressure in this area has led to the depletion of mangrove forest and changes in the coastal environment. Conversion to aquaculture area and land reclamation for housing have been major factors affecting the depletion of Mengkabong mangrove forest area. According to the Sabah Fisheries Department (2012), shrimp pond activity has been conducted in the Mengkabong area since the early 2000s. This aquaculture activity has been conducted extensively by a private aquaculture company and local people. **Figure 4.1** depicts the conditions of mangrove forest and the degradation activities in Mengkabong.

With this impetus, this chapter determines the ability of the decision-tree learning method to classify mangrove forest land cover and to detect changes of mangrove forest land cover in the Mengkabong area from multi-temporal Landsat data series (TM, ETM+, and OLI_TIRS). The rule set applied in this study was derived from data from 2013 to 1990, 1995, 2000, and 2005, in order to detect changes of mangrove forest over the periods. We anticipate that the decision-tree method should be able to improve the performance of mangrove forest monitoring via multi-temporal Landsat data and ancillary GIS data.



Source : Field survey photographs, 2013

Figure 4.1 Condition of mangrove and degradation activities in the Mengkabong area

4.2 Objectives

The main objective of this study is to determine the potential of the machine learning method for classifying and detecting changes of mangrove forest land cover in the Mengkabong area using multi-temporal Landsat data series. The specific objectives of this study follow:

1. To determine the potential of the decision-tree learning method for classifying mangrove forest land cover in the Mengkabong area.
2. To detect changes of Mengkabong mangrove forest land cover using the multi-temporal Landsat data series integrated with the decision-tree learning method.

4.3 Materials and Methods

4.3.1 Materials of Satellite Images and Reference Data

(i) Acquisition and Selection of Landsat Data Series

The Landsat data series (TM, ETM+, and OLI/TRS) used in this study were downloaded free from the Earth Explorer US Geological Survey (USGS) website (<http://earthexplorer.usgs.gov/>). Details of the data acquisition and the data selection protocols were presented in the previous chapter (Chapter 3) of this study. The multi-temporal Landsat data series (TM, ETM+, and OLI_TIRS) used in this study included the years 1990, 1995, 2000, 2005, 2010, and 2013.

Due to the failure of the Scan Line Corrector (SLC) in the ETM+ sensor, there were lines of error in the Landsat ETM+ data of the years 2005 and 2010. Therefore, supplementary data for both of these years were needed to produce a corrected image using gap-filling analysis. The details of the gap-filling analysis protocols were presented in Chapter 3 of this research. **Table 4.1** shows the data specifications that were used in this study. **Figure 4.2** shows a true color composite of Landsat images of the study area.

Table 4.1 Specifications of multi-temporal Landsat data series used in this study

Landsat series	Year	Date acquired	Date of supplementary data for interpolation	Cloud cover (%)	Multispectral bands
L4 TM	1990	19.06.1990	None	20	
L5 TM	1995	01.02.1995	None	5.25	1-5, 7
	2000	07.12.2000		13.46	
L7 ETM+ SLC-off	2005	20.02.2005	02.10.2005*	6.18 & 32.15*	
	2010	06.03.2010	13.08.2010*	9.00 & 15.86*	
L8 OLI_TIRS	2013	23.04.2013	None	11.57	2 - 7

Note: (*) represents supplementary data

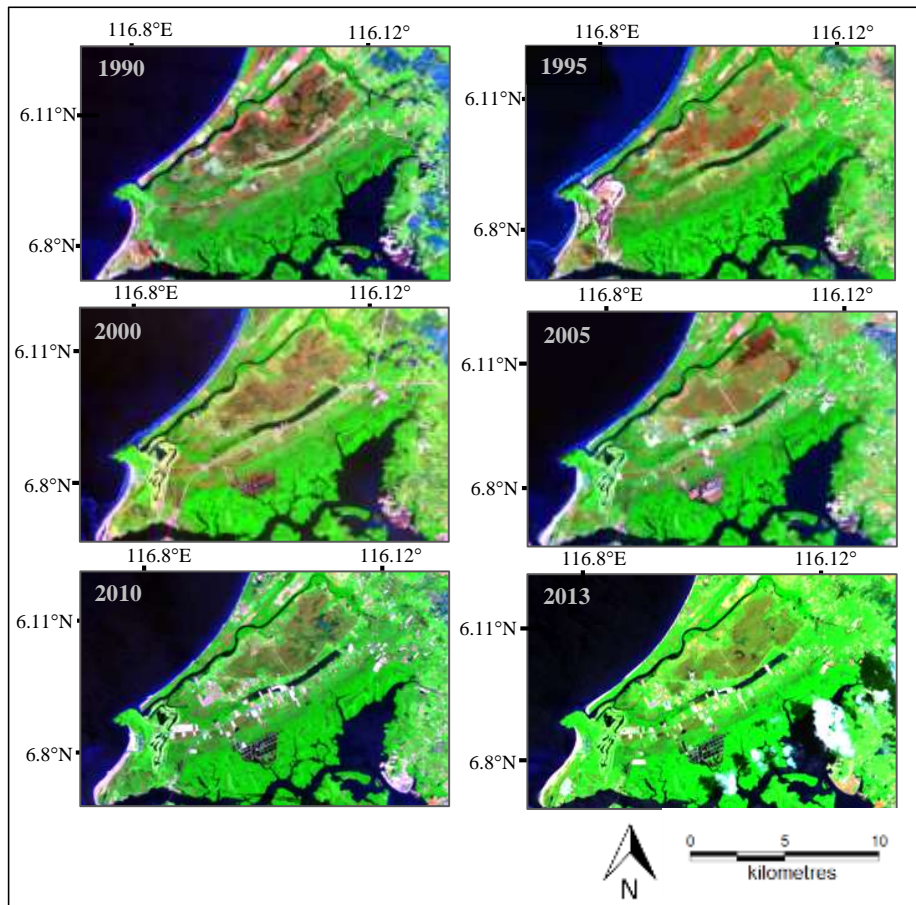


Figure 4.2 True-color composite (RGB) of Landsat series images (TM, ETM+, and OLI_TIRS) of the study area

(ii) Field Data and Reference Data

The reference data used to validate the results of this study included mainly field data, topography data, and vegetation maps. The field survey protocol was explained in detail in the Chapter 3 of this study. A detailed topographic map and vegetation map at the scale of 1:50,000 were obtained from the Sabah Survey and Mapping Department and the Sabah Forestry Department (SFD), respectively. Another reference data were the GIS ancillary data that contained digital elevation model and distance to the coastline data. These data were used to classify forest land cover into specific elevation categories.

4.3.2 Methodology

This study integrated multi-temporal Landsat data series with the decision-tree learning classification method. In this process, all multi-temporal Landsat data were analyzed for the data analysis. The analysis conducted involved (1) pre-processing, (2) generating the decision-tree learning classification, (3) *M*-statistics, and (4) accuracy assessment. The Environment for Visualizing Images (ENVI) 4.7 and 5.1 software and MS Excel 2010 were used to analyze the data.

4.3.2.1 Data Pre-processing

The Landsat data selected in this study were analyzed for pre-processing analysis. The pre-processing analysis consisted of radiometric calibration, creating multispectral data, subsetting the data, gap-filling analysis, cloud masking, and statistical analysis. The standard protocols for the pre-processing data analysis are those described in the previous chapter (Chapter 3) of this research. The purpose of the pre-processing analysis was to normalize the data, correct atmospheric effects, reduce noise, and allow intercomparison between data. Subsequently, the processed Landsat data were analyzed via the decision-tree learning classification method.

4.3.2.2 Applying the Decision-Tree Learning Method

The decision-tree method is a non-parametric classification method that repeatedly partitions a dataset into smaller subsets based on the test defined at each node of the tree (Liu *et al.*, 2008). According to Friedly & Brodley (1997), the decision-tree learning technique provides the flexibility of classification process that the statistical distribution of the data is not important. Another benefit of decision-tree classification is that several data sources, other than the remote sensing inputs, can be utilized to enhance the classification process (Horssen *et al.*, 2002; Li *et al.*, 2010). Decision-tree learning is illustrated in **Figure 4.3**.

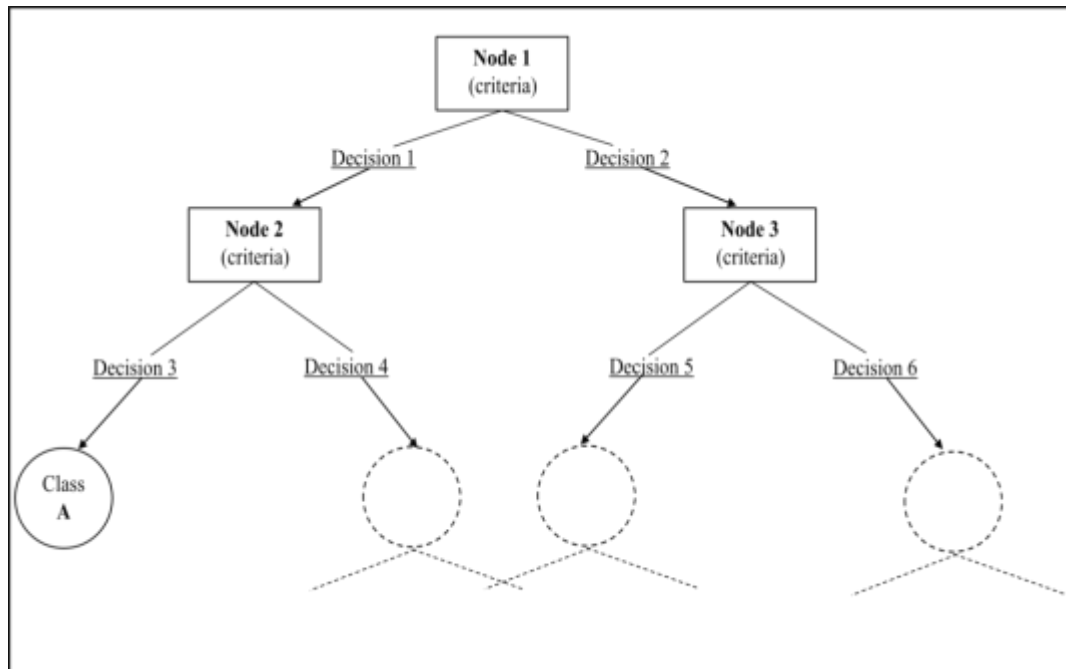


Figure 4.3 Sample of the decision-tree learning method

At each node of the tree, one or more criteria can be defined that produce a binary result (or two branches). Repeatedly, new criteria can be developed for each decision branch that transform the branch into a new node and yields two more branches from it. In this way, the process can be continued until the desired level of classification is attained. The initial nodes of the classification tree are generally targeted to

distinguish the general classes, but proceeding further can yield more specific classes and increase the complexity of the tree.

In this study, a dataset was comprised from the multi-temporal Landsat data and topographic variables. Because the majority of our study area was forest area, we focused mainly on using the spectral patterns of key features. The spectral patterns of these features in the multi-temporal Landsat data were extracted using tasselled cap transformation (TCT), normalized vegetation index (NDVI), band ratios and reflectance bands (bands 4, 5 and 7). The extracted features then were selected for the attributes rules (initial nodes) for the decision-tree learning classification method. The details of the feature extraction are explained in the following paragraphs.

(i) Feature Extraction and Determining the Attributes

(a) Tasselled Cap Transformation (TCT)

The TCT index extracted the greenness, brightness, and wetness features from the related six bands (1–5, 7) and (2–7) of TM, ETM+, and OLI_TIRS, respectively. This technique is useful for enhancing the spectral information content of Landsat data (MSS, TM, ETM+, OLI_TIRS) (Ali Baig *et al.*, 2014; Crist & Cicone, 1984; Healey *et al.*, 2005; Huang *et al.*, 2010;) and was optimized for data viewing for vegetation studies (Cohen *et al.*, 1995; Zhan *et al.*, 2002). The features were extracted using following expression:

$$\text{tas. cap}_i = (\text{coeff}_1 * \text{band}_1) + (\text{coeff}_2 * \text{band}_2) + (\text{coeff}_3 * \text{band}_3) + (\text{coeff}_4 * \text{band}_4) + (\text{coeff}_5 * \text{band}_5) + (\text{coeff}_7 * \text{band}_7), \quad (4.1)$$

where tas. cap_i is the calculated tasselled cap index for brightness, greenness, or wetness depending on the coefficients used and the bands are the top of atmosphere (TOA) reflectance (Grant & Carter, 2011). All Landsat data used in this study were previously

converted to TOA reflectance value during the pre-processing analysis. Therefore, the TCT index was processed directly using ENVI 4.7 software.

The TCT coefficients used for the TM, ETM+, and the OLI_TIS data are from the studies by Huang *et al.* (2002) and Ali Baig *et al.* (2014), respectively (**Tables 4.2 and 4.3**). The six bands of the TM, ETM+, and OLI_TIRS data were the basic attributes used for the decision-tree learning classification. **Figure 4.4** shows the images of brightness, greenness, and moisture of the Landsat data that were extracted using the TCT index.

Table 4.2 Tasseled cap coefficient for Landsat TM and ETM+ at satellite reflectance

Index	Band 1	Band 2	Band 3	Band 4	Band 5	Band 7
Brightness	0.3561	0.3972	0.3904	0.6966	0.2286	0.1596
Greenness	-0.3344	-0.3544	-0.4556	0.6966	-0.0242	-0.263
Moisture	0.2626	0.2141	0.0926	0.0656	-0.7629	-0.5388
Fourth	0.0805	-0.0498	0.195	-0.1327	0.5752	-0.7775
Fifth	-0.7252	-0.0202	0.6683	0.0631	-0.1494	-0.0274
Six	0.4000	-0.8172	0.3832	0.0602	-0.0602	0.0985

Table 4.3 Tasseled cap coefficient for Landsat OLI_TIRS at satellite reflectance

Index	Band 1	Band 2	Band 3	Band 4	Band 5	Band 7
Brightness	0.3029	0.2786	0.4733	0.4733	0.5599	0.508
Greenness	-0.2941	-0.243	-0.5424	-0.5424	0.7276	0.0713
Moisture	0.1511	0.1973	0.3283	0.3283	0.3407	-0.7117
Fourth	-0.8239	0.0849	0.4396	0.4396	-0.058	0.2013
Fifth	-0.3294	0.0557	0.0557	0.1056	0.1855	-0.4349
Six	0.1079	-0.9023	-0.9023	0.4119	0.0575	-0.0259

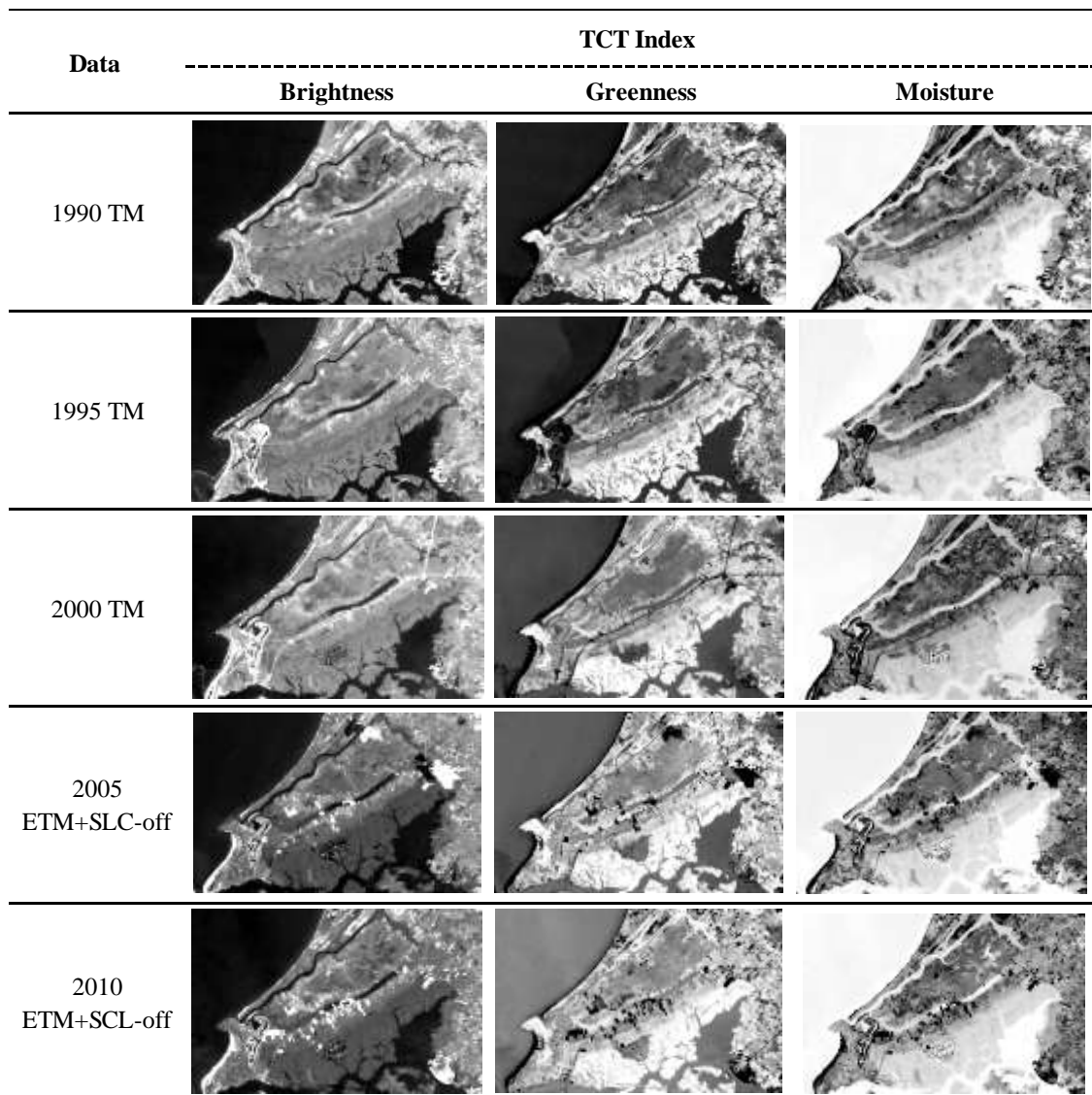


Figure 4.4 Tasseled cap transformation indexes of brightness, greenness, and moisture of the Landsat data

(b) Normalized Difference Vegetation Index (NDVI)

The normalized difference vegetation index (NDVI) was also included as one of the major attributes for representing vegetation conditions. The NDVI is a simple numerical indicator that can be used to analyze remote sensing measurements whether the target object being observed contains live green vegetation or not.

The NDVI was calculated from the following equation:

$$\text{NDVI} = \frac{(\text{NIR} + \text{Red})}{(\text{NIR} - \text{Red})}, \quad (4.2)$$

where *Red* and *NIR* refer to the spectral reflectance measurement acquired in the red and near-infrared wavelength, respectively. In this study, we used the spectral reflectance of bands 3 and 4 of the Landsat data of TM and ETM+ and those of bands 4 and 5 of OLI_TIRS, which are closely related to the wavelengths of the red and NIR bands, respectively. **Figure 4.5** shows the NDVI of the Mengkabong area that were extracted using the Landsat data. The spectral patterns of key features were then extracted using the help endmember extraction tool available in the ENVI software to distinguish among the various vegetation.

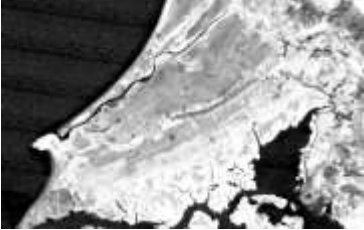




Data	NDVI extracted of Landsat bands
1990 TM	
1995 TM	
2000 TM	
2005 ETM+SLC-off	
2010 ETM+SLC-off	

Figure 4.5 NDVI extracted using bands 3 and 4 of the Landsat data series

(c) Band Ratio

Band ratio indices were used to enhance the spectral differences between bands and to reduce the effects of topography. The band ratios 5/4 and 3/5 (Green *et al.*, 1998) are

always used in mangrove discrimination studies. Therefore, both of these band ratios were selected in this study to improve the difference between mangrove and non-mangrove areas.

(d) Band 4

Band 4 of the Landsat data were frequently applied to monitor vegetation moisture content and vegetation densities. Based on the spectral profile classification result in the Chapter 3 of this study, band 4 very useful to distinguish the mangrove forest from other vegetation. Mangrove has high reflectance value in band 4 compared with others vegetation classes due to high moisture contents in the leaves. Therefore, band 4 was selected as an attribute rule for mangrove discriminating in this study.

(e) Bands 5 and 7

Bands 5 and 7 of the Landsat data also were frequently applied to monitor vegetation moisture content. The spectral profiles of bands 5 and 7 show a lower reflectance value within mangrove forest compared with other classes (Alsaaidh *et al.*, 2011). This makes bands 5 and 7 very useful for distinguishing mangrove forest from other vegetation.

(ii) Generating Decision-Tree Learning

The decision-tree learning classification method was conducted using ENVI 5.1 software. The attributes rules comprised spectral attributes values of Landsat bands (4, 5 and 7, greenness, moisture, and NDVI), elevation attributes (DEM), and distance attributes (distance to coastline) (**Table 4.4**).

Table 4.4 Attributes used for the decision-tree learning method

Attributes	Acquisition Method	Value Range
1. Spectral Attributes (Landsat data bands: 1-5,7),TCT index (Greeness & Moisture),NDVI	TCT method ,band ratio & NDVI	NDVI (-1 to 1)
2. Elevation attributes (DEM)	Sample of DEM Image in ARC/INFO Grid	0-500 integer
3. Distance attributes (Distance to the Coastline)	EucuDistance of ARC/INFO Grid	Distance 0-20 km

The field survey conducted for this study found that mangrove forests were not distributed at elevations higher than 6 m. Therefore, the digital elevation model (DEM) was used to exclude non-mangrove pixels that have similar spectral attributes with mangrove pixels but were above the limiting elevation line. In addition, mangrove in this study area were unlikely to be found beyond 1 km from the coastline.

The class label has two possible values. Mangrove forest is represented by C1, and non-mangrove forest is by represented C2. The classification results were overlain to detect mangrove changes and were calculated statistically. **Figure 4.6** shows the decision-tree learning classification procedure applied in this study.

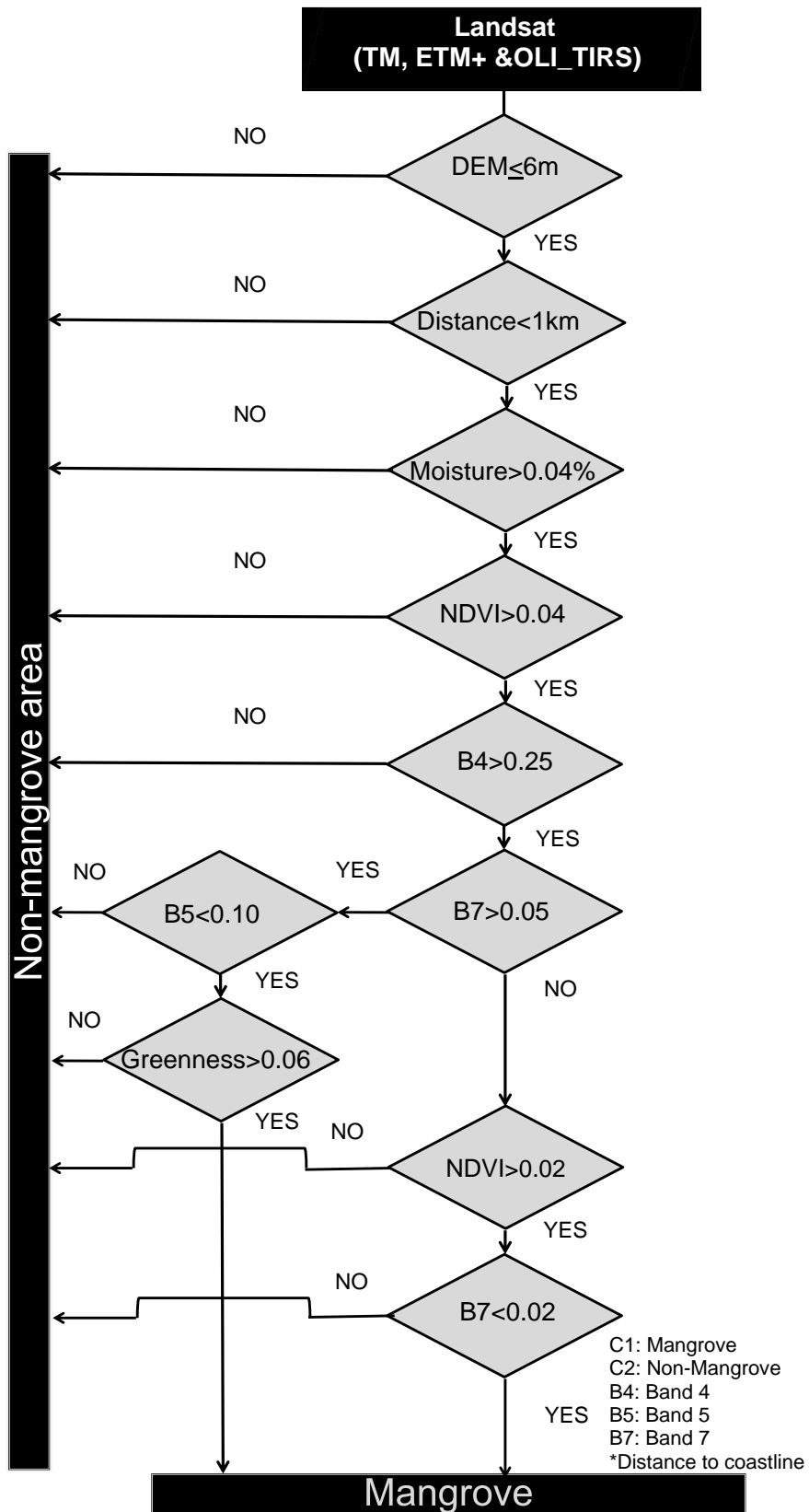


Figure 4.6 Decision-tree learning classification method

4.3.2.3 *M*-statistic

The *M*-statistic was adopted for identifying the accuracy of the features selection. It quantitatively assesses the separability of two classes in terms of mean distance and standard deviation (Zhang *et al.*, 2011). A greater separability is preferable. This also means that the feature is useful for object recognition. The formula for normalizing mean distance follows:

$$M = \frac{|\mu_1 - \mu_2|}{\sigma_1 + \sigma_2} , \quad (4.3)$$

where *M* is the normalized mean distance and μ_1 and μ_2 are the means for classification feature of two samples with two different types of objects. σ_1, σ_2 refer to the standard deviations of the classification feature of two samples with different types of objects.

4.3.2.4 Assessment of Classification

The classified land cover maps derived from the satellite data were used further for accuracy assessment. The confusion matrix method, integrated with ground-truth data from the field survey, topographic map data, and Google Earth, was used for the accuracy analysis. The accuracy assessment procedures were explained in detail in Chapter 3. **Figure 4.7** shows a flowchart of the overall decision-tree learning classification using the multi-temporal Landsat series (1990–2013) data.

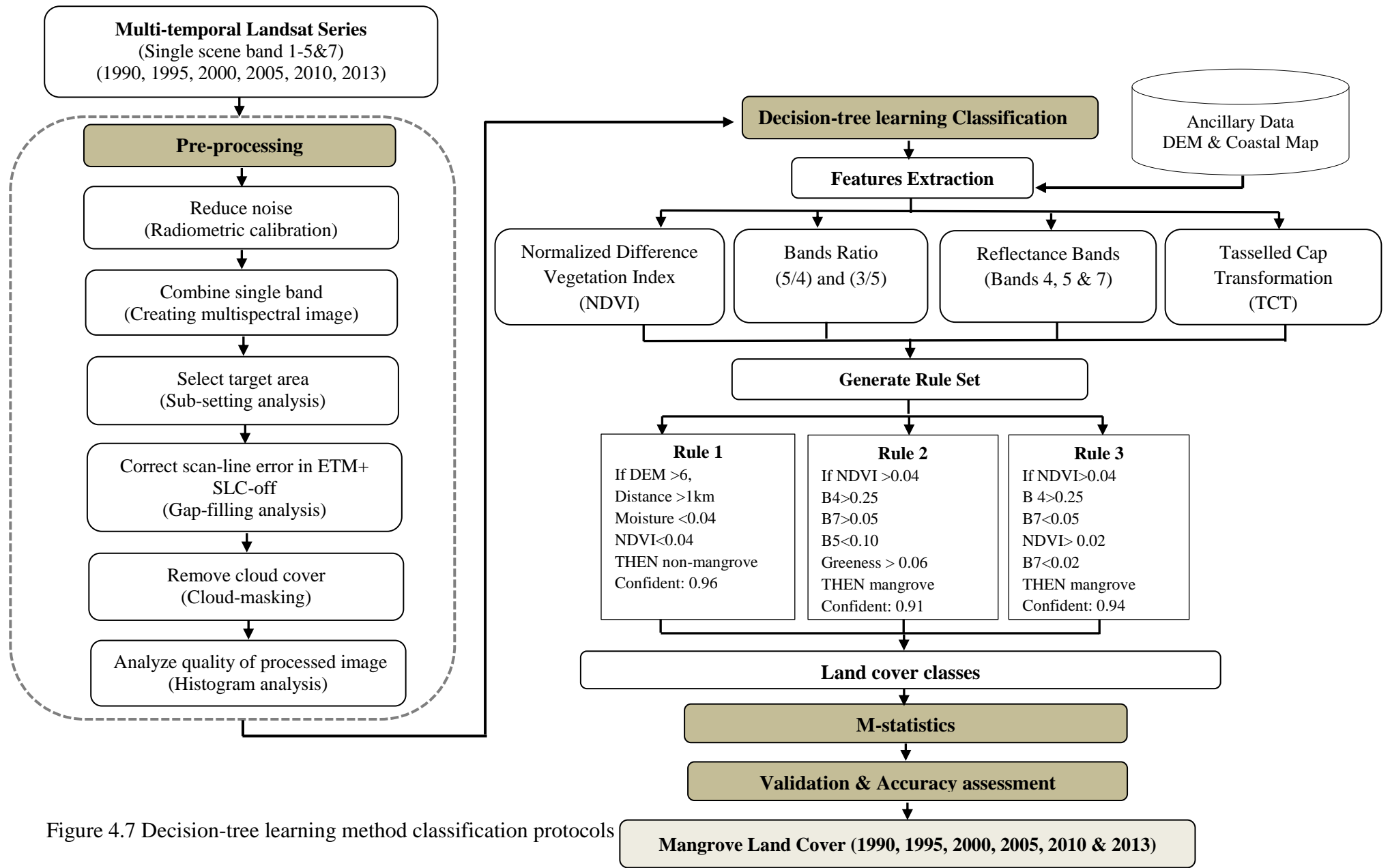


Figure 4.7 Decision-tree learning method classification protocols

4.4 Results and Discussion

4.4.1 Decision-Tree Learning Classification of Mengkabong Mangrove Land Cover

This study demonstrates the potential of the decision-tree learning method for classifying land covers in the Mengkabong area. Seven land cover types were classified: mangrove, open water, built-up, water–mixed vegetation, secondary forest, grassland, and bare soil. **Table 4.5** shows the resulting M -statistic values for separability among the land covers classes. Only the M -statistic values of moisture, greenness and Band 4 were large, thus the separability between terrestrial vegetation, mangrove, and water–vegetation mixed pixels was better.

The mangroves class in all the data recorded the largest M -statistic value of moisture, with a highest value of 3.26 in 1990 and 3.22 in 2013. Mangrove forests are known to be hydrophytic, a term which means that the plants grow in water or in very wet soil. Therefore, the background of the environment reflects the moisture of the mangrove canopy (Ajithkumar *et al.*, 2008). Furthermore, moisture is an indicator of water bodies and moisture content in the vegetation canopy (Crist *et al.*, 1986).

The mangrove vegetation shows the largest M -statistics value of Band 4 in all the data (1990-2013). The highest value was recorded in the years 1990, 1995 and 2013 and its show of high of mangrove distributions in that year. The Band 4 is useful to discriminate mangrove with others vegetation plants. Result of spectral profile classification in the Chapter 3 of this study also shows that mangrove has high reflectance value in the Band 4 due to high of moisture content in the mangrove leaves. The results of this study also supported from the previous studies by USGS (2004) and Rahman *et al.* (2013).

Because the mangrove environment is a mixture with water areas, the water–vegetation mixed pixel class was identified. The greenness of the TCT index measures the contrast between the near-infrared and visible bands, and the large M -statistic value

in greenness index could be useful for separating the water–vegetation mixed pixel class. The highest value of *M*-statistic of greenness, a value of 2.23, was recorded in the 2013 data. This means the water–vegetation mixed pixel distribution was highest in 2013.

Table 4.5 *M*-statistics value between mangrove area and non-mangrove area

Data	Classification Features	Terrestrial Vegetation area	Mangrove area	Water-Vegetation mixed pixel	Built-up Area	Water
19061990 TM	Greenness	0.83	0.93	1.93	2.14	4.72
	Moisture	2.59	3.26	0.47	1.26	0.18
	Brightness	1.15	1.05	0.94	4.16	4.56
	NDVI	1.56	1.52	1.28	2.90	4.39
	Band 5/Band 4	2.27	2.32	0.67	0.03	1.56
	Band 3/Band 5	1.62	1.72	0.91	4.91	0.70
	Band 4	2.22	2.69	1.69	0.26	0.05
	Band 5	1.45	1.60	0.52	1.24	0.84
	Band 7	1.22	1.20	0.46	1.08	0.72
01021995 TM	Greenness	0.63	0.98	1.95	2.12	4.71
	Moisture	2.47	3.22	0.43	1.25	0.17
	Brightness	1.12	1.06	0.92	4.12	4.53
	NDVI	1.48	1.48	1.24	2.98	4.37
	Band 5/Band 4	2.29	2.23	0.63	0.07	1.54
	Band 3/Band 5	1.58	1.67	0.93	4.98	0.71
	Band 4	2.18	2.60	1.48	0.23	0.04
	Band 5	1.32	1.54	0.51	1.23	0.83
	Band 7	1.18	1.16	0.47	1.03	0.73
07122000 TM	Greenness	0.62	0.86	1.98	2.10	4.77
	Moisture	2.36	3.18	0.41	1.23	0.15
	Brightness	1.18	1.22	0.95	4.11	4.51
	NDVI	1.38	1.38	1.21	2.97	4.35
	Band 5/Band 4	2.26	2.21	0.61	0.06	1.51
	Band 3/Band 5	1.48	1.58	0.95	4.99	0.73
	Band 4	2.12	2.48	1.34	0.21	0.05
	Band 5	1.28	1.47	0.48	1.22	0.81
	Band 7	1.15	1.17	0.43	1.01	0.75
20022005 ETM+	Greenness	0.64	0.78	2.18	2.08	4.79
	Moisture	2.28	3.13	0.42	1.21	0.13
	Brightness	1.2	1.28	0.93	4.13	4.53
	NDVI	1.36	1.35	1.23	2.95	4.35
	Band 5/Band 4	2.28	2.18	0.63	0.07	1.53
	Band 3/Band 5	1.46	1.48	0.97	5.01	0.69
	Band 4	2.1	2.36	1.26	0.18	0.03
	Band 5	1.25	1.39	0.49	1.21	0.79
	Band 7	1.13	1.13	0.41	1.00	0.73
13082010 ETM+	Greenness	0.72	0.75	2.21	2.11	4.81
	Moisture	2.73	3.18	0.43	1.23	0.11
	Brightness	1.24	1.25	0.91	4.11	4.51
	NDVI	1.37	1.33	1.21	2.97	4.31
	Band 5/Band 4	2.22	2.11	0.67	0.06	1.51
	Band 3/Band 5	1.35	1.35	0.95	5.05	0.71
	Band 4	1.98	2.28	1.2	0.16	0.02
	Band 5	1.10	1.37	0.47	1.23	0.73
	Band 7	1.08	1.11	0.39	1.11	0.79
23042013 OLI_TIRS	Greenness	0.71	0.78	2.23	2.13	4.97
	Moisture	2.75	3.22	0.41	1.21	0.13
	Brightness	1.21	1.27	0.89	4.1	4.63
	NDVI	1.35	1.31	1.2	2.93	4.42
	Band 5/Band 4	2.18	2.18	0.65	0.05	1.57
	Band 3/Band 5	1.25	1.28	0.93	5.07	0.69
	Band 4	1.95	2.54	1.18	0.14	0.03
	Band 5	1.08	1.33	0.43	1.21	0.77
	Band 7	1.05	1.12	0.37	0.08	0.81

According to Crist (1986), greenness is responsible for enhancing the absorption in the visible spectra caused by plant pigments, including chlorophyll, and the high reflectance in the infrared region due to the internal structure of the leaves. Many previous studies supported the usefulness of greenness and moisture in mangrove recognition (Baker *et al.*, 2006; Crist *et al.*, 1986; Razali & Nuruddin, 2012; Zhang *et al.* 2013). Therefore, the greenness and moisture that were extracted using the TCT were chosen during the mangrove identification.

However, the *M*-statistic values were very small when using the original reflectance values of band 5 and band 7 for the mangrove identification. The highest *M*-statistic value for band 5 of only 1.60 was recorded in 1990. It may have resulted from the high biomass of mangrove forest in 1990, when there were no deforestation activities. These results may support the report by the Sabah Forestry Department (SFD) released in 2010.

Other non-mangrove areas, such as a built-up area, could be identified using the band ratio index. This ratio is useful for the determination of barren land and built-up areas (Quinn, 2001). The large values of *M*-statistic for band ratio 3/5 of 4.91–5.07 in 1990 to 2013, respectively, could be useful for differentiating built-up areas from other classes. Barren-land and built-up areas appear in a light tone compared to forest, water body, and crop plant areas, which appear in a dark tone.

Figure 4.8 shows the band ratio images of mangrove and built-up areas in this study. Based on the field survey and other reference data such as the vegetation map and Google Earth, the built-up area in the study area was actually referred to shrimp pond development. Mangrove areas have been reclaimed for shrimp pond farming since 2000 (SFD, 2010).

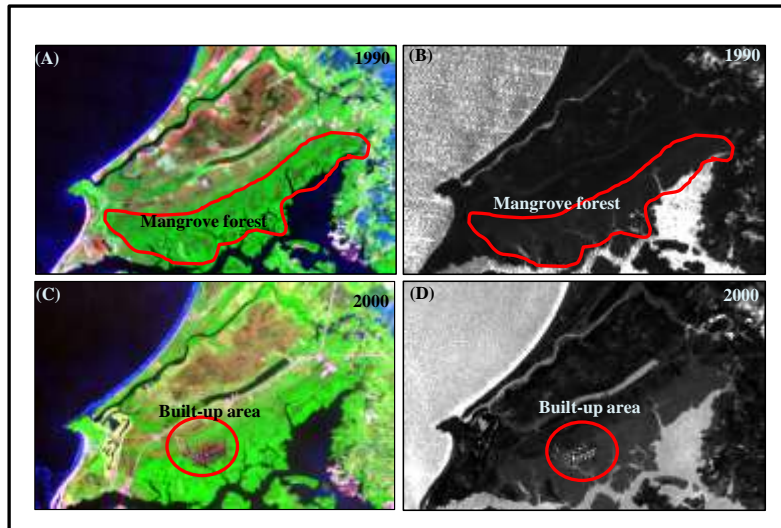


Figure 4.8 Landsat images of 1990 and 2000 (bands 7, 4, and 2 as R, G, and B). (A) Mangroves forest area (mostly in green color). (B) Band ratio of mangrove forest area (dark tone). (C) Built-up area (light red color). (D) Band ratio of built-up area (light tone).

The use of spectral reflectance as a key feature was able to confirm the different land cover classes in the Mengkabong area, which produced significant differences in spectral profile characteristics. **Figures 4.9** and **4.10** show the spectral characteristics of the mangrove and the non-mangrove land covers in this study area using the Landsat data attributes.

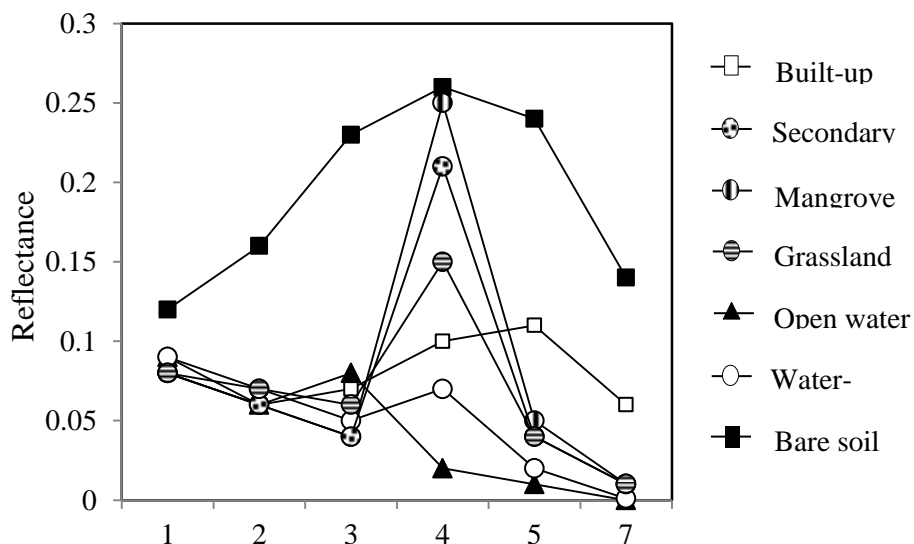


Figure 4.9 Spectral characteristics of mangrove and non-mangrove land cover types using Landsat data series (TM, ETM+, and OLI_TIRS)

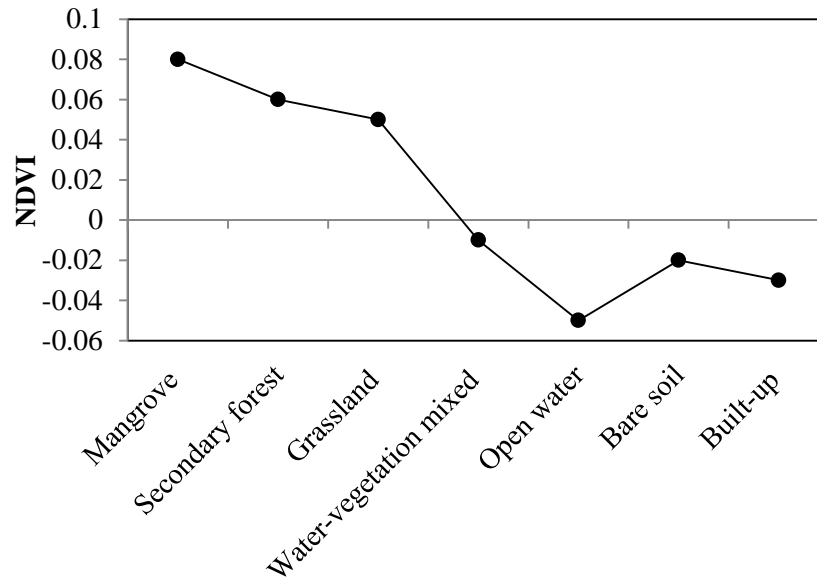


Figure 4.10 Spectral characteristics of mangrove and non-mangrove land cover types using NDVI value

Previous studies by Froidefond *et al.* (2002), Morel *et al.* (2012), and Rahman *et al.* (2013) confirmed that the spectral profile of remote sensing data can be useful for identifying the specific features of land cover types. In addition, the use of NDVI attributes was useful for differentiating different classes of vegetation and non-vegetation areas (Karaburun, 2010; Ramachandra & Kumar, 2004; Xie *et al.*, 2010).

The mangrove and secondary forest have high NDVI values of 0.08 and 0.06, respectively. The result of this study confirmed that the Mengkabong area is dominated by a very high density of mangrove species such as *Rhizophora apiculata*. A study by John and David (1999) suggested that the standard of high NDVI values, from 0.4 to 1, corresponds to the density of vegetated area. Negative NDVI values represent water, built-up areas, and bare soil areas.

The decision-tree classification in this study demonstrated that the selection of good attributes for mangrove classification promoted high accuracies of the result. The use of DEM and GIS data promoted the effectiveness of delineating the spatial distributions and temporal changes of the mangrove forest. Liu *et al.* (2008) suggested that a combination of Landsat data containing multi-temporal images and GIS data, such as DEM and distance to the coast data, is useful for delineating mangrove forest both spatially and temporally.

4.4.2 Results of Change Detection

The details of the detected changes of mangrove forest and other types of land cover in the study area are presented in the **Table 4.6**. The total area of Mengkabong is 4981.68 ha. According to the results of this study, mangrove forests were distributed extensively in the Mengkabong area in 1990, when they had an area of 1145.16 ha (almost 25% of the total area). However, there was a significant decrease from 1990 to 2000 (1145.16 ha to 945.72 ha) and a slight increase from 2010 to 2013 (997.20 ha to 1185.12 ha). Generally, the total area of mangrove forest declined (a reduction of 40 ha from 1990 to 2013) and fragmentation was obvious.

Table 4. 6 Changes in mangrove forest and other land cover types from 1990 to 2013

Land Cover	1990		1995		2000		2005		2010		2013	
	ha	%	ha	%	ha	%	ha	%	ha	%	ha	%
Open water	1531.26	30.74	1555.20	31.22	1593.81	31.99	1616.67	32.45	1549.80	31.11	1536.84	30.85
Mangroves	1145.16	22.99	1024.20	20.56	945.72	18.98	872.82	17.52	997.20	20.02	1185.12	23.79
Secondary forest	846.90	17.00	826.20	16.58	780.12	15.66	627.21	12.59	518.40	10.41	499.14	10.02
Built-up	921.42	18.50	1037.34	20.82	1142.19	22.93	1186.83	23.82	1309.05	26.28	1048.50	21.05
Bare soil	342.00	6.87	253.17	5.08	198.72	3.99	266.85	5.36	246.33	4.94	270.54	5.43
Grassland	132.75	2.66	238.77	4.79	277.38	5.57	371.52	7.46	324.18	6.51	407.16	8.17
Water-Veg.	62.19	1.25	46.80	0.94	43.74	0.88	39.78	0.80	36.72	0.74	34.38	0.69

Figure 4.11 clearly shows the changes in percentage of mangrove forest and other land cover types from 1990 to 2013. The field investigation showed that most of the mangrove forest in the Mengkabong area has been lost. Most of the mangrove areas have been converted to shrimp ponds and housing settlements. As discussed in the previous chapter (Chapter 3), shrimp pond activity in this area has occurred since 2000 (Department of Fisheries Sabah, 2012).

Thus, the results of this study may support the report by the Department of Fisheries Sabah. Only certain areas are well protected. Other land cover areas show similar trends over the study period, and the changes in these land cover areas were linear. Specifically, built-up areas expanded continuously, while secondary forest and water-vegetation mixed areas shrank continuously. The open water and bare soil areas showed an increasing-decreasing pattern.

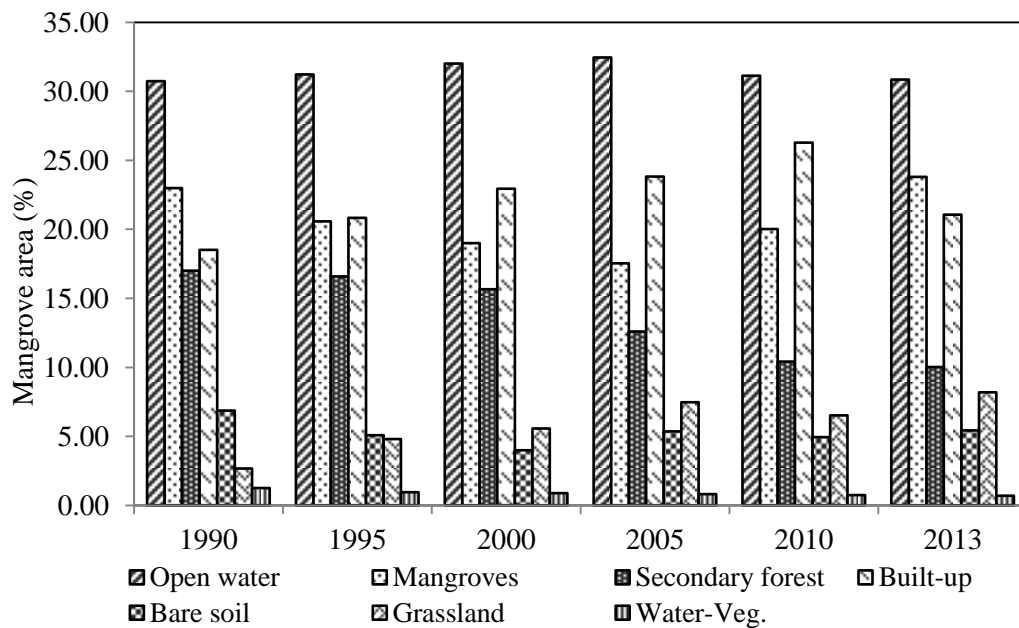


Figure 4.11 Changes in mangrove forest and other land cover types from 1990 to 2013

4.4.3 Assessment of Classification

The error matrices for the six years and their corresponding kappa values are listed in **Table 4.7**. The result of the classification assessment of the decision-tree learning method with GIS ancillary data shows that the highest kappa coefficient and the total accuracy of mangrove identification were 0.82 and 90.8%, respectively.

Table 4.7 Error matrices of decision-tree learning classification for 1990, 1995, 2000, 2005, 2010, and 2013

Classified Data		Reference Data		Total Accuracy (%)	Kappa Coefficient
		Non-Mangrove	Mangrove		
TM 1990	Non-Mangrove	234	16	84	0.68
	Mangrove	64	186		
TM 1995	Non-Mangrove	221	29	82	0.64
	Mangrove	61	189		
TM 2000	Non-Mangrove	226	24	87.2	0.74
	Mangrove	40	210		
ETM+ 2005	Non-Mangrove	230	18	89.6	0.79
	Mangrove	32	218		
ETM+ 2010	Non-Mangrove	238	12	90.8	0.82
	Mangrove	34	216		
OLI- TIRS 2013	Non-Mangrove	218	24	89.2	0.78
	Mangrove	22	228		

Note: Total accuracy and kappa coefficient calculations can be referred to the accuracy assessment analysis in the **Section 3.4.2.5**

4.5 Summary

In summary, this study successfully classified mangrove and non-mangrove areas in the Mengkabong area by integrating the decision-tree learning method with multi-temporal Landsat series and GIS ancillary data. The selection of good attributes, from the spectral features of Landsat data and from topographic data (DEM and distance to coastline) from the GIS database, for the mangrove classification promoted the high accuracy of result of 90.8%.

Chapter 5

Detection of Regional-scale Conversion of Sabah's Mangrove to Aquaculture Using Change-point Analysis of MODIS Time-series Data

5.1 Introduction

Mangrove forests occur in coastal environments at tropical and subtropical latitudes and are among the most productive terrestrial ecosystems in the world (Kuenzer *et al.*, 2011; Myint *et al.*, 2008). These forests play an important role in providing ecological and societal goods and services to local communities (Giri *et al.*, 2008; Wang *et al.*, 2004; Zhang *et al.*, 2003) by stabilizing shorelines and reducing the destructive impacts of natural disasters, such as tsunamis and cyclones (Giri *et al.*, 2008; Zhang *et al.*, 2007), serving as a breeding and nursing ground for marine and pelagic species (Giri *et al.*, 2008), and providing food, medicine, and fuel, as well as building materials, and opportunities for aquaculture (Myint *et al.*, 2008; Thu & Populus, 2007).

According to Clough (1992), the clay soil with high salinity levels in mangrove areas is very suitable for aquaculture systems, especially for shrimp pond cultures. Furthermore, FAO (1987) stated that clayey soil stabilizes the bed of the pond and absorbs large quantities of nutrients, which increases the productivity of the pond. Thus, such clayey soil is an important factor contributing to the productivity of shrimp pond farming, which is frequently found in coastal mangrove forest.

Shrimp farming areas in mangrove areas have been expanding rapidly, especially in Asian countries (Giri *et al.*, 2008; Primavera *et al.*, 2007). FAO (2007) found that the high economic return of shrimp farming has caused it to be promoted as a way to increase its national economic potential to serve as a source of income for local communities, especially in developing countries such as Malaysia, Vietnam, and

Myanmar. In Malaysia, shrimp farming is conducted by using the pond system and is generally established along mangrove coastal areas (Abdullah *et al.*, 2013).

According to Othman (2008), the total area of shrimp pond farming in Malaysia has increased from 2,600 ha in 1995 to 7,500 ha in 2007. The major brackish-water shrimp species for commercial purposes are banana shrimp (*Penaeus vanamei*) and tiger shrimp (*Penaeus monodon*) (Abdullah *et al.*, 2013). The highest concentrations of shrimp pond farming operations were found in Sabah, Perak, Penang, Johor, and Selangor.

Due to the high demand for tiger and banana shrimps, both species are cultured extensively and commercially in Sabah's mangrove area. Sabah is also the largest producer of tiger shrimp in Malaysia (Ng *et al.*, 2010). For example, more than 20,000 metric tonnes of production of tiger species were harvested in 2010 (DFS, 2011). However, the high concentrations of shrimp pond farming have led to a decrease of thousands of hectares of mangrove area in Malaysia (Consumer Association of Penang, 2010).

Sabah has the largest distribution of mangrove forest in Malaysia. However, Jakobsen *et al.* (2007) reported that more than 10,000 ha of mangrove area has been converted to shrimp pond farming. Some of these aquaculture activities have been conducted illegally without permission from the Sabah Forestry Department and the Department of Fisheries Sabah. A majority of the illegal shrimp pond farming areas are operated by local communities for only short periods of time. The high cost of shrimp pond maintenance and limited support facilities have been factors resulting in the increase of inactive shrimp pond farming areas (Department of Fisheries Sabah, 2010).

As a result, the destruction of mangrove forest will bring a certain level of direct and indirect economic loss to the coastal community, and the total cost of recovering the forest also will be high. According to the Sabah Forestry Department (SFD) (2010), about RM 5 million was expended for the mangrove replanting project in Sabah from 2006 to 2010. This project was implemented because the mangrove forests in Sabah

were decreasing at an alarming rate and also to protect the coastal areas from erosion. Furthermore, continuous monitoring should be conducted to manage the restoration of mangrove areas and also to identify potential sites for the mangrove replanting project.

Many remote sensing studies to monitor mangroves have been carried out in the last two decades (Seto & Frangkias, 2007). A review of recent advancements in remote sensing data and techniques for large-scale monitoring of mangrove is given by Hueman (2011). Traditional pixel-based classifications of aerial and remote sensing imagery and the more recent application of radar or LIDAR data combined with texture-based analyses have demonstrated increased potential for the application of remote sensing for mangrove mapping and change detection.

However, another recent review by Kuenzer *et al.* (2011) provided an overview of the limitations of the currently used remote sensing methods. Most aerial photography and high satellite imagery suffers from high cost, scarcity of data, small coverage area, and lack of automation. Hyperspectral data are also very expensive and not yet available for large area coverage. Radar and LIDAR data have restricted data access due to their low availability and the complexity involved in the process and also have low spatial and temporal resolution.

To overcome these limitations, Moderate Resolution Imaging Spectroradiometer (MODIS) time-series data at 250 m pixel size were used in this study. MODIS data, which are available at no cost, have potential for detecting anthropogenic-driven land cover changes that usually occur at this spatial resolution. Vegetation indices (VIs) of MODIS data can be used to identify vegetation density in coastal ecosystems and can also cover a large area (Hansen *et al.*, 2002).

Temporal pattern analysis using MODIS enhanced vegetation index (EVI) datasets has significant advantages for both capturing the actual timing of change events and monitoring vegetation growth. Wardlow *et al.* (2007) suggested that MODIS EVI time-series data have potential for offering new opportunities for detailed, large-area vegetation mapping, with large geographic coverage and low cost. For example,

Setiawan & Yoshino (2012) found that change in land use type can be recognized through change in the pattern of the long-term vegetation dynamics of MODIS EVI time-series data. Thus, the aim of this study is to determine the potential of low-cost satellite MODIS data for detecting and monitoring the deforestation of the mangrove area. A method is developed to track the conversion of mangrove land cover for a 14-year period (2000–2013) using statistical change detection.

5.2 Objectives

The main objective of this study is to demonstrate the potential of MODIS time-series data and an applicable method for detecting the deforestation of mangrove forest in Mengkabong, Sabah. To achieve this objective, the following specific objectives of this study were established:

1. To delineate patterns of mangrove and aquaculture from the MODIS satellite imagery time series.
2. To develop applicable methods for tracking more than 10 years of Mengkabong mangrove land cover change using MODIS vegetation index time series.
3. To examine the possibilities of applying remote sensing for monitoring aquaculture development and land use change in the study area.

5.3 Materials and Methods

5.3.1 Study Area

The study area is located in Mengkabong, Sabah. The total study area extends from 6°8'24" N to 6°11'24" N latitude and from 116°08'6" E to 116°12'54" E longitude (Google Earth, 2012) (**Fig. 5.1**). Prior to the 1990s, the study area was almost entirely covered with *Rhizophora apiculata*, which is a healthy and dense mangrove species (Sabah Forestry Department, 2010).

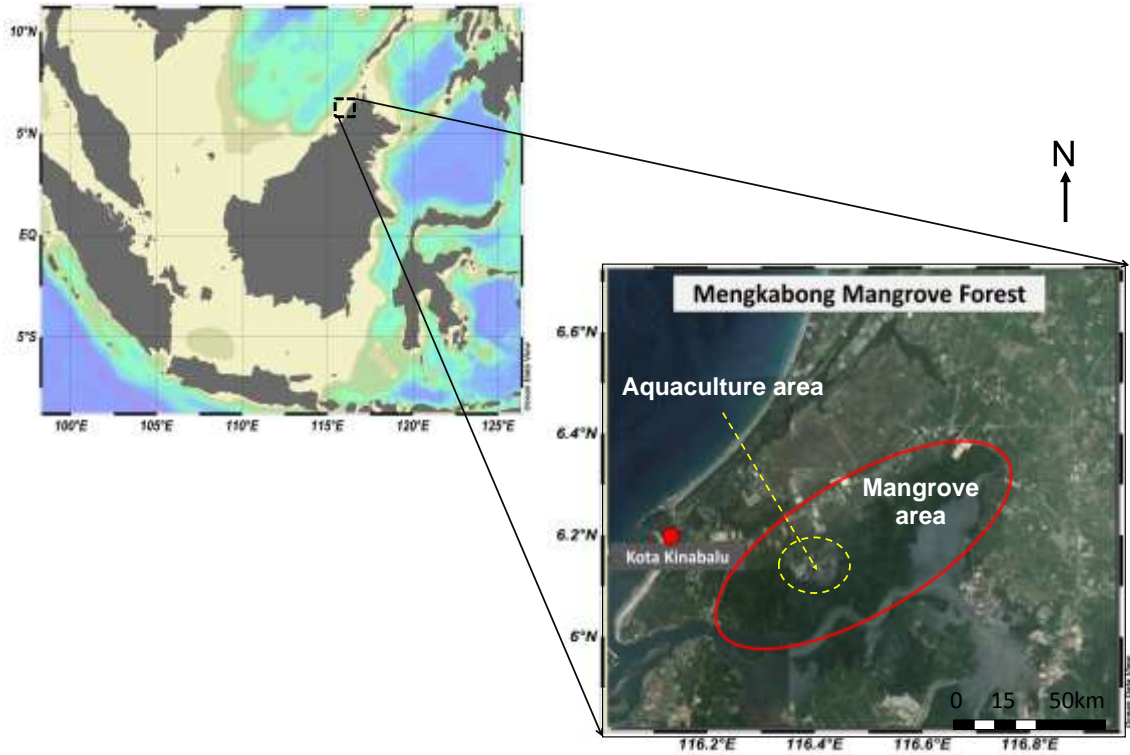


Figure 5.1 Location of study area. The red line shows the mangrove area and the yellow line shows the aquaculture area

However, in the early 2000s, more mangrove areas were cleared for shrimp pond farming activities. The activities have been expanding gradually, resulting in increases in the number of pond areas (Department of Fisheries Sabah, 2014). **Figure 5.2** shows the conditions of mangrove coverage and shrimp pond systems in the study area. A study by Polpanish *et al.* (2009) reported that the total number of shrimp pond areas in Mengkabong increased from 6 to 19 from 1998 to 2008.

The average total area of each pond is 2.5 ha. An increased demand for tiger shrimp (*Penaeus monodon*) has been a factor in the increase of shrimp pond areas in Mengkabong. The shrimp pond area is the largest of the aquaculture operations in the Tuaran District area. Therefore, this area was selected for detection of land cover changes and aquaculture development in the mangrove area of Sabah over the past 10 years.

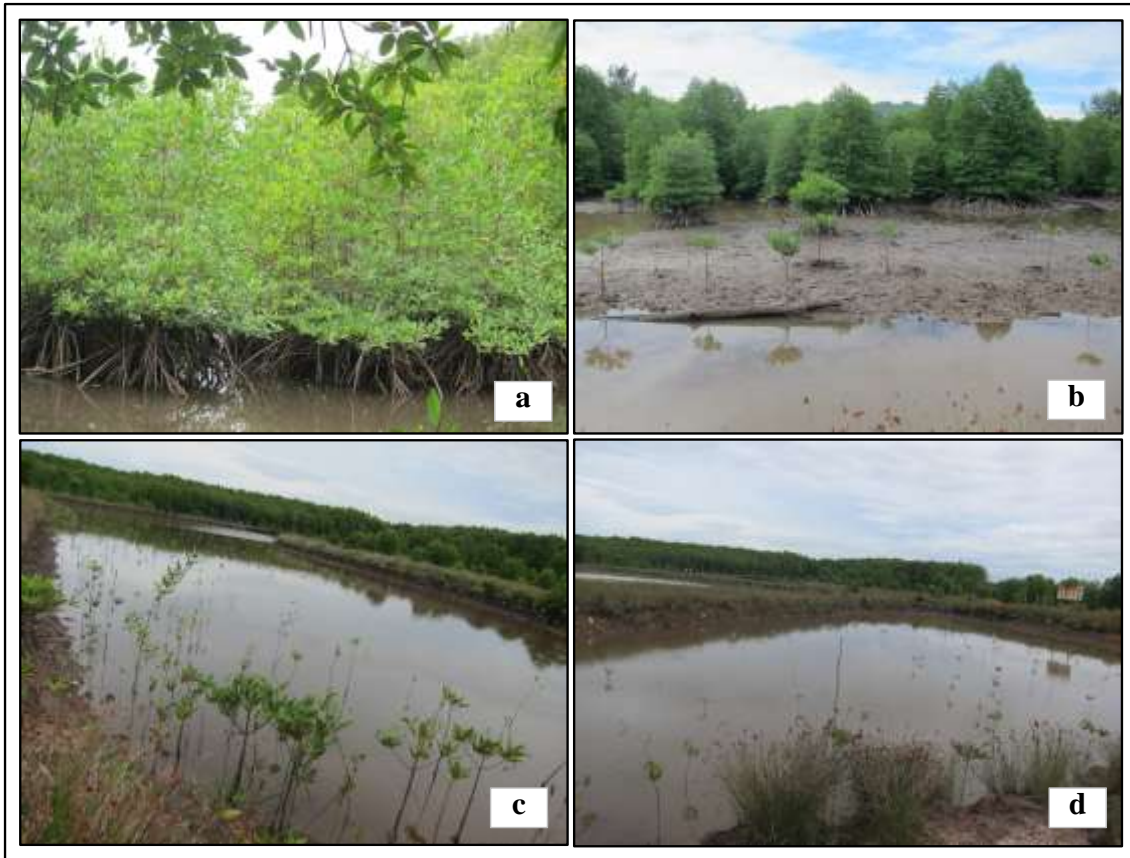


Figure 5.2 Example of mangrove coverage and schematic sketch of an integrated shrimp–mangrove pond farming system in Mengkabong area. (a) Dense and healthy mangroves species (*Rhizophora apiculata* sp.). (b) Degraded mangrove area. (c) Inactive shrimp pond with mangrove seedlings of the replanting project (d) Active shrimp pond in mangrove area. (Source: Field survey photographs, 2013)

5.3.2 Acquisition of Remote Sensing Data

Time-series MODIS EVI data were selected and downloaded from the Oak Ridge National Laboratory (ORNL) Distributed Active Archive Center (DAAC) website. The data were acquired for the period from January 2000 until December 2013 (14 years) with a 16-day (half-monthly) interval. Quarterly temporal periods (e.g., January–March, April–June, July–September, and October–December) were used for the analysis. January was chosen as the starting point of our 3-month periods to conform to the

calendar year. A total of 56 data segments of EVI time series at quarterly temporal intervals were used in this study.

Other data, such as land surface reflectance (MODIS MOD 09Q1) and MODIS land–water mask (MODIS MOD 44W), were also included in this study. The MODIS land–water mask data were used to cut out the boundaries of the EVI data. Both of these data also were acquired from the ORNL DAAC website. **Figure 5.3** shows the protocols of the MODIS data acquisitions using the ORNL DAAC website.

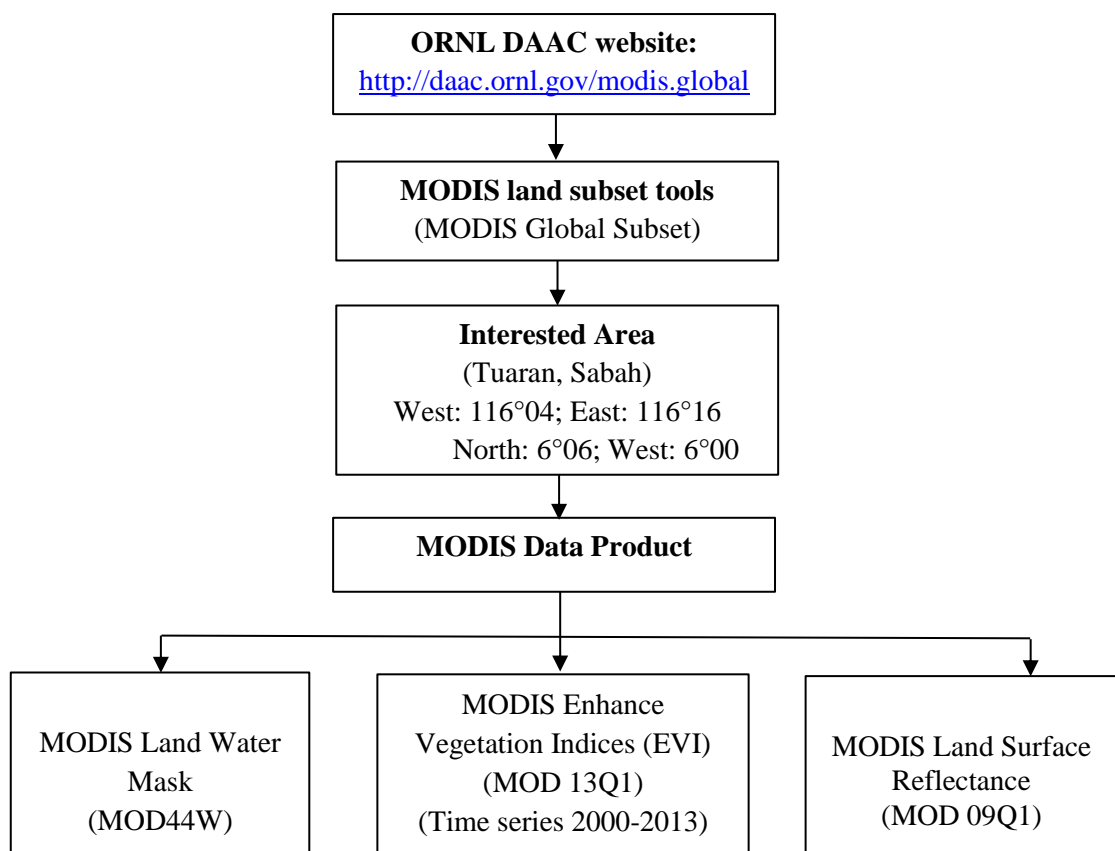


Figure 5.3 Access protocols of MODIS data using the ORNL DACC website

The ORNL website has *MODIS global subset tools* that provide several time series of MODIS data for a specific area worldwide. This site is intuitive and it provides step-by-step instructions for downloading the data. Another advantage of this site is that the data can be downloaded as Geo-tiff files in latitude–longitude format, which can be

opened easily by any image processing software program. **Table 5.1** shows the data characteristics used in this study.

Table 5.1 MODIS data characteristics used in this study

Sensor	Code	Product	Temporal Resolution /Bands	Processing Level	Spatial Resolution
	MODIS MOD 13Q1	Enhance Vegetation Index	16-day interval yearly temporal		
MODIS Terra	MODIS MOD 09Q1	Surface Reflectance	Band 1&2	Level 3	250 m
	MODIS MOD 44 W	MODIS Water Mask	Global		

5.3.3 Data Pre-processing

All of the downloaded MODIS-EVI time-series datasets (2000–2013) were pre-processed to reduce noise and normalize the data. The EVI time-series data also contain errors caused by disturbances such as atmospheric variability and aerosol scattering, along with some residual errors (Lu *et al.*, 2004; Xiao *et al.*, 2003). These errors would degrade the quality of the data and confuse the temporal sequence analysis. Wavelet transformation for noise reduction analysis (Setiawan *et al.*, 2011) was applied to the MODIS-EVI time-series datasets to filter noise from the data. Thus, the purpose of the pre-processing analysis is to correct, smoothen, and normalize the data. **Figure 5.4** shows the MODIS data preparation and pre-processing protocols that were used in this study.

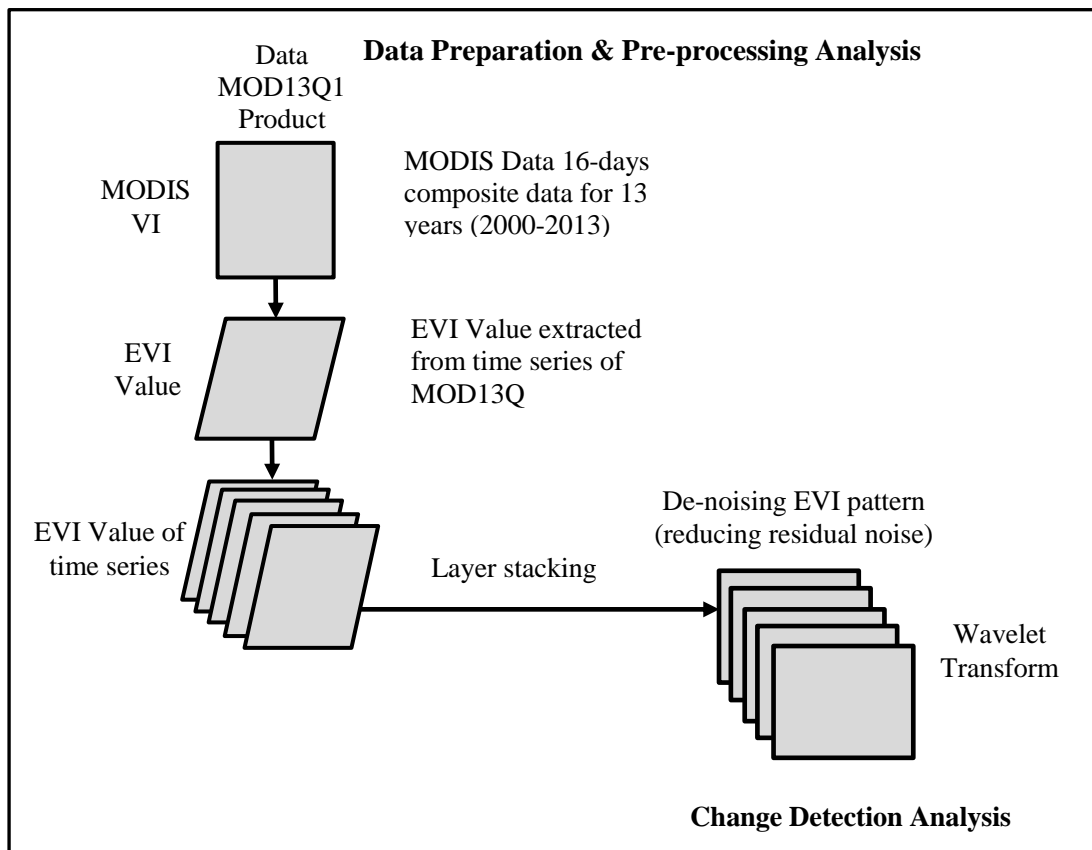


Figure 5.4 Data preparation and pre-processing analysis of the MODIS data

5.3.4 Change-point Analysis

Next, the MODIS EVI time-series datasets were proceeded to the change detection using change-point analysis. Change-point analysis is used in this study to detect whether a pixel was deforested and when the deforestation occurred. Taylor (2000) stated that change-point analysis is a powerful tool for determining whether a change has taken place and that it is capable of detecting subtle changes missed by control charts. Furthermore, this technique is simple to use and interpret, especially for large datasets and/or when multiple changes have occurred.

The EVI datasets for the years of 2000–2013 captured the temporal signatures of greenness of each pixel in the Mengkabong area. Examples of two scenarios (mangrove and shrimp pond) in the EVI temporal profile are shown in **Figure 5.2(a)**. If the pixels

of land cover do not change significantly during the period of study, the EVI temporal profile will show no significant changes. However, there may be some temporal variation in the EVI signal of any pixel due to shedding of old leaves, growth of new leaves, or random noise signals (Rahman, 2013). In contrast, if a mangrove pixel was fully or partially converted to shrimp pond area, the profile would then show a significant drop in EVI values and would remain low after the changes (**Figure 5.2(b)**).

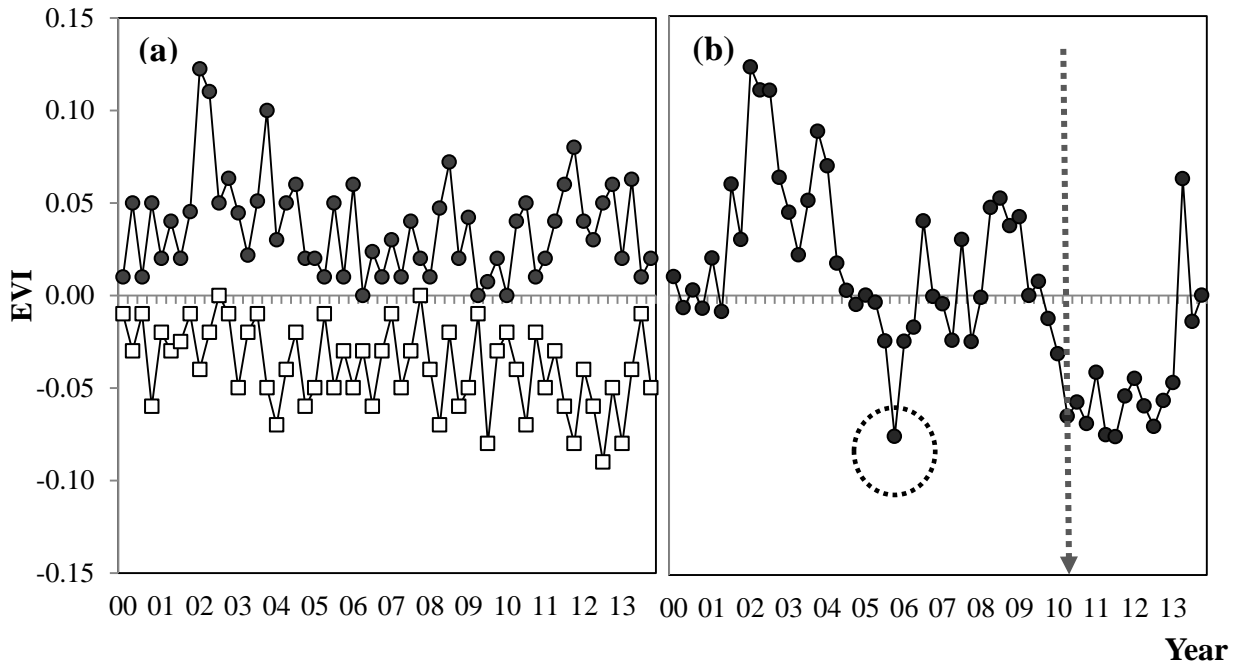


Figure 5.5 Identification of temporal change in EVI temporal profile using change-point analysis. (a) Example of EVI time series for two scenarios: unchanged mangrove area (top) and unchanged shrimp pond area (bottom). (b) Conversion of mangrove area to shrimp pond area. The vertical dotted line shows the occurrence of a change and the estimated time when the change occurred. The dashed circle shows outlier data.

Thus, the aims of the change-point analysis were to determine significant changes in the mean distribution across the time series and to identify when the changes occurred. Cumulative sum (CUSUM) and bootstrapping were used in this change-point analysis (Taylor, 2000). The analysis was performed using Microsoft Excel 2010. In this study, the CUSUM of the difference between each EVI value of a pixel and the long-term mean of EVI values of that pixel was used to determine the timing and

magnitude of the changes in terms of mean EVI value. The CUSUM time series of the EVI data was calculated as follows:

$$S_i = S_{i-1} + (X_i - \bar{X}), \quad (\text{Eq. 1})$$

where X_i represents the consecutive 56 quarterly values of any pixel ($i = 1, 2 \dots 56$), \bar{X} represents the average of 56 quarterly values of EVI data, and S_i represents the CUSUM of the time series.

In the absence of significant changes in the EVI time series, the CUSUM curve shows a relatively horizontal random path along the x -axis. If a change takes place, the CUSUM shows peaks (either positive or negative) that correspond to the mean of the changes. In this case, the difference between the maximum (S_{max}) and minimum (S_{min}) values of the CUSUM is the magnitude of the changes (S_{diff}). A total of 1,000 synthetic datasets were generated from the observed time series by random sampling without replacement. S_{diff} was calculated for each dataset as follows:

$$S_{diff} = S_{max} - S_{min} , \quad (\text{Eq. 2})$$

where

$$S_{max} = \max S_i , i = 0 \dots 56$$

$$S_{min} = \min S_i , i = 0 \dots 56 .$$

Once S_{diff} was calculated, bootstrap analysis of the 56 datasets, denoted as $X^0_1, X^0_2 \dots X^0_{56}$, was performed. Bootstrap analysis is a numerical sampling technique in which the data sampled are resampled with replacement (John, 2011). The bootstrap CUSUM, denoted as $S^0_1, S^0_2 \dots S^0_{56}$, were calculated as in Equation 1. The maximum, minimum, and difference of the bootstrap CUSUM, denoted as S^0_{min}, S^0_{max} , and S^0_{diff} , respectively, were calculated as in Equation 2. Then, it was determined whether or not the difference bootstrap, S^0_{diff} , was less than the original difference, S_{diff} . The level of confidence that change occurred as a percentage was determined as follows:

$$\text{Confidence level} = 100 \frac{X}{N} \% \quad (\text{Eq. 3})$$

Once a change was detected, the estimation of the changes occurred could be made using the following equation:

$$\text{MSE (m)} = \sum_{i=1}^m (E_i - \bar{E}_1)^2 + \sum_{i=m+1}^{56} (E_i - \bar{E}_2)^2, \quad (\text{Eq.4})$$

where MSE (m) is the mean square error estimator. Points 1 to m estimate the last point before the change occurred, and points m+1 to 56 estimate the first point after the change of two different means (E1 and E2). Once the occurrence of a significant change was established for any pixel, the forest fraction of that pixel was determined separately using the mean EVI values before and after the change point. For the pixels that showed no significant change across the study period, the entire EVI time series (all 56 values) was used to calculate the forest fraction. The procedure for the data analysis used in this study is shown in **Figure 5.6**.

5.3.5 Validation

Significant change patterns were validated based on the reference data derived from the field survey, Landsat data series images (TM, ETM+, and OLI_TIRS), high-resolution images from Google Earth, and other secondary data. The secondary data of aquaculture activities and status of mangrove area were obtained from the Department of Sabah Fisheries and the Sabah Forestry Department.

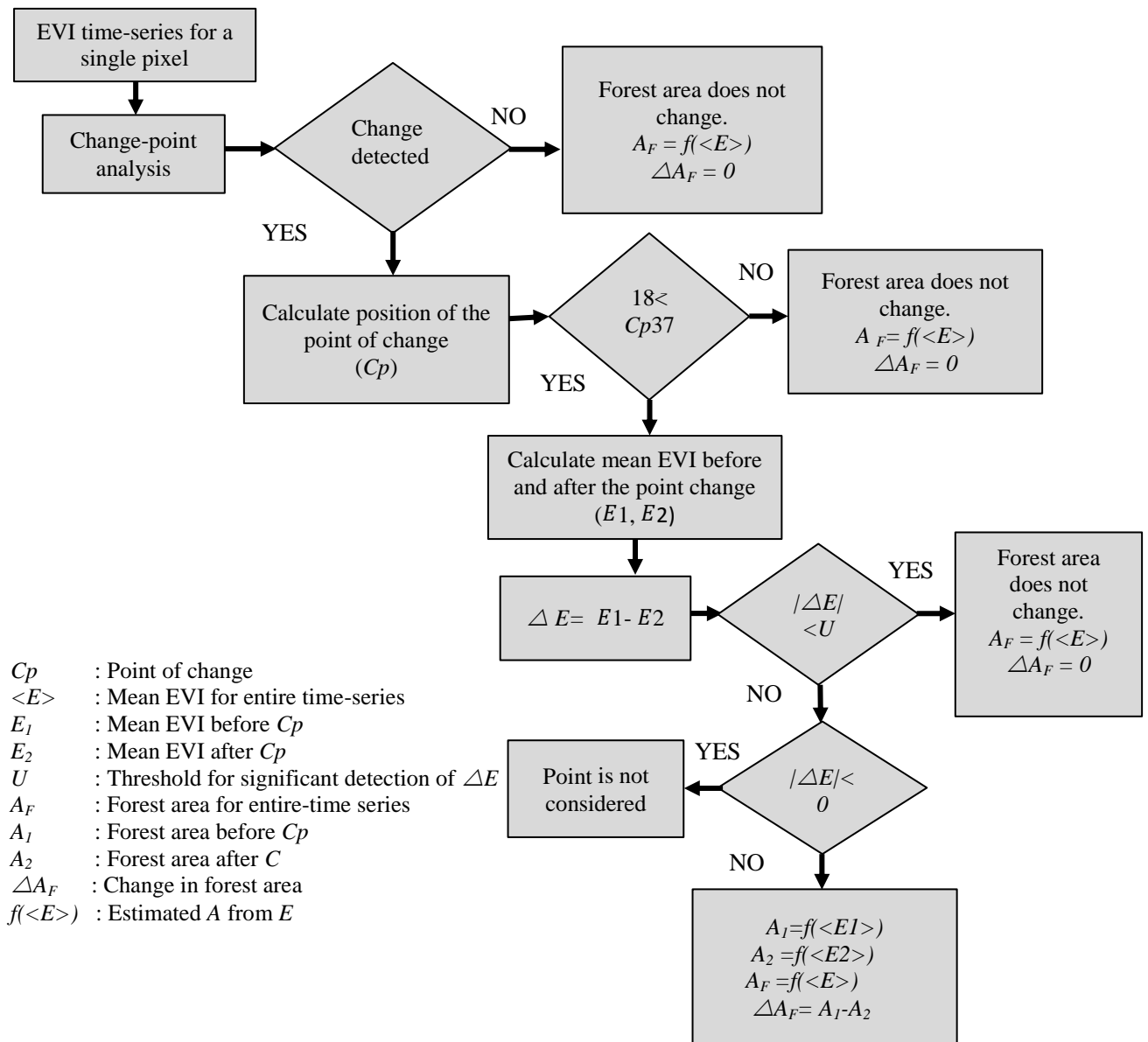


Figure 5.6: Flow diagram of the change-point analysis used in this study

5.4 Results and Discussion

5.4.1 Change Detection

The results of the change-point analysis showed significant changes in the EVI time series of Mengkabong's mangrove areas at the 95% confidence level. The significant drop in EVI values in the negative values shows that the mangrove areas were partially deforested and converted to shrimp pond areas. Several significant changes of EVI values (drop in the negative values) were detected from the MODIS pixels in the years 2000–2001, 2004–2006, 2007–2008, and 2009–2013 (Figure 5.7). The negative values (-0.1 to -0.3) of EVI in 2000–2001 demonstrate that the biomass of mangrove area decreased, with the area converted to shrimp pond farming.

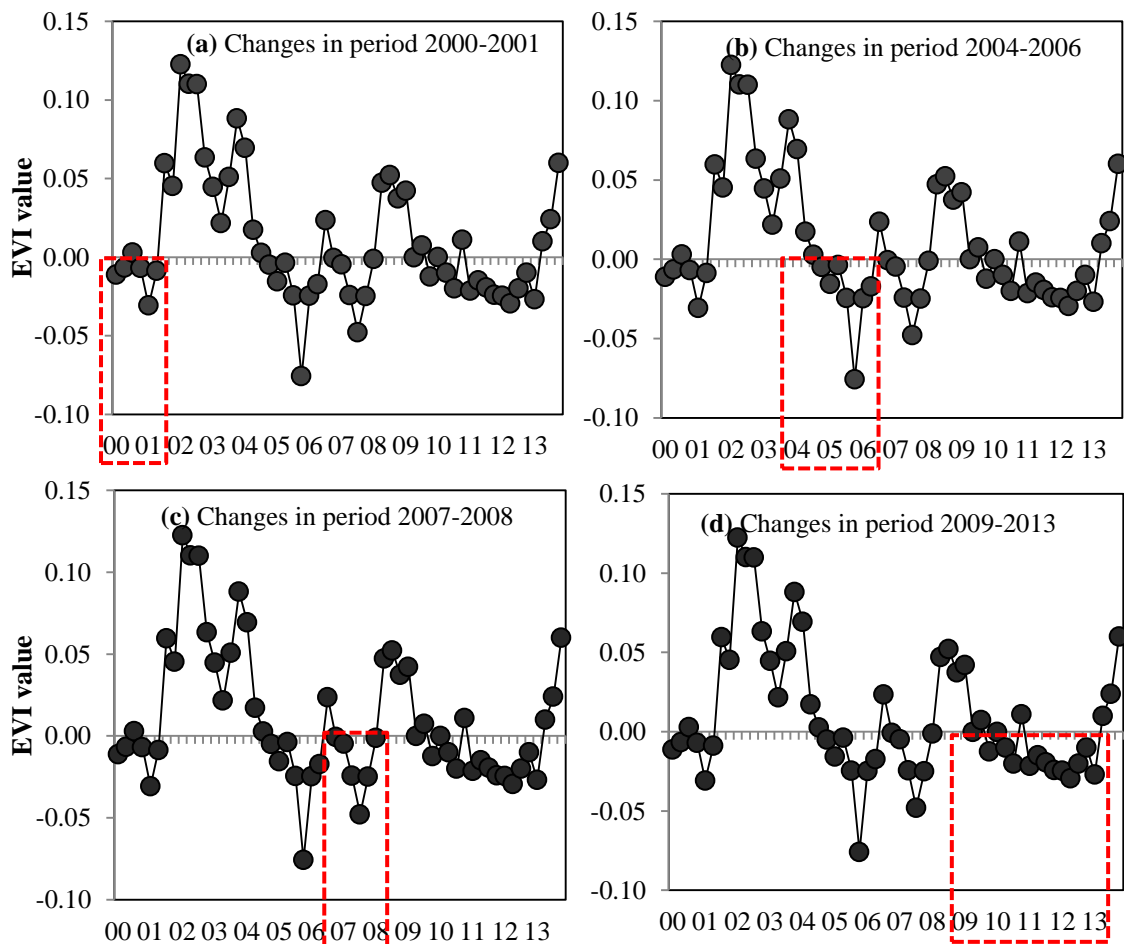


Figure 5.7: Several significant changes of EVI value from a single MODIS pixel that was assigned as the actual change of mangrove area to shrimp pond area

The results of this study are supported by the findings of SFD (2010), whereby more than 15 ha of mangrove areas were converted to shrimp ponds with an average pond size of 2.5 ha in 2000, which was followed by an expanded loss of mangrove to 20 ha in 2001. Eckert *et al.* (2015) confirmed that a decrease of EVI values in the negative values shows that the vegetation area was deforested. In addition, a decrease of EVI values indicates a decrease of biomass of vegetation regions (Huete *et al.*, 2002). The shrimp pond farming activity that began in Mengkabong in the early 2000s may have caused the start of the decrease of the mangrove area EVI values.

Another significant decrease of EVI values, with a range from -0.2 to -0.8, was detected in 2004 to 2006. This decrease was then followed by decreases in 2007–2008 (-0.1 to -0.5) and 2009–2013 (-0.01 to -0.03). These decreases may be due to an increase of shrimp pond areas. Secondary data analysis of the total shrimp pond area in Mengkabong from 2000 to 2013 (**Figure 5.8**) supports the results of this study. The trend of shrimp pond areas in Mengkabong correlates with the decreased pattern of EVI values in the MODIS time-series data. The number of shrimp ponds in Mengkabong increased to more 40, with a total area of almost 90 ha, from 2000 to 2013 (DFS, 2013). The drastic increase of shrimp pond areas led to the deforestation of mangrove forests in the study area.

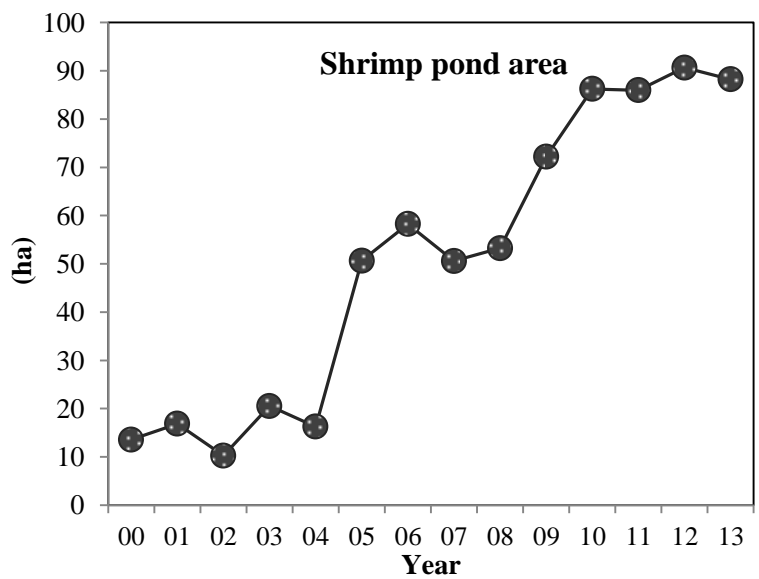


Figure 5.8 Total area of shrimp pond in Mengkabong

The temporal mangrove distributions in Mengkabong for each quarter of the study period are presented in **Figure 5.9**. Based on this figure, mangrove areas decreased significantly from October–December 2005 to October–December 2007, revealing the extent and temporal trend of the extensive mangrove-to-shrimp pond conversion in Mengkabong. However, mangrove areas started to increase in January–December 2008, then slowly decreased in January–March 2009. In April–June 2009, mangrove areas increased again until October–December 2010. Then, they decreased slowly from July–September 2011 until October–December 2012.

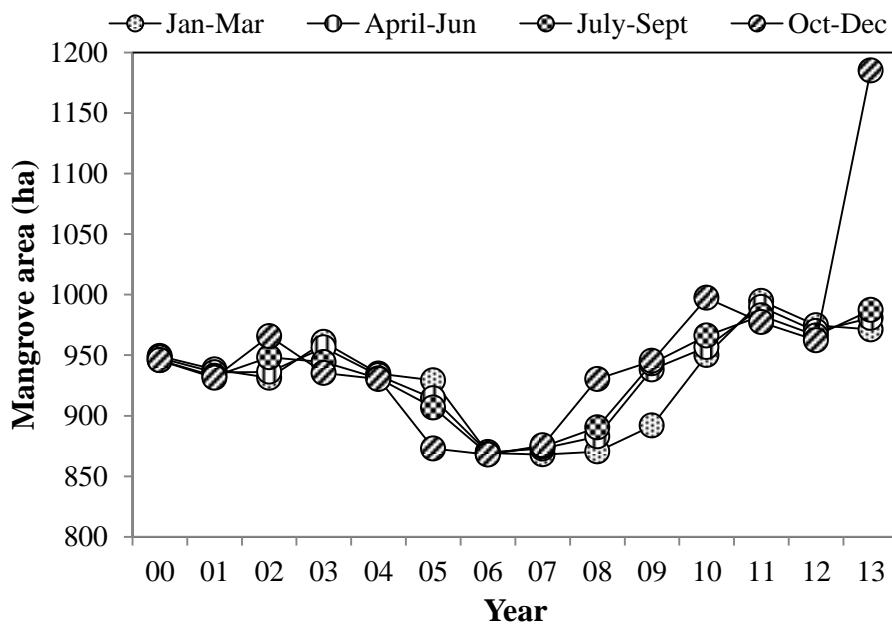


Figure 5.9 Temporal distribution of Mengkabong mangrove area for each quarter of each year

The increases mentioned above may be related to the mangrove replanting and restoration project in Mengkabong. The project, costing approximately RM 5 mil, was implemented in Sabah by the SFD from the end of 2006 to 2010. This project was implemented because of the decreasing mangrove forests in Sabah and to protect the coastal areas from erosion. However, the unsuccessful project faced several problems, including the red tide phenomenon, strong currents, and disturbances by the barnacle

population and livestock, causing high mortality of the mangrove seedlings (SFD, 2010). The low level of public awareness about the importance of mangrove restoration was also a reason for the failure of the project.

The increase of mangrove areas in October–December 2013, with almost 1,200 ha, was due to an extensive mangrove replantation project that was conducted by the Kota Kinabalu Wetland (KKW) Centre and SFD. Many international non-government organizations were involved, and these organizations contributed funds and expertise that helped make the project successful. Under the project, 25,000 mangrove seedlings were replanted in the mangrove areas (SFD, 2013).

5.5 Summary

In this study, the combination of MODIS EVI time series and change detection was used to generate a virtual reconstruction through 14 years (2000–2013) of the conversion of mangrove areas to shrimp ponds in Mengkabong using a spatial resolution of 250 m and a temporal resolution of 3 months. The significant decreases in MODIS EVI time-series negative values in 2000–2001, 2004–2006, 2007–2008, and 2009–2013 confirmed that the mangrove areas in Mengkabong were partially deforested and converted to shrimp pond areas. The temporal patterns of the mangrove distributions for each quarter of each year clearly showed the timing of the deforestation of Mengkabong's mangrove areas. With the continuation of satellite data acquisition by MODIS, it will be useful to monitor and verify changes of Sabah's mangrove forests in the future.

Chapter 6

Satellite Monitoring Procedures for Mangrove Change Detection and Conservation Management Plan in Sabah

6.1 Introduction

Satellite remote sensing monitoring has been found to be a valuable tool for application in forest management, including management of mangroves. The advantages of this application tool are not only in monitoring, but also for carrying out relevant observations that can reveal the impact of deforestation on global climate. Mangrove change detection using satellite data is a powerful tool to visualize, measure, and better understand trends of mangrove ecosystems (Binh *et al.*, 2005; Seto *et al.*, 2007; Thu & Populus, 2004; Wang *et al.*, 2003). It enables the evaluation of subtle changes over a long period of time (as trends), as well as the identification of sudden changes due to natural or anthropogenic impacts (e.g., tsunami destruction or conversion to shrimp farms) (Giri *et al.*, 2008; Ramachandran *et al.*, 2000; Sirikulchayon *et al.*, 2008; Thu & Populus, 2004).

The multi-temporal remotely sensed Landsat series (TM, ETM+, and OLI_TIRS) and MODIS data have been suggested to be more applicable to the identification of mangrove deforestation area, mapping the growth of mangrove forest area, and tracing the major changes in mangrove land cover (Blasco *et al.*, 1998; Giri *et al.*, 2007; Green *et al.*, 1998; Karthisen & Birgham, 2001; Kuenzer *et al.*, 2011). The application of these remotely sensed data in mangrove studies has shown many advantages, such as high cost-effectiveness, large-scale monitoring, time savings, and long-term data access (Aschbacher *et al.*, 1995; Blasco *et al.*, 1998; Green *et al.*, 1998; Hernandez *et al.*, 2005; Manson *et al.*, 2003; Mironga, 2004; Mumby *et al.*, 1999; Lee & Yeh, 2009; Wang *et al.*, 2003). In addition, both of these remotely sensed datasets are freely

available from the National Aeronautics and Space Administration (NASA) and the U.S. Geological Survey (USGS).

Application of Landsat series and MODIS remotely sensed data in mangrove studies has been performed extensively since the 1970s and the 2000s, respectively. Among these data, Landsat TM and ETM+ have been used widely in the mangrove studies. The improvement by several additions of infrared bands and the spatial resolution of 30 meters of TM and ETM+ have promoted the application of both these data for mangrove monitoring (Green *et al.*, 1998). In addition, the new development of the Landsat series OLI_TIRS data in the year 2013 has made available the new advantages of these remotely sensed data.

Many previous studies have successfully measured, visualized, and monitored the changes of mangrove forest using multi-temporal Landsat series and MODIS data (Giri *et al.*, 2007; Sirikulchayon *et al.*, 2008; Sulong *et al.*, 2002; Thu & Populus, 2004). One of the special characteristics of MODIS data for providing a large spatial coverage is the ability to observe an entire region or a whole country at the same time with almost the same atmospheric conditions, which simplifies data processing and analysis (Doung, 2004; Rahman *et al.*, 2013; Vo *et al.*, 2013).

Furthermore, MODIS data are available in short revisit time (1 to 2 days). Thus, these data offer the possibility of creating a cloud-free composite, which is essential for the establishment of a multi-temporal dataset, a very important need for environment monitoring. Therefore, the availability of continuously acquired MODIS data has promoted the application of these data for mangrove monitoring and mapping (Rahman *et al.*, 2013; Vo *et al.*, 2013).

In Sabah, satellite monitoring of mangrove forests is not yet well applied, even though there have been massive mangrove deforestations. Increases in population occurring simultaneously with the expansion of agricultural land, aquaculture activities, industrial activities, and urban development have caused a significant proportion of Sabah's mangrove forest area to be destroyed (Jakobsen *et al.*, 2007; Polpanish, 2008;

Sabah Forestry Department, 2012). Although, the mangrove replanting project has been conducted to manage the degraded areas, limited continuous monitoring contributes to the lack of success of this project. According to the Sabah Forestry Department (SFD) (2010), about RM 5 million was expended on the mangrove replanting project in Sabah from 2006 to 2010. However, the expenditure might increase due to the high cost of maintenance of this project. Thus, applying the satellite remote sensing technology for mangrove change detection and monitoring will promote the effectiveness of the management plan for mangrove conservation in Sabah.

6.2 Objectives

The main objective of this study is to develop schematic procedures of the satellite remote sensing application for change detection and monitoring for mangrove forest management in Sabah. To achieve this objective, the following specific were established:

1. To simplify procedures for Landsat and MODIS remotely sensed data application for a mangrove change detection and monitoring program in Sabah.
2. To assess the potential of the cost-effectiveness of the remotely sensed for mangrove studies in Sabah.

6.3 Materials and Methods

Eight major steps of the change detection and monitoring process for mangrove studies in Sabah using remotely sensed data were developed, as described in the following.

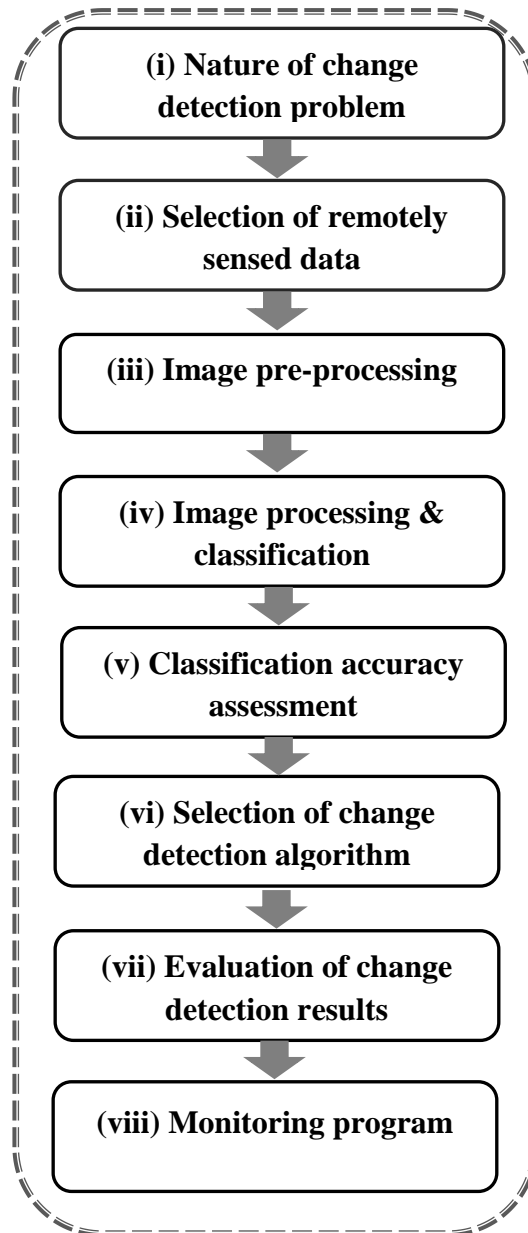


Figure 6.1 Eight major steps of remote sensing-based land cover change detection and monitoring procedures for mangrove studies in Sabah

6.3.1 The Nature of Change Detection Problems

Before a change detection assessment is conducted in a specific study area, it is very important to clearly define the research problems that need to be solved, the objectives,

the location, and the size of the study area (Jensen, 2005). These issues directly affect the selections of remotely sensed data and the selection of change detection algorithms. Detailed descriptions of the nature of the problem in this study follow.

(i) Mangrove Deforestation Problem in Sabah

Recently, deforestation of mangrove forest in Sabah has been occurring at an alarming rate. The continuous pressures from socioeconomic activities such as aquaculture and urbanization and the large-scale commercial exploitation of mangrove resources have caused partial destruction of the mangrove in Sabah. The mangrove areas at risk include Kota Kinabalu, Tuaran, and the problem is increasing extensively in Tawau, Sandakan, and Semporna, where the demand for land for both commercial uses and housing development is high (Sabah Forestry Department, 2012). **Figure 6.2** shows the current condition of mangrove areas in Sabah. However, due to limited study time, only the Tuaran area was selected in this research. The background of the Tuaran study site was explained in detail in Chapters 3, 4, and 5 of this research.

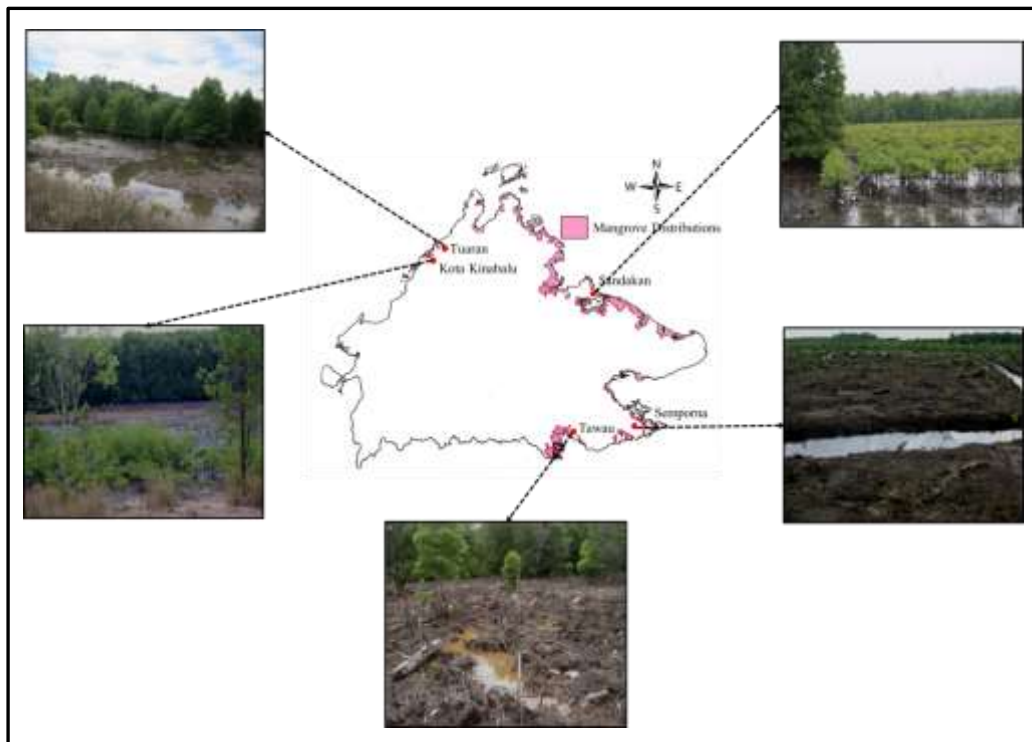


Figure 6.2 Current conditions of mangrove forest in Sabah

6.3.2 Preparation and Selection of Remotely Sensed Data

Many remotely sensed data generated from both airborne and spaceborne sensors with different spatial, radiometric, spectral, and temporal resolutions are available. In order to select suitable datasets for a specific study, it is important to understand the strengths and weaknesses of the various types of sensor data. In addition, cost-effective, large-scale, and long-term temporal remotely sensed data are recommended for mangrove study in the Sabah area. Thus, Landsat data series (TM, ETM+, and OLI_TIRS) and MODIS data were proposed for the data selections. The protocols of both the satellite remotely sensed data acquisition and the selections that were made in this study are described in the following.

(i) Acquisition and Selection of Landsat Data Series

The Landsat data series (TM, ETM+, and OLI/TRS) were downloaded freely from many websites, including the following sites:

- 1) Earth Explorer US Geological Survey (USGS) (<http://earthexplorer.usgs.gov/>)
- 2) Global Visualization Viewer (<http://glovis.usgs.gov/>)
- 3) Landsat Org (<http://www.Landsat.org>)
- 4) Global Land Facility (<http://glcf.umd.edu.>)

All of these websites provide thousands of free satellite imagery of the Landsat series for any interest of any study area. The United States Geological Survey (USGS) announced on April 21, 2008, that it will provide all Landsat data archives for free. Landsat has been providing standard processing algorithms for data and applied terrain correction, making it very easy to use. There are three types of Landsat data-level corrections: standard terrain correction (Level 1T), systematic terrain correction (Level 1GT), and systematic correction (Level 1G) (USGS, 2013). The selection of the data types depends on the particular study.

However, all of these types of Landsat data are very compatible for mapping, change detection, and monitoring of the mangrove ecosystem (Churches *et al.*, 2014; Fatoyinbo *et al.*, 2008; Liu *et al.*, 2008). In addition, the quality level of the remotely sensed data, such as less cloud cover and being accurately co-registered, was controlled by the choices from the mentioned websites. Only multispectral bands were thought be suitable for selection for the analysis. Panchromatic and thermal bands were not used during the analysis to avoid the complexities involved with dealing with data at different spatial resolutions. The details of the Landsat data accessing protocols are described in Chapter 3 of this research.

(ii) Acquisition and Selection of MODIS Data

MODIS satellite data were downloaded freely from the following several websites:

- 1) The Land Processes Distributed Active Archive Centre (LP DAAC)
(<http://lpdaac.usgs.gov/>)
- 2) Reverb (<http://riverb.echo.nasa.gov/riverb>)
- 3) Data Pool (<http://lpdaac.usgs.datapool.datapool.asp>)
- 4) Oak Ridge National Laboratory (ORNL) DAAC
(<http://daac.ornl.gov/modis.global>)

All of these websites also provide thousands of free satellite imagery of MODIS data for any interest of any study area. MODIS data include a lot of remotely sensed data with specific code products. Vegetation indices such as NDVI and EVI of MODIS data are commonly used to measure reliable spatial and temporal photosynthetic activity and canopy structure variety of vegetation (Hansen *et al.*, 2002; Morton *et al.*, 2006; Wessel *et al.*, 2004; Zhan *et al.*, 2002).

Therefore, NDVI and EVI are useful for mangrove studies. The vegetation indices of MODIS data (NDVI and EVI) are embedded in the MODIS MOD 13Q1 product. All of these data can be derived at 8-day, 16-day, and monthly intervals for accurate seasonal and interannual monitoring of earth's vegetation both spatially and temporally.

For each site from which MODIS subset data were downloaded, all of the data were saved as a text file in various formats (ASCII format, comma separated, no header) with a log file listing all the unique downloads and their download status. The data saved in this format can be easily reread into any image processing software, such as ENVI software. The details of the MODIS data accessing protocols were described in Chapter 5 of this research.

6.3.3 Remotely Sensed Data Processing (Pre-processing and Processing)

All of the remotely sensed data (Landsat and MODIS) downloaded from the websites were proceeded to the data processing. In the remotely sensed data processing, several steps of pre-processing and image processing were suggested in the previous chapter of this research as being useful for application to mangrove study in Sabah. For the Landsat data, the details of the processing procedures that were developed in the previous chapter (Chapter 3) are suggested to be the standard protocol for the remotely sensed data processing. The gap-filling analysis developed in the pre-processing analysis is useful for correcting the scan-line error in the ETM+ SLC-off data. This analysis has the potential to produce good spatial data of ETM+ SLC-off data for use in further analysis. As discussed in the previous chapter, there are significant differences in land cover classification results before and after the gap-filling process of ETM+ SLC-off data.

In addition, the details of the processing procedures that were developed in Chapter 5 of this research are suggested to be the standard protocol for MODIS data. The MODIS data also contain disturbance caused by some errors such as atmospheric variability (Huete & Liu, 1994), aerosol scattering (Xiao *et al.*, 2003), and residual errors (Lu *et al.*, 2007). Thus, noise reduction analysis on the observed data is required before the analysis of temporal dynamics can be determined. Within this context, a variety of methods has been proposed to process the time series of the satellite image data. Time series smoothing and the residual error method were applied in the previous chapter (Chapter 5).

The remotely sensed data processing in this research was performed using image processing software, such as the Environment for Visualizing Images (ENVI) software and MS Excel 2010. The ENVI software is an image processing system designed for multispectral and hyperspectral data analysis and information extraction.

6.3.4 Classification Analysis

Classification analysis is used to classify the remotely sensed data information that is needed. In this study, the mangrove forest was the main target of the classification analysis. There are many classification techniques (conventional and advanced) that have been suggested for use in mangrove studies. However, only classification techniques such as spectral profile, normalized difference vegetation index (NDVI), maximum likelihood, and decision-tree learning classification integrated with Landsat data series were applied to classify the Mengkabong mangrove in the Tuaran area.

In addition, decision-tree learning is one of the recent advanced classification techniques that can be both accurate and efficient for land cover classification (Defries *et al.*, 1998; Friedl & Brodley, 1997; Friedl *et al.*, 1999; Hansen *et al.*, 1996; Swain & Hauska, 1977). All of these techniques were analyzed using image processing, such as by ENVI software and MS Excel 2010.

6.3.5 Classification Accuracy Assessment

Integrating remotely sensed data with reference data, such as field data, topography, and vegetation, improves the accuracy of the classification. The topographic and vegetation maps used in this study were obtained from the Survey and Mapping Department and the Forestry Department, respectively. After obtaining suitable reference data, the classification results were analyzed for accuracy assessment.

Classification accuracy refers to the degree of correspondence between the classification of remote sensing data and the reference information (Congalton, 1991). Confusion matrices and cross-tabulation of the mapped class were useful for computing

the accuracy of the mangrove classification statistically (Campbell, 2011; Congalton, 1991; Foody, 2002). The details of the mangrove classification using the Landsat data series procedures were described in Chapters 3 and 4 of this research.

6.3.6 Selection of Change Detection Algorithms

There are many change detection methods that can be applied to study land cover change, such as algebraic, transformation, classification, advanced model, geographic information system, and visual analysis approaches (Lu *et al.*, 2004). In this study, the classification, visual analysis, and transformation methods were applied to detect the mangrove change in the Tuaran area. First, the classification and visual analysis methods integrated with the Landsat data series were applied to detect the mangrove change in the Tuaran area. The areas of the mangrove land cover classes were calculated and the land cover change was analyzed statistically.

Then, the enhanced vegetation index (EVI) of the MODIS time-series data integrated with the change-point method was applied to detect the mangrove change in Tuaran. The change-point method is useful for analyzing the changes of MODIS EVI time series (Rahman *et al.*, 2013). From a statistical point of view, a change point is a point in a time series where the distribution of the mean of the observed data changes significantly (Chen & Gupta, 2000). Change-point analysis can answer the two key questions of whether there are significant distributions of mean across the time series and when does change occur (Taylor, 2000). The change detection algorithms that were applied in this study were described in detail in Chapters 3, 4, and 5 of this research.

6.3.7 Evaluation of Change Detection Results

Next, change detection analysis was applied to evaluate the accuracy of the result. The standard accuracy assessment technique was developed mainly for single-date remotely sensed data (Congalton, 1991; Congalton & Green, 2008). However, the error matrix-based accuracy assessment method is the most common and valuable method for evaluation of change detection results (Congalton & Green, 2008), and this method was

applied in the previous chapters (Chapters 3 and 4) of this study. Then, the results of the mangrove land cover change were presented in either maps or graphs. The details of the Landsat and MODIS data processing that were used in this research are presented in **Figures 6.3a** and **6.3b**, respectively.

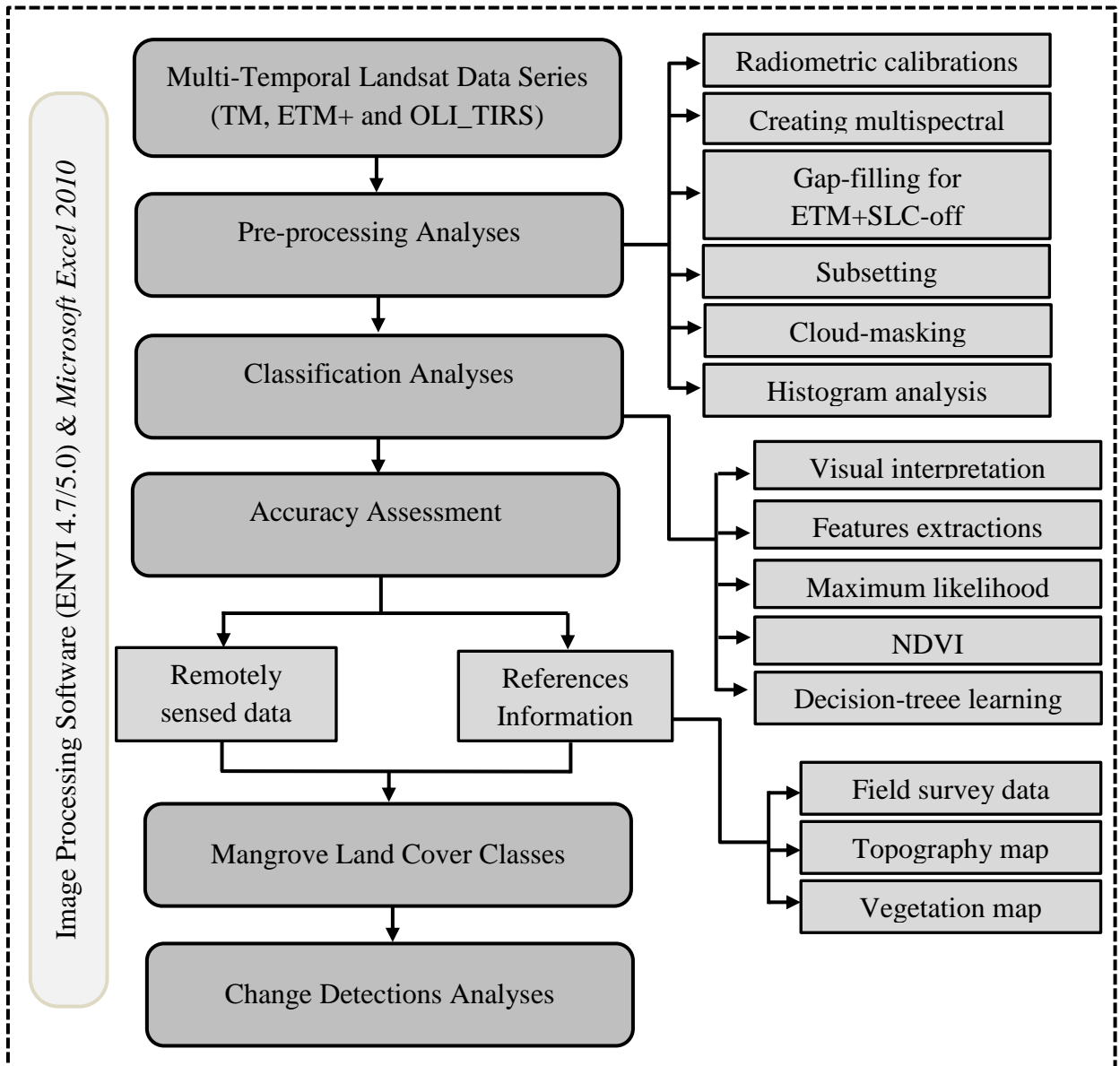


Figure 6.3(a) Mangrove classification and change detection protocols for Landsat data series

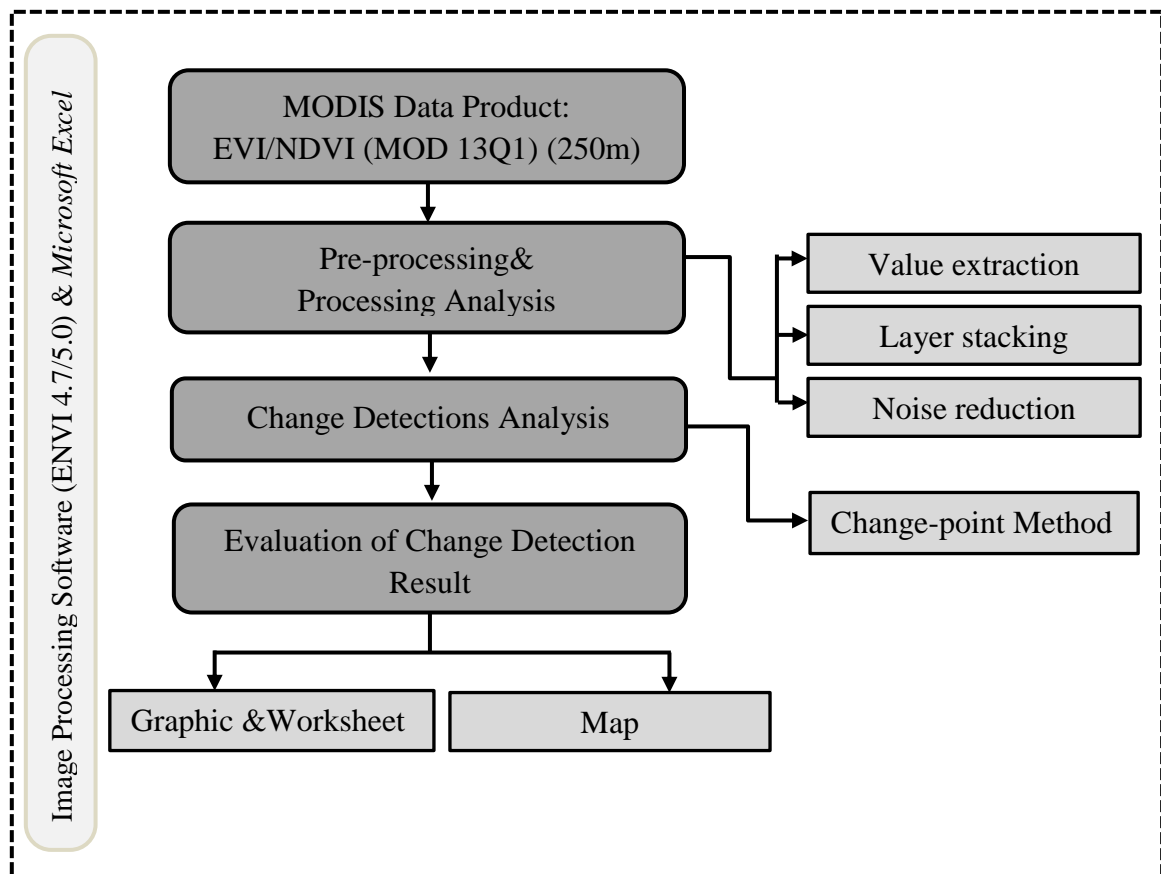


Figure 6.3(b) Mangrove change detection protocols for MODIS (VI) time-series data.

6.3.8 Monitoring Program

Since the schematic procedures for mangrove change detection were developed, the monitoring program using remote sensing technology has been applied extensively. In addition, the integration of cost-effectiveness, large scale, long-term temporal remotely sensed data, and better accuracy, such as by using Landsat series and MODIS, promotes the many advantages of applying remote sensing tools for mangrove forest monitoring, especially in Sabah. Therefore, mangrove monitoring using remote sensing tools has been implemented in the mangrove conservation management plan.

6.4 Results and Discussion

The availability of the developed protocols for application of remotely sensed data and the other results of this study have promoted the mangrove monitoring program in the Tuaran area.

6.4.1 The Nature Change Detection Problem

The Tuaran area is located within the region of 6°8'24" N to 6°11'24" N latitude and 116°08'6" E to 116°12'54" E longitude (Google Earth, 2012) (**Fig. 6.4**). Prior to the 1990s, the Tuaran area was almost entirely covered with *Rhizophora apiculata*, a healthy and dense mangrove species (Sabah Forestry Department, 2010). The total mangrove area in the 1990s was 1260 ha. However, this area experienced a 15% decrease from 1990 to 2000.

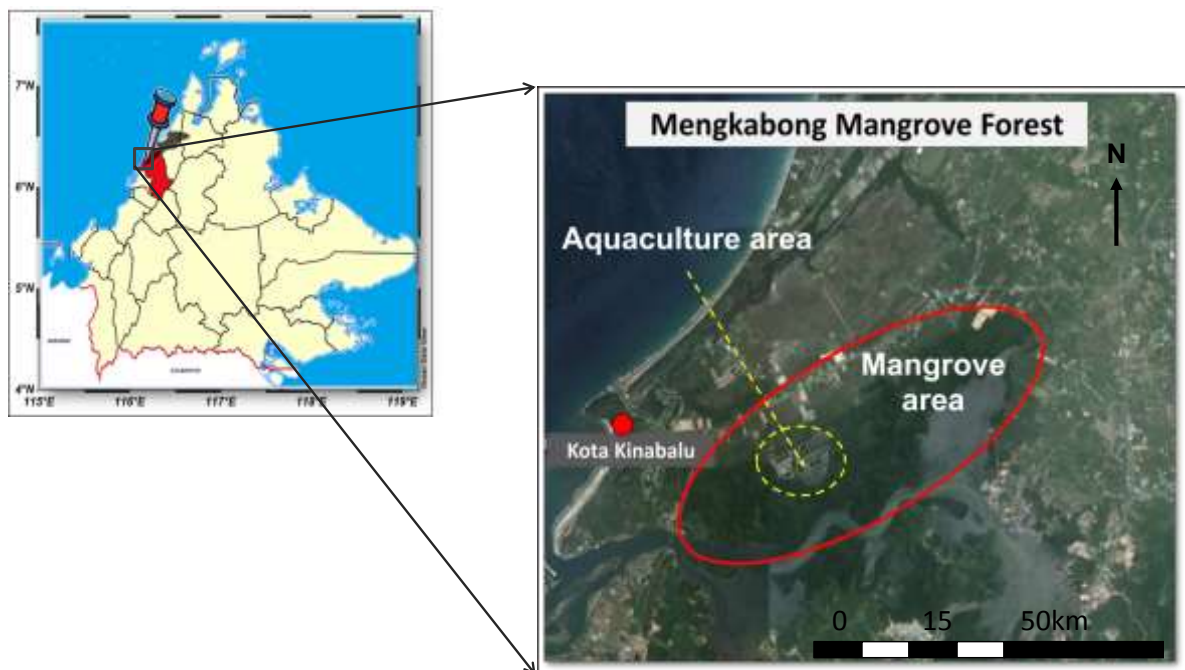


Figure 6.4 Location of study area

The main factor affecting the reduction of Tuaran mangrove was shrimp pond farming activity. This activity began in the early 2000s, after which more than 15 ha of mangrove area were converted to shrimp ponds with an average area of 2.5 ha for each pond. These activities have been continuing gradually, resulting in increases in the number of pond areas. The increased demand for tiger shrimp (*Penaeus monodon*) has been a factor in the increase of shrimp pond areas in Tuaran. The drastic increase of shrimp pond areas led to deforestation of the mangrove forests in the study area. **Figure 6.5** shows the shrimp pond farming in the Tuaran mangrove forest, which was acquired during the field survey in November 2011 and September 2013.



Figure 6.5 Shrimp pond in the Tuaran mangrove area
(Source: Field survey photographs)

6.4.2 Selection of Remotely Sensed Data

The available free data access websites and acquisition developed protocols promotes the selection process for good satellite data of Landsat series and MODIS in this study. The used of both data provided an advantages of the cost-effective, large-scale, and long-term temporal of remotely sensed data for the mangrove study in Tuaran. In addition, the Landsat has been providing standard processing algorithms data and terrain correction applied, making it very easy to use. The used of temporal pattern MODIS enhanced vegetation index (EVI) datasets has significant advantages for both capturing the actual timing of change events and monitoring of mangrove growth.

6.4.3 Remotely Sensed Data Processing (Pre-processing and Processing)

The use of the processed multi-temporal Landsat data series (1990–2013) and the MODIS data with the developed protocols improves the potential for producing high quality satellite data. The gap-filling analysis developed in the pre-processing analysis is useful for correcting the scan-line error in the ETM+ SLC-off data. The selection of an appropriate gap-filling analysis process produced a good spatial result in the final ETM+ SLC-off data. The result of this analysis was supported the study by Singh & Sherman (2010). **Figure 6.6** shows the final ETM+ SLC-off data produced by the gap-filling analysis.

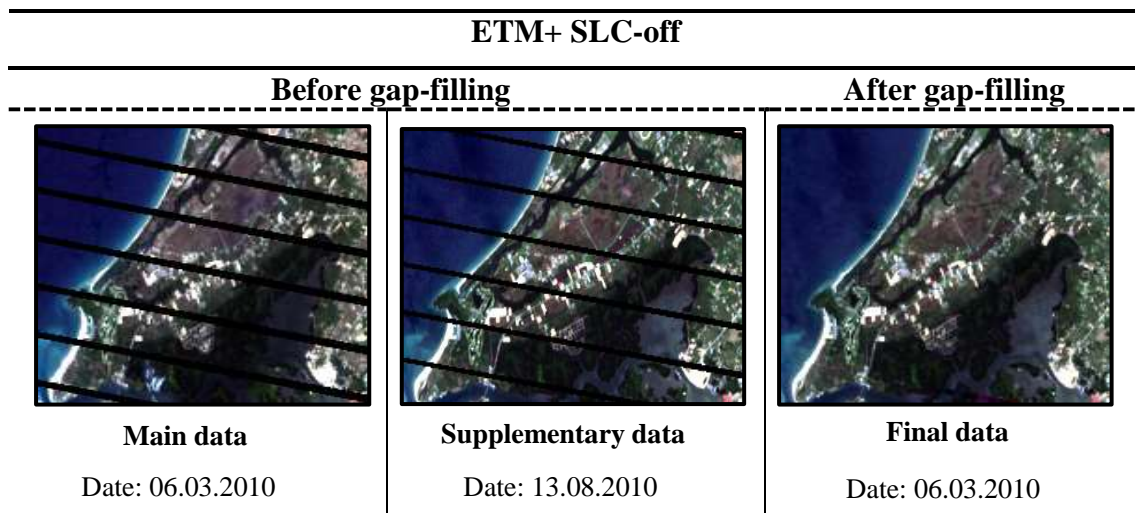


Figure 6.6 Landsat ETM+ SLC-off data before and after gap-filling analysis

The cloud masking technique that was applied in this study is useful for removing cloud cover in the Landsat images. The protocol of the analysis was explained in detail in Chapter 3. Furthermore, the processing procedures that were developed for correcting disturbance in the MODIS data produced a smoothed time-series MODIS EVI. Therefore, the pre-processing analysis that was applied in this study has the potential to produce good results of processed Landsat data for further use, especially for mangrove study.

6.4.4 Classification Analyses and Accuracy assessment

The use of the classification protocols integrated with conventional (visual interpretation, spectral profile, NDVI, and maximum likelihood) and advanced (decision-tree learning) remote sensing techniques showed high accuracy of mangrove and non-mangrove classification in the Tuaran area. The use of the NDVI classification technique in MS Excel and the spectral profile technique should improve the effectiveness of mangrove classification in the Tuaran area.

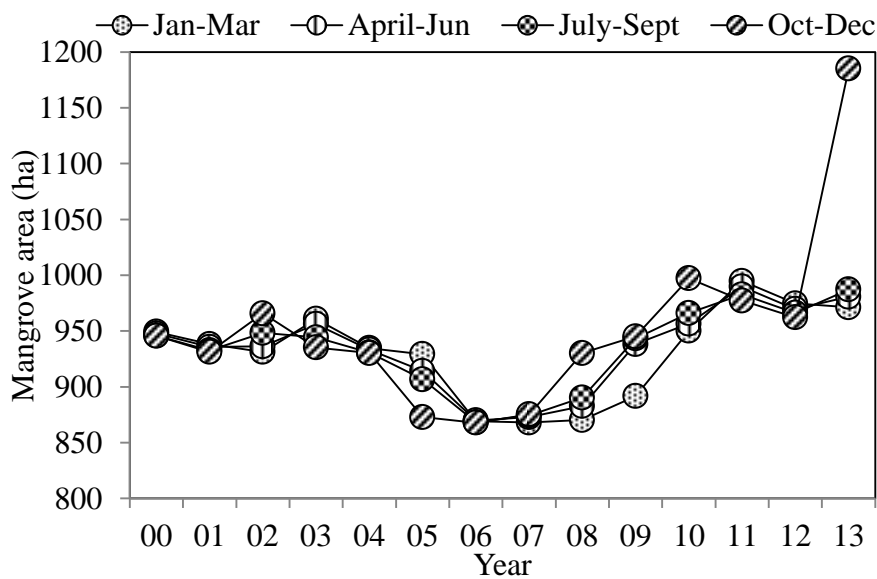
Furthermore, the application of the decision-tree learning technique integrated with GIS ancillary data successfully classified mangrove and non-mangrove areas. The selection of good attributes from the spectral features of Landsat and from the topographic data (DEM and distance to coastline) from the GIS database for mangrove classification promoted a highly accurate result (90.8% accuracy).

6.4.5 Selection of Change Detection Algorithm

The use of change-point analysis integrated with enhanced vegetation index (EVI) MODIS time-series data revealed the history of the destruction of mangrove forest and the aquaculture activities in the Tuaran area. The significant decrease in MODIS EVI time-series negative values confirmed that Tuaran's mangrove areas were partially deforested and converted to shrimp pond areas. Temporal patterns of mangrove distribution for each quarter of each year clearly showed the timing of deforestation of Mengkabong's mangrove areas.

Figure 6.7 shows the temporal distributions of Mengkabong mangrove area for each quarter of each year. This result confirmed that the shrimp pond farming started in 2000. The result of increasing mangrove area in 2010 to 2013 was supported by the replanting project that was conducted by the Sabah Forestry Department in early 2010. In 2010, the Sabah Forestry Department did its first transplantation project but it was unsuccessful (decrease of area from 2011-2012) because of livestock disturbance and red tide.

The increase of mangrove area in year 2013 might have been caused by the second mangrove seedling transplantation done by Sabah Forestry Department. According to Sabah Forestry Department (2013), more than 25,000 mangrove seedlings (6-8 months old; 40-50 cm height) were successfully transplanted in the area. **Figure 6.8** shows the mangrove in the replanting areas. The details of mangrove replanting area are shown in the appendix of this dissertation. With the continuation of satellite data acquisition by MODIS, it will be useful to continue to monitor and verify the changes of Sabah's mangrove forests in the future.



6.7 Temporal distribution of Mengkabong mangrove area for each quarter of each year



(Source: Field survey photograph, 2013)

Figure 6.8 Mangroves in replanting area

6.4.6 Evaluation of Change Detection Result

The details of the change detection of the Tuaran mangrove area are presented in the **Table 6.1**. According to the results of this study, Tuaran mangrove forests were distributed extensively in the Mengkabong area in 1990 (1145.16 ha). However, there was a significant decrease from 1990 to 2000 (1145.16 ha to 945.72 ha) and a slight increase from 2010 to 2013 (997.20 ha to 1185.12 ha). Generally, the total area of mangrove forest has been declining (a reduction of 40 ha from 1990 to 2013) and fragmentation is obvious. The change of mangrove forest in the Tuaran area was affected by shrimp pond activities, as discussed in the previous chapter of this study. Furthermore, the integration of remotely sensed data with secondary data acquired from various departments, such as the Sabah Forestry Department, Sabah Fisheries Department, and Survey and Mapping department, supported the results of this study.

Table 6.1 Total Tuaran mangrove area from 1990–2013

Multi-temporal Landsat data	Mangrove area (ha)
1990	1145.16
1995	1024.20
2000	945.72
2005	872.82
2010	997.20
2013	1185.12

6.4.7 Monitoring Program

The mangrove monitoring program using remote sensing technology has been applied frequently in the Tuaran mangrove forest. The availability of schematic procedures promotes the use of the monitoring program for mangrove replanting and rehabilitation projects in the Tuaran area. The combination of cost-effectiveness, large scale, long-term temporal availability, and improved accuracy of the Landsat series and MODIS

data promotes the application of these remote sensing tools for mangrove forest monitoring, especially in Sabah.

6.5 Summary

In summary, remote sensing technology offers considerable advantages in mangrove studies and has become a useful tool for monitoring the changes of the mangrove ecosystem in Sabah. In addition, the availability of schematic procedures for applying the remotely sensed data of the Landsat series and MODIS data to mangrove change detection should encourage the potential use of these data for mangrove monitoring in Sabah in the future.

Chapter 7

Evaluation of Developed Protocols for Monitoring Protected Mangrove Forest in Sabah

7.1 Introduction

Uncontrolled exploitation of protected mangrove forest in Sabah was an impetus for conducting this study. As discussed in Chapter 1, the aim of this study was to develop and apply new remote sensing techniques using low-cost satellite data to monitor changes of protected mangrove in Sabah.

This study was carried out after considering the limitations of the the remote sensing technology currently used for mangrove study. The high cost of high-resolution remotely sensed data with small area coverage, limitations in applying medium-resolution data integrated with recent advanced remote sensing techniques, and lack of availability of free data access protocols with data processing were identified as limitations of the technology often currently used in mangrove studies.

Therefore, the model studies of Chapters 3, 4, 5, and 6 for mangrove study in Sabah developed techniques using low-cost remotely sensed data. The Landsat series and MODIS data are proposed as potential low-cost remotely sensed data that can be used for mangrove monitoring in Sabah.

The results of the model studies show the potential of the remotely sensed data used and the protocols developed for classifying and detecting changes of protected mangrove in Sabah. Thus, this chapter provides an evaluation of the effectiveness of the developed protocols by evaluating the selection of satellite data characteristics, calculating the estimated cost, estimating the time required, and considering the required degree of expertise.

7.2 Objectives

The main objective of this study is to evaluate the effectiveness of the developed protocol for monitoring mangrove forest in Sabah. Specific objectives of this study follows:

1. To evaluate the selection of data characteristics of low-cost remotely sensed data for mangrove study in Sabah.
2. To compare the cost-effectiveness between medium-resolution and high-resolution data.
3. To evaluate the time and degree of expertise required for use of the developed the protocols.

7.3 Materials and Methods

7.3.1 Evaluation of Satellite Data Characteristics

The characteristics of low-cost (Landsat, MODIS) and high-cost (e.g., QuickBird, SPOT-5) satellite data such as spatial resolution, spectral information, temporal frequency data, discrimination level, free data access, and coverage area were variously selected to evaluate the effectiveness of data used for mangrove monitoring in Sabah.

7.3.2 Cost Analysis of Low-cost Satellite Data

The cost was determined based on the types of satellite data, software needs, and processing components. For the cost comparison with high-cost satellite data, the price list of satellite data was obtained from the Malaysia Remote Sensing Agency. The price list included the basic processing components for the satellite data. Furthermore, the price list of software was obtained from the Environmental Systems Research Institute (ESRI) Malaysia.

7.3.3 Time Requirement

The time requirement was evaluated by the time used for the data processing and validation. For the data processing components, time was noted for downloading, interpretation, and analysis.

7.3.4 Degree of Expertise

The degree of expertise was evaluated based on the work required to complete the developed protocols of the satellite data preparation, data analysis, and survey work.

7.3.5 Accuracy of Method

The accuracy of the method was evaluated based on the classification and change detection results for the mangrove forest in the study area with the satellite data used. Secondary data such as the mangrove distributions in Sabah were acquired from the Sabah Forestry Department and were used to validate the results of this study.

7.4 Results and Conclusion

7.4.1 Evaluation of Satellite Data Characteristics

Table 7.1 shows comparisons of satellite data characteristics between the low-cost and the high-cost remotely sensed data. The data characteristics included spectral information, discrimination level, temporal frequency data, coverage area, and free access. All of the selected data characteristics illustrate the benefits and advantages of using low-cost satellite data for mangrove monitoring.

Kuenzer *et al.* (2011) also reported that the selection of satellite data characteristics depends on the purpose of the user's study. As discussed in the first chapter, the main purpose of this study was to develop cost-effective protocols for

mangrove monitoring in Sabah. Therefore, the data characteristics of Landsat and MODIS data described in this study promote the effectiveness of these data for mangrove monitoring in Sabah.

Table 7.1 Comparison of satellite characteristics between low-cost and high-cost satellite data

Satellite Data Characteristics	Low-cost (Landsat series & MODIS)	High-cost (Quickbird, IKONOS, SPOT-5)
Spatial resolution	To coarse / Low (meter)	Very high (centimetre to meter)
Spectral information	Several multispectral bands (R, G, B, NIR, mid-NIR & thermal band)	Relatively few spectral bands (R, G, B, & NIR)
Discrimination level	(i)Mangrove and non-mangrove (ii) Condition status	Down to species level
Temporal frequency data	Available over three decades	Limited
Coverage area	Large-area	Small-area
Free-data access	Yes	No

7.4.2 Cost Calculation

Table 7.2 shows the estimated costs of medium-resolution remotely sensed data and high-resolution data for the total study area. The Landsat series and MODIS data that were used in this were acquired at no cost. Due to the availability of free data acquisition protocols for these data, it is easy to download data and select good data with less cloud cover. Furthermore, the data covered the large area of the study area (>1000 ha). The only cost incurred is for the software packages used, such as ENVI and Arc GIS. The estimated costs of software were obtained from the Environmental Systems Research Institute (ESRI) Malaysia. However, the software packages that were used in this study were financed by Kyoto University.

For the data processing components, the basic processing for the satellite data used in this study was performed at no cost. The developed protocols for the data processing produced good processed satellite data, especially for the Landsat ETM+ SLC-off data. Furthermore, the developed protocol of the pre-processing also could be useful for removing the small amount of cloud cover in the satellite data. The several available websites promotes the selection of good satellite data.

High-resolution data, such as QuickBird, SPOT, and IKONOS data, have high cost compared to medium-resolution data. To acquire data such as SPOT data, at least 200,000 JPY are needed for coverage of the study area. Furthermore, the cost excludes the other data processing levels and other materials needed for the analysis, such as the software.

Therefore, the results show that the low-cost remotely sensed data that were used in this study are very cost-effective compared to high-cost satellite data. Previous studies have also confirmed that the use of Landsat and MODIS data promote the cost-effectiveness of using remote sensing technology in mangrove studies.

Table 7.2 Cost comparison of low-cost and high-cost satellite data

No.	Item	Amount (JPY) (1000 ha)				
		Low-cost data			High-cost data	
		Landsat Series	MODIS	Quickbird	SPOT	IKONOS
1.	Satellite data with Processing level (Pre-processing)	No cost		600,000	200,000	430,000
2.	Softwares :					
	Environment Visualization Image (ENVI)+IDL (Single user)	204,000			204,000	
	Arc GIS Desktop Basic (Single user)	45,000			45,000	
	Microsoft excel			No cost		
	Total	249,000		849,000	449,000	679,000

7.4.3 Time Requirement

The time requirement was evaluated by considering the time used for satellite data preparation, such as downloading, processing, interpretation, and validation. In the beginning of this study, the time used for data preparation took more than a month, excluding the data processing, interpretation, and validation. However, since the method has now been developed, the data preparation, interpretation, and processing should take less than a month. For validation, the collection of reference information such as field survey data and secondary data took a long time compared with the interpretation using the remote sensing data. However, in this study, field surveying for the validation process was conducted only two times. Thus, the time requirement using the developed protocol and field surveying method is more effective than the use of only a conventional method, such as field surveying.

7.4.4 Degree of Expertise

To complete the developed protocols of the satellite data preparation, data analysis, and survey work, a certain degree of expertise is needed. However, the expertise required for the data preparation is only a minimum level (basic level). For the data analysis and surveying work, a reasonable degree of expertise is needed at least for processing the data and knowing how to use the image processing software. However, minimal training of less than a month could be conducted for the beginner.

7.4.5 Method Accuracy

The result of total mangrove area that was produced using the developed protocol was not very different from the secondary data that were acquired from the Sabah Forestry Department. For example, in 2000, the total mangrove area from the developed protocol was 945 ha and that from the secondary data was 950 ha. Thus, the results show that the developed protocol has high accuracy for mangrove study in Sabah.

7.5 Summary

This chapter evaluated the effectiveness of the developed protocols for monitoring protected mangrove in Sabah. The selection of the Landsat and MODIS data characteristics and the cost-effectiveness of the methods promote effective use of low-cost satellite data for mangrove monitoring and change detection studies.

Chapter 8

Conclusions and Recommendations

8.1 Conclusions

Mangrove forests provide critical ecosystem services, fulfill important socioeconomic and environmental functions, and support coastal livelihoods. These forests are also among the most vulnerable ecosystems, both to anthropogenic disturbance and climate change. Even though mangrove forests in Sabah have large distribution, they are declining at an alarming rate due to the conversion to agricultural, shrimp pond farming, and urban development areas, along with other types of deforestation. In order to cope with these problems, the application of satellite technology for estimating and monitoring changes of mangrove forests in Sabah was developed and evaluated in this research. The conclusions of the work are explained as follows.

Chapter 2 provided the available literature pertaining to basic information about mangroves and satellite technology. The basic information on mangroves was introduced in terms of mangrove characteristics, mangrove distribution, mangrove importance, and the threats to mangrove. The satellite technology information began with research identifying the characteristics of mangrove using remotely sensed data and describing the potential of recent and advanced mangrove technologies, including their benefits and limitations.

Chapter 3 highlighted the potential of applying the processed Landsat data series (TM, ETM+, and OLI_TIRS) for classifying the mangrove forest land cover in Tuaran, Sabah. A standard protocol for Landsat data processing was developed for the mangrove classification. The gap-filling processing that was used in this study showed good results for producing Landsat ETM+ SLC-off gap-filled data. The application of Landsat data series in this study demonstrated the advantages of using low-cost

remotely sensed data for mangrove studies. The NDVI and maximum likelihood classification techniques that were applied to the processed Landsat data series (TM, ETM+, and OLI_TIRS) showed good results of land cover classification. However, there remain several limitations and challenges in the interpretation of mangrove by using these conventional methods. Thus, recent advanced classification techniques should be applied to processed Landsat data series for greater validation. This recommendation was applied in Chapter 4 of this thesis.

Chapter 4 examined the potential of recent advanced remote sensing techniques for mangrove research. A decision-tree learning method integrated with multi-temporal Landsat series (TM, ETM+, and OLI_TIRS) was determined and applied for classifying and detecting rapid changes of the Mengkabong mangrove forest area. The results of this study showed that the application of the decision-tree learning method in combination with a dataset comprised of multi-temporal Landsat series (TM, ETM+, and OLI_TIRS) and GIS data can be effective at delineating spatial and temporal changes of the mangrove forest. The integration of various sources of remote sensing data, such as the sources of remote sensing data such as greenness, vegetation moisture content, and reflectance band values improved the classification accuracy of mangrove due to the similarity of the spectra of forest and water–vegetation mixed pixels.

Chapter 5 examined the potential of MODIS time series data for detecting and identifying the conversion of mangrove area to shrimp pond farming in Mengkabong. A simple and robust statistical method of change analysis was developed and applied to the MODIS enhanced vegetation index (EVI) time-series data. The findings of this study confirmed that the technique developed could be applied to determine the history of mangrove deforestation and the development of aquaculture in the Mengkabong area for a 14-year period (2000–2013). With the continuation of satellite data acquisition by the MODIS sensor, this method should be useful for future monitoring and verification of changes of Sabah's mangroves.

Chapter 6 examined the development of a simplified methodology for application of remotely sensed data for mangrove monitoring in Sabah. The cost-effective and long-

term multi-temporal nature of remotely sensed data such as Landsat series and MODIS data were suggested for the specified applications. The schematic procedures started with identify the nature change detection problems. Five potential study sites were identified around Sabah. These study sites were facing mangrove destruction due to human activities such as aquaculture and urbanization. Then, the procedures of remotely sensed data preparation, pre-processing, and classification analysis including selection of change detection algorithms and evaluation of change detection results were followed. Next, monitoring program procedures for the mangrove conservation management plan were suggested.

Chapter 7 evaluated the effectiveness of the developed protocol for monitoring protected mangrove forest in Malaysia. The selection of the Landsat and MODIS data characteristics, the time requirement, and the cost-effectiveness of the methods will promote the use of these low-cost satellite data for mangrove monitoring and change detection studies.

8.2 Recommendations

The results of this study indicated that the low-cost remotely sensed Landsat series and MODIS data have high potential for classifying and monitoring changes in mangrove forests in Sabah. The following recommendations are provided for future studies:

1. Satellite monitoring using cost-effective remotely sensed data should be applied extensively to mangrove monitoring around Sabah in order to gain a better understanding of the trends of mangrove forest change.
2. It is recommended that this research be used as a baseline study to promote the effective use of remotely sensed data for mangrove studies in Sabah.
3. The integration of satellite technology and field surveying for mangrove monitoring in Sabah should be an effective method in the future.
4. The mangrove management plan in Sabah should be involved in the satellite monitoring protocols in order to provide spatiotemporal trends of mangrove distribution and deforestation.

5. Lastly, it is recommended that the people in Sabah be educated regarding the importance of mangrove forest. This effort will raise awareness, making it easier to manage these valuable resources in the future.

REFERENCES

- Abdullah, A.M., Ismail, M.M., Khai, N.X. & Durham, S. (2013). Mangrove Conservation Awareness among Shrimp Culturist in Malaysia. *Pertanika Journal Social Science & Humanities*, 21, 47-62.
- Ahmed, E.A. & Abdel-Hamid, K. (2007). Along the Red Sea Coast, Egypt. *World Applied Sciences Journal*, 2 (4), 283-288.
- Ajithkumar, T.T., Thangaradjou, T. & Kannan, L. (2008). Spectral Reflectance Properties of Mangrove Environment, Tamil Nandu. *Journal of Environmental Biology*, 29 (5), 785-788.
- Ali Baig, M.H., Zhang, L., Shuai, T. & Tong, Q. (2014). Derivation of a Tasseled Cap Transformation Based on Landsat-8 at- Satellite Reflectance. *Remote Sensing Letters*, 5 (5), 423-431.
- Alongi, D.M. (2008). Mangrove Forest: Resilience, Protection from Tsunami and Responses to Global Climate Change. *Estuarine Coastal and Shelf science*, 76, 1-13.
- Alongi, D. M. (2009). *The Energetics of Mangrove Forests*. Dordrecht Springer.
- Al Habshi, A., Youssef, T., Aizpuru, M. & Blasco, F. (2007). New Mangrove Ecosystem Data along the UAE Coast using Remote Sensing. *Aquatic Ecosystem Health Management*, 10, 309-319.
- Almeida, R. A. & Shimabukuro, Y. E. (2002). Digital Processing of a Landsat-TM Time Series for Mapping and Monitoring Degraded Areas Caused by Independent Gold Miners, Roraima State, Brazilian Amazon. *Remote Sensing of Environment*, 79, 42-50.
- Al-Rahmahie. (2012). Spectrally Comparison between TM5 & ETM+7 Bands. *Iraqi Journal of Science*, 53 (2), 454-464.
- Al Saaideh, B., Al-Hanbali, A., Tateishi, R., Kobayashi T. & Hoan, N.T. (2011). Mangrove Forest Mapping in the Southern Part of Japan using Landsat ETM+ with DEM. *Journal of Geographic information System*, 5, 369-377.
- Araújo, R.J., Jaramillo, J.C. & Snedaker, S.C. (1997). LAI and Leaf Size Differences in Two Red Mangrove Forest Types in South Florida. *Bulletin Marine Science*, 60, 643-647.

- Aschbacher, J., Ofren, R., Delsol, J.P., Suselo, T.B., Vibulsresth, S. & Charrupat, T. (1995). An Integrated Comparative Approach to Mangrove Vegetation Mapping using Advanced Remote Sensing and GIS Technologies: Preliminary Results. *Hydrologica*, 295, 285-295.
- Baker, C., Lawrence, R., Montagne, C. & Patten, D. (2006). Mapping Wetlands and Ririparian areas using Landsat ETM+ Imagery and Decision-Tree-Based Model. *Journal of Wetlands*, 26 (2), 456-474.
- Barua, P., Chowdhury, M. S. N. & Sarker, S. (2010). Climate Change and Its Risk Reduction by Mangrove Ecosystem of Bangladesh. *Bangladesh Research Publications Journal*, 4 (3), 218-225.
- Béland, M., Goïta, K., Bonn, F. & Pham, T.T. (2006). Assessment of Land Cover Changes Related to Shrimp Aquaculture using Remote Sensing Data: A Case in the Giao Thury District, Vietnam. *International Journal Remote Sensing*, 27, 1491-1510.
- Benfield, S.L., Guzman, H.M. & Mair, J.M. (2005). Temporal Mangrove Dynamics in relation to coastal development in Pacific Panama. *Journal Environmental Management*, 76, 263-276.
- Berlanga-Robles, C.A. & Ruiz-Luna. (2002). A Land Use Mapping and Change Detection in the Coastal Zone of Northwest Mexico Using Remote Sensing Techniques. *Journal Coastal Resource*, 18, 514-522.
- Blaschke, T. (2010). Object Based Image Analysis for Remote Sensing. *ISPRS Journal of Photogrammetry and Remote sensing*, 65, 2-16.
- Blaschke, T., Burnett, C. & Pekkarinen, A. (2004). New Contextual Approaches using Image Segmentation for Object-based Classification. In: De Meer, F., de Jong, S. (Eds.), *Remote Sensing Image Analysis: Including the spatial domain*. Kluwer Academic Publishers, Dordrecht, pp. 211-236.
- Blasco, F., Gauquelin, T., Rasolofoharinoro, M., Denis, J., Aizpuru, M. & Caldairou, V. (1998). Recent Advances in Mangrove Studies using Remote sensing Data. *Marine Freshwater Resource*, 49, 287-296.
- Binh, TNKD., Vromant, N., Hung, N.T., Hens, L. & Boon, E.K. (2005). Land Cover Changes between 1968 and 2003 in Cai Nuoc, Ca Mau Peninsula, Vietnam. *Environment Development Sustainability*, 7, 519-536.

- Biro, K., Pradhan, B., Buchroithner, M.F. & Makeschin, F. (2013) Land use/ land-cover change impacts on soil properties in the northern part of Gadarif region, Sudan. *Land Deg & Develop*, 24, 90-102.
- Breiman, L., Friedman, J. H., Olshen, R. A. & Stone, C. J. (1984). Classification and Regression Trees. New York. Chapman and Hall.
- Campbell, J.B. & Wynne, R.H. (2011). Introduction to Remote Sensing, 5th ed.; *The Guilford Press*: New York, NY, USA.
- Carlos, A.D. & Cebrih, J. (1996). The Fate of Marine Autotrophic Production. *Limnology and oceanography*, 41 (8), 1758-1766.
- Chander, G., Xiong, X., Choi, T. & Angal, A. (2010). Monitoring on-orbit Calibration Stability of the Terra MODIS and Landsat 7 ETM+ Sensors using Pseudo-invariant Test Sites. *Remote Sensing Environment*, 114, 925-939.
- Chauvaud, S., Bouchon, C. & Maniere, R. (2001). Thematic Mapping of Tropical Marine Communities (coral reefs, seagrass beds and mangroves) using SPOT Data in Gua- deloupe Island. *Oceanologica Acta*, 24, 3-16.
- Chen, J., Zhu, X., Vogelmann, J.E., Gao, F. & Jin, S. (2011) A Simple and Effective Method for Filling Gaps in Landsat ETM+ SLC-off Images. *Remote Sensing Environment*, 115, 1053-1064.
- Chen, J. & Gupta, A.K. (2000). Parametric Statistical Change Point Analysis. Birkhauser, pp. 220.
- Chouhan, R. & Rao, N. (2011). Vegetation Detection in Multispectral Remote sensing Images: Protective Role-analysis of Coastal Vegetation in 2004 Indian Ocean Tsunami. Geo-Information for Disaster Management, Turkey.
- Churches, C.E, Wampler, P.J, Sun, W. & Smith, A.J. (2014). Evaluation of Forest Cover Estimates for Haiti using Supervised Classification of Landsat data. *International Journal of Applied Earth Observation and Geoinformation*, 30, 203-216.
- Clough, B.F. (1992). Primary Productivity and Growth of Mangrove Forests. In: A.I. Robertson and D.M. Alongi (Eds.) *Tropical Mangrove Ecosystems*. American Geophysical Union, Washington, D.C. pp. 225-249.
- Congalton, R. G. (1991). A Review of Assessing the Accuracy of Classifications of Remotely Sensed Data. *Remote Sensing of Environment*, 37, 35-46.

- Congalton, R. G. & Green, K. (2008). Assessing the Accuracy of Remotely Sensed Data: Principles and Practice, (Second Edition). 183, Boca Raton: CRC Press/Taylor & Francis Group.
- Cohen, W.B., Spies, T.A. & Fiorella, M. (1995). Estimating the Age and Structure of Forests in a Multi-ownership Landscape of Western Oregon, USA. *International Journal Remote Sensing*, 16,721-746.
- Colstoun, E. C. B., Story, M. H., Thompson, C., Commisso, K., Smith, T.G. & Irons, J. R. (2003). National Park vegetation mapping using multitemporal Landsat 7 data and a decision tree classifier. *Remote Sensing of Environment*, 85, (3) 16-27.
- Conchedda, G., Duriex, L. & Mayaux, P. (2008). An Object-based Method for Mapping and Change Analysis in Mangrove Ecosystem. *ISPRS Journal of Photogrammetry and Remote Sensing*, 63, 578-589.
- Consumer Association of Penang (CAP). (2010). Call off shrimp farming. Retrieved from <http://www.consumer.org.my>.
- Corcoran, J.M., Knight, F.J. & Gallant, A.L. (2013). Influence of Multi-Source and Multi-Temporal Remotely Sensed and Ancillary Data on the Accuracy of Random Forest Classification of Wetlands in Northern Minnesota. *Remote Sensing*, 5, 3212-3238.
- Corvalán, C. F. (2005). Ecosystems and Human well-being: A Report of the Millennium Ecosystem Assessment. 53.
- Costanza, R., Arge, R., Groot, R. De, Farberk, S., Grasso, M., Hannon, B., Limburg, K., Naem, S., O'Neill, R. V., Paruelo, J., Rakin, R.G., Sutton, P. & Belt, M.V.D. (1997). The Value of the World's Ecosystem Services and Natural Capital. *Journal of Nature*, 387 (5), 253-260.
- Crist, E. & Cicone, R. (1984). A Physically Based Transformation of Thematic Mapper Data: The TM Tassled Cap. *IEEE Transactions on Geoscience and Remote Sensing*, 22, 256-263.
- Crist, E. P., Laurin, R. & Cicone, R. C. (1986). Vegetation and soils information contained in transformed thematic mapper data, in Proceedings, IGARSS '86 Symposium, Zurich, Switzerland, 8-11 September 1986, ESA Publ. Division, SP-254, pp. 1465-1470. ISBN 99-0600888-1.

- Defries, R. S., Hansen, M., Townshend, J.R.G. & Sohlberg, R. (1998). Global Land Cover Classifications at 8 km Spatial Resolution: The Use of Training Data Derived from Landsat imagery in Decision Tree Classifiers. *International Journal of Remote Sensing*, 19 (31), 41-68.
- Duong, N.D. (2004). Land Covers Mapping of Vietnam using MODIS 500M 32-day Global Composites. International Symposium on Geoinformatics for Spatial Infrastructure Development in Earth and Allied Sciences.
- DFS (Department Fisheries Sabah) (2011). Annual Fisheries Statistics 2004. Department of Fisheries Sabah (DFS), Kota Kinabalu.
- Dvorak, M., Vargas H, Fessl, B. & Tebbich, S. (2004). On the Verge of Extinction: A Survey of the Mangrove Finch *Cactospiza Heliobates* and its Habitat on the Galapagos Islands. *Journal of Conservation*, 38 (2), 171-179.
- Eckert, S., Husler, F., Liniger, H., & Hodel, E. (2015). Trend analysis of MODIS NDVI time-series for detecting land degradation and regeneration in Mongolia. *Journal Arid. Environment* 113, 16-28
- Everitt, J.H., Escobar, D.E. & Judd, F.W. (1991). Evaluation of Airborne Video Imagery for Distinguishing Black Mangrove (*Avicennia germinans*) on the Lower Texas Gulf Coast. *Journal of Coastal Research* 7, 1169-1173.
- FAO (Food and Agriculture Organization). (2007). The World's Mangroves 1980–2005. FAO Forestry Paper 153. FAO, Rome.
- FAO (Food and Agriculture Organization). (1987). Soil Quality Considerations in the Selection of Sites for Aquaculture. Fisheries and Aquaculture Department. pp. 36.
- Fatoyinbo, T.E., Simard, M., Washington-Allen, R.A, & Shu-gart, H.H. (2008). Landscape-scale Extent, Height, Bio-mass, and Carbon Estimation of Mozambique's Mangrove Forests with Landsat ETM and Shuttle Radar Topography Mission elevation data. *Journal of Geophysical Research – Biogeosciences*, 113, 02-06.
- Figueredo, A.J., Ross, D.M. & Petrinovich, L. (1992). The Quantitative Ethology of the Zebra finch: A Study in Comparative Psychometrics. *Multiv. Behav. Res.*, 27, 435-458.
- Foody, G.M. (2002). Status of Land Cover Classification Accuracy Assessment. *Remote Sens. Environ*, 80, 185-201.

- Friedl, M.A. & Brodley, C.E. (1997). Decision Tree Classification of Land Cover from Remotely Sensed Data. *Remote Sensing of Environment*, 61, 399-409.
- Friedl, M. A., Brodley, C. E. & Strahler, A. H. (1999). Maximizing Land Cover Classification Accuracies Produced by Decision Trees at Continental to Global Scales. *IEEE Transactions on Geoscience and Remote Sensing* 37, 969-77.
- Froidefond, J.M., Gardel, L., Guiral, D., Parra, M. & Ternon, J.F. (2002). Spectral Remote Sensing Reflectance of Coastal Waters in French Guiana under the Amazon Influence. *Remote Sensing of Environment*, 80, 225-232.
- Fromard, F., Vega C. & Proisy, C. (2004). Half a Century of Dynamic Coastal Change Affecting Mangrove Shorelines of French Guiana: A Case Study Based on Remote Sensing Data Analyses and Field Surveys. *Marine Geology*, 208, 265-280.
- Gang, P. O. & Agatsiva, J. L. (1992). The Current Status of Mangroves Along the Kenyan Coast, A Case Study of Mida Creek Mangroves Based on Remote sensing. *Hydrobiologia*, 247, 29-36.
- Gao, J.A. (1999). Comparative Study on Spatial and Spectral Resolutions of Satellite Data in Mapping Mangrove Forests. *International Journal Remote Sensing*, 20, 2823-2833.
- Gibson, P. J. & Power, C. H. (2000). Introductory Remote Sensing: Digital Image Processing and Applications. Routledge.
- Gillespie, T.W., Foody, G.M., Rocchini, D., Giorgi, A.P. & Saatchi, S. (2008) Measuring and Modelling Biodiversity from space. *Progress in Physical Geography*, 32, 203-221.
- Gilman, E., Ellison, J., Duke, N.C. & Field, C. (2008). Threats to Mangroves from Climate Change and Adaptation Options: A Review. *Journal of Aquatic Botany*, 89 (2), 237-250.
- Giri, C., Long J. & Tieszan, L. (2011). Mapping and Monitoring Louisiana`s mangroves in the aftermath of the 2010 Gulf of Mexico oil spill. *Journal Coastal Research*, 27,1059-1064.
- Giri, C., Ochieng, E., Tieszen, L.L., Zhu, Z., Singh, A., Loveland, T., Masek, J. & Duke, N. (2010). Status and Distribution of Mangrove Forests of the World using Earth Observation Satellite Data. *Global Ecology and Biogeography*, 20, 154-159.

- Giri, C., Zhu, Z., Tieszen, L. L., Singh, A., Gillette, S. & Kelmelis, J. A. (2008). Mangrove Forest Distributions and Dynamics (1975–2005) of the Tsunami-affected Region of Asia. *Journal of Biogeography*, 35 (3), 519-528.
- Giri, C., Pengra, B., Zhu, Z., Singh, A., & Tieszen, L.L. (2007). Monitoring Mangrove Forest Dynamics of the Sundarbans in Bangladesh and India using Multi-temporal Satellite Data from 1973 to 2000. *Estuarine Coastal Shelf Science*, 73, 91-100.
- Giri, C.P., Kratzschmar, E., Ofren, R.S., Pradhan, D. & Shrestha, S. (1996). Assessing Land Use/Land Cover Dynamics in Two Identified-Hot Spot Areas: Oudomxay Province of Lao P.D.R. and Mekong Delta of Vietnam. In *Proceeding of the 17th Asian Conference on Remote Sensing*, Colombo, Sri Lanka, November 4-8.
- Grant, J.F. & Carter, L. (2011). Calculating Vegetation Indices from Landsat 5 TM and Landsat 7 ETM+ data. Colorado View, Colorado University.
- Green, E. P., Clark, C. D., Mumby, P. J., Edwards, A. J. & Ellis, A. C. (1998). Remote sensing techniques for mangrove mapping. *International Journal of Remote Sensing*, 19 (5), 935-956.
- Green, E.P., Mumby, P.J., Edwards, A.J., Clark, C.D. & Ellis, A.C. (1997). Estimating Leaf Area Index of Mangroves from Satellite Data. *Aquatic Botany*, 58, 11-19.
- Green, E.P., Mumby, P.J., Edwards, A.J. & Clark, C.D. (1996). A Review of Remote Sensing for the Assessment and Management of Tropical Coastal Resources. *Coastal Management*, 24, 1-40.
- Hamdan, O., Mohd Azahari, F., Audi Hani, A. & Khairul Azwan, M. (2012). Distribution and extent of mangrove. Pp. 60-87 in Hamdan O, Khali Aziz H & Raja Barizan RS (Eds.) *Status of Mangrove in Peninsular Malaysia*. Gemilang Press Sdn. Bhd. Sungai Buloh.
- Hansen, M. C., DeFries, R. S., Townshend, J. R. G., Sohlberg, R., Dimiceli, C. & Carroll, M. (2002). Towards an Operational MODIS Continuous Field of Percent Tree Cover Algorithm: Using AVHRR and MODIS Data. *Remote Sensing of Environment*, 83, 303-319.
- Hansen, M., Dubayah, R. & DeFries, R. (1996). Classification Trees: An Alternative to Traditional Land Cover Classifiers. *International Journal of Remote Sensing*, 17 (1), 75-81.

- Harbison, P. (1986). Mangrove Muds a Sink and a Source for Trace-Metals. *Journal of Marine Pollution Bulletin*, 17 (16), 246-250.
- Healey, S.P., Cohen, W.B., Zhiqiang, Y. & Krankina, O.L. (2005). Comparison of Tasseled Cap-Based Landsat data Structures for Use in Forest Disturbance Detection. *Remote Sensing of Environment*, 97, 301-310.
- Helmer, E. H., Kennaway, T. A., Pedreros, D. H., Clark, M. L., Marcano-Vega, H., Tieszen L. L., Ruzzycki, T. R., Schill, S. & Carrington, C. M. S. (2008). Land Cover and Forest Formation Distributions for St. Kitts, Nevis, St. Eustatius, Grenada and Barbados from Decision Tree Classification of Cloud-Cleared Satellite Imagery. *Caribbean Journal of Science*, 44(2), 175-198.
- Hernandez, C.R., Koedam, R., Luna R, Troell, M. & Dahdouh, G.F. (2005). Remote Sensing and Ethnobotanical Assessment of the Mangrove Forest Change in the Navachiste-San Ignacio-Macapule Lagoon Complex, Sinaloa, Mexico. *Ecology and Society*, 10 (1), 1-16.
- Hord, R. & Brooner, W. (1996). Land Use Map Accuracy Criteria. *Photogrammetric Engineering and Remote Sensing*, 42, 671-77.
- Horsen, P. W., Pebesma, V. E. J. & Schot, P. P. (2002). Uncertainties in spatially aggregated predictions from a logistic regression model. *Ecological Modelling* 154, 93-101.
- Huang, X. Q. & Jensen, J. R. (1997). A machine-learning approach to automated knowledge-based building for remote sensing image analysis with GIS data. *Photogrammetric Engineering and Remote Sensing*, 63, 1185-94.
- Huang, C., Wylie, B., Yang, L., Homer, C. & Zylstra, G. (2010). Derivation of a Tasseled Cap Based on Landsat 7 at- Satellite Reflectance. *International Journal of Remote Sensing*, 23 (8), 1741-1748.
- Huemann, B.W. (2011). An Object-Based Classification of Mangrove Using a Hybrid Decision Tree-Support Vector Machine Approach. *Remote Sensing*, 3, 2440-2460.
- Huete, A., Didan, K., Miura, T., Rodriguez, E. P., Gao, X. & Ferreira, L. G. (2002). Overview of the radiometric and biophysical performance of the MODIS vegetation indices. *Remote Sens. Environ.*, 83, 195-213.

- Huete, A.R. & Liu, H.Q. (1994). An Error and Sensitivity Analysis of the Atmospheric-Correction and Soil-Correcting Variant of the NDVI for the MODIS-EOS. *IEEE Transaction on Geoscience and Remote Sensing*, 32 (4), 897-905.
- Hussain, Z. & Acharya, G. (1994). Mangroves of the Sundarbans,,: Bangladesh. IUCN Wetlands Programme, IUCN- The World Conservation Union Switzerland, 2, 257.
- Ibrahim, Z.Z, Arshad, A., Lee, S.C, Bujang, J.S, Law, A.T, Nik Mustapha, R.A, Abdullah, R. & Maged, M.M. (2000). *East Coast of Peninsular Malaysia in Seas at the Millennium: An environmental Evaluation*. The Netherlands, Elsevier Science. Ltd.
- Islam, M.A., Thenkabail, P.S., Kulawardhana, R.W., Alankara, R., Gunasinghe, S. & Edussriya, C. (2008). Semi-automated Methods for Mapping Wetlands using Landsat ETM plus and SRTM data. *International Journal of Remote Sensing*, 29, 7077-7106.
- Ivan, V., Jennifer, L.B. & Joanna, K. Y. (2001). *Journal of BioScience*, 51 (10), 807-815.
- Jakobsen, F., Hartstein, N., Frachisse, J. & Golingi, T. (2007). Sabah Shoreline Management Plan (Borneo, Malaysia): Ecosystems and Pollution. *Journal of Ocean & Coastal Management*, 50 (1-2), 84-102.
- Jensen, J.R., Lin, H., Yang, X., Ramsey III, E.W., Davis, B.A., Thoemke, C.W. (1991). The Measurement of Mangrove Characteristics in Southwest Florida using SPOT Multispectral Data. *Geocarto International*, 6, 13-21.
- Jensen, J.R. (1995). Introductory Digital Image Processing. *A Remote Sensing Perspective*. (Second Edition). Englewood Cliffs: Prentice-Hall.
- Jensen, J. R. (2005). Introductory Digital Image Processing: *A Remote Sensing Perspective*, (Second Edition). 526 Upper Saddle River, NJ: Prentice Hall.
- Jiang, N., Zhu, W, Zheng, Z., Chen, G. & Fan, D. (2013). A Comparative Analysis between GIMSS NDVIg and NDVI3g for Monitoring Vegetation Activity Change in the Northern Hemisphere during 1982–2008. *Remote sensing*, 5, 4031- 4044.
- John, W. & David, H. (1999), Measuring Vegetation (NDVI & EVI), Earth Observatory, NASA, USA.
- Jones, J., Dale, P., Chandica, A.L. & Breitfuss, M.J. (2004). Changes in the Distribution of the Grey Mangrove *Avicennia marina* (Forsk.) using Large Scale Aerial Color

- Infrared Photographs: Are the Changes Related to Habitat Modification for Mosquito Control. *Estuarine Coastal and Shelf Science*, 61, 45-54.
- Kairo, J.G., Kiviyatu, B. & Koedam, N. (2002). Application of Remote Sensing and GIS in the Management of Mangrove Forests within and Adjacent to Kiunga Marine Protected Area, Lamu Kenya. Remote Sensing and GIS in the Sustainable Management of Tropical Coastal Ecosystems. *Environment Development and Sustainability*, 4, 93-112.
- Kairo, J.G., Dahdouh-Guebas, F., Bosire, J. & Koedam, N. (2000). Restoration and Management of Mangrove systems with a special reference on East Africa. *South African Journal of Botany*, 67, 383-389.
- Kamal, M. & Phinn, S. (2011). Hyperspectral Data for Mangrove Species Mapping: A Comparison of Pixel-Based and Object-Based Approach. *Remote Sensing*, 3, 2222-2242.
- Karaburun, A. (2010). Estimation C Factor for Soil Erosion Modelling using NDVI in Buyukcekmece Watershed. *Asian Journal of Applied Sciences*, 3 (1), 1943-2429.
- Kathiresan, K. & Rajendran, N. (2005). Coastal Mangrove Forests Mitigated Tsunami. *Journal of Estuarine, Coastal and Shelf Science*, 65 (3), 601- 606.
- Kathiresan, K. & Bingham, B. L. (2001). Biology of Mangrove and Mangrove Ecosystems. *Journal of Advances in Marine Biology*, 40, 81-251.
- Komiyama, A., Ong, J. E. & Pongpan, S. (2008). Allometry, Biomass, and Productivity of Mangrove Forests: A Review. *Journal of Aquatic Botany*, 89 (2), 128-137.
- Kuenzer, C., Bluemel, A., Gebhardt, S., Quoc, T. V. & Dech, S. (2011). Remote Sensing of Mangrove Ecosystems: A Review. *Journal of Remote Sensing*, 3, 878-928.
- Laegdsgaard, P. & Johnson, C. (2001). Why Do Juvenile Fish Utilise Mangrove Habitats. *Experimental Marine Biology and Ecology*, 257, 229-253.
- Lee, T.M. & Yeh, H.C. (2009). Applying Remote Sensing Techniques to Monitor Shifting Wetland Vegetation: A Case Study of Danshui River Estuary Mangrove communities, Taiwan. *Ecological Engineering*, 35, 487-496.
- Li, X. & Yeh, A. G. O. (2004). Data Mining of Cellular Automata's Transition Rule. *International Journal of Geographical Information Science*, 18 (8): 723-744.

- Liew, C. (2001). Image processing and analysis: Tutorial: Centre for Remote Sensing and Image Processing.
- Li, M.S, Mao, L.J, Shen, WJ, Liu, S.Q. & Wei, A.S. (2013). Change and Fragmentation trends of Zhanjiang mangrove forests in southern China using multi-temporal Landsat imagery (1977-2010). *Estuarine, Coastal and Shelf Science*, 130, 1-10.
- Liu, K, Li, X., Shi, X. & Wang, S.G. (2008). Monitoring Mangrove Forest Changes using Remote sensing and GIS Data with Decision-Tree Learning. *Wetlands*, 28, 336-346.
- Lo Man, W., Andy, R.M. & Ejiria, S. (2011). Diversity of Mangrove Ecosystem in Malaysia in Semporna Mangrove Forest. *Borneo Science*, 9-17.
- Li, P., Wu, X., Hu, X., Liang, Q., Gao, Y. (2010). A Random Decision tree Ensemble for Mining Concept Drifts from Noisy Data Streams. *Applied Artificial Intelligence* 24, 680-710.
- Li, X.J., Wang, Z., Song, K., Zhang, B., Liu, D. & Guo, Z. (2007). Assessment for Salinized Wasteland Expansion and Land Use Change using GIS and Remote Sensing in the West part of Northeast China. *Environmental Monitoring and Assessment*, 131 (1–3), 421–437.
- Lu, D., Mausel, P., Brondizio, E. & Moran, E. (2004). Change Detection Techniques. *International Journal Remote Sensing*. 25, 2365-2401.
- Malaysia Department Statistics. (2013). Area of mangrove forest in Malaysia. Environmental Statistic Time Series. Pp 44-47.
- Manson, F. J., Loneragan, N. R. & Phinn, S. R. (2003). Spatial and Temporal Variation in Distribution of Mangroves in Moreton Bay, Subtropical Australia: A Comparison of Pattern Metrics and Change Detection Analyses Based on Aerial Photographs. *Journal of Estuarine, Coastal and Shelf Science*, 57 (4), 653-666.
- Maselli, F. (2002). Improved Estimation of Environmental Parameters through Locally Calibrated Multivariate Regression Analyses. *Photogrammetric Engineering and Remote Sensing*, 68 (11), 1163-1171.
- Mastaller, M. (1996). Destruction of Mangrove Wetlands Causes and Consequences. *Natural Resources and Development*, 43 (44), 37-57.

- Mironga, J.M. (2004). Geographic Information Systems (GIS) and Remote sensing in the Management of Shallow Tropical Lakes. *Applied Ecology and Environmental Research*, 2, 83-103.
- Mohd Lokman, H. & Sulong, I. (2001). Mangrove of Terengganu. MARU. KUSTEM and FDPM. 58 pp.
- Mohammady, M., Moradi, H.R. & Zeinivand, H. (2013). Validating Gap-Filling of Landsat ETM+ Satellite Images in the Golestan Province, Iran. *Arab Journal Geoscience*, doi 10.1007/s12517-013-0967-5.
- Morel, A. C., Fisher, J. B. & Malhi. Y. (2012). Evaluating the Potential to Monitor Aboveground Biomass in Forest and Oil Palm in Sabah, Malaysia, for 2000-2008 with Landsat ETM+ and ALOS-PALSAR. *International Journal of Remote Sensing*, 33, 3614-3639.
- Mumby, P. J., Green, E. P., Edwards, A. J. & Clark, C. D. (1999). The Cost-effectiveness of Remote sensing for Tropical Coastal Resources Assessment and Management. *Environmental Management*, 55, 157-166.
- Myint, S.W., Giri, C.P., Wang, L., Zhu, Z. & Gillette, S.C. (2008). Identification Mangrove Species and Their Surrounding Land Use and Land Cover Classless using an Object-Oriented Approach with a Lacunarity Spatial Measure. *GIS Science & Remote Sensing*, 45 (2), 188-208.
- Morton, D. C., DeFries, R. S., Shimabukuro, Y. E., Anderson, L. O., Arai, E., del Bon Espirito-Santo, F., Freitas, R. & Morissette, J. (2006). Cropland Expansion Changes Deforestation Dynamics in the Southern Brazilian Amazon. *Proceedings of the National Academy of Sciences of the USA*, 103 (39), 14,637-14,641.
- National Housing Department (2012). Annual Report, (2011/2012). Online web: <http://www.hdb.gov.sg/fi10/fi10320p.nsf/w/AboutUsAnnualReports?OpenDocument>
- Ng, X-K., Shaufique, F. S., Wei, T-Z., & Mohd Mansor, I. (2010b). Identification of Target Area of Concentration (TAC) for shrimp farming in Malaysia. *OPTIONS*, 16 (2).
- Nezry, E, Mougin, E., Lopes, A. & Gastellu-Etchegorry, J.P. (1993). Tropical Vegetation Mapping with Combined Visible and SAR Spaceborne data. *International Journal of Remote Sensing*, 14, 2165-2184.

- Norasma, D. (2007). Traditional Practices, Contemporary Perspectives and Policy Review in Shrimp Farming in Sabah, Malaysia. *PhD Thesis*. University Malaysia Sabah.
- Othman, M. F. (2008). Challenges ahead in meeting aquaculture production in Malaysia under the Third National Agricultural Policy, Nap3 (1998- 2010). Food and Fertilizer Technology Centre Publication Database.
- Ozesmi, S.L. & Bauer, M.E. (2002) Satellite Remote sensing of Wetlands. *Wetlands Ecol. Manage*, 10, 381-402.
- Paola, J.D. & Schowengerdt, R.A. (1997). The Effect of Neural-Network Structure on a Multispectral Land-use/Land-cover Classification. *Photogrammetric Engineering and Remote Sensing*, 63, 535-544.
- Perry, C. R. & Lautenschlager, L. F. (1984). Functional Equivalence of Spectral Vegetation Indices. *Remote Sensing of the Environment*, 14, 169-182.
- Polpanisch, O., Shing, W.C., Collin, J.A., Talib, & Samarakoon, L. (2008). Mangrove Conversion Aquaculture Development in Sabah, Malaysia. Remote sensing-GIS-Based Approach for Assessing Land Use Change in Sabah.
- Primavera, J. H. (1997). Socioeconomic Impacts of Shrimp Culture. *Journal of Aquaculture Research*, 28 (10), 815-827.
- Primavera, J.H., Altamirano, J. P., Lebata, M. J. H. L., de los Reyes, A. A. Jr. & Pitogo, C. L. (2007). Mangroves and shrimp pond culture effluents in Aklan, Panay Is., central Philippines. *Bull. Mar. Sci.*, 80, 795-804.
- Pringle, M.J., Schmidt, M. & Muir, J.S. (2009) Geostatistical Interpolation of SLC-off Landsat ETM plus images. *ISPRS J Photogrammetry, Remote Sensing*, 64 (6), 54-66.
- Quinlan, J. R. (1993). Programs for Machine Learning. Morgan Kaufmann, California.
- Quinn, J.W. (2001). Band Combination. (<http://web.www.pdx.edu/emch/ipl/band/bandcombination.html>).
- Rahman, M.M. (2013). Temporal Change Detection of Vegetation Coverage in Patuakhali Coastal Area of Bangladesh using GIS & Remotely Sensed Data. *International Journal of Geomatic and Geoscience*, 4, 36-46.
- Rahman, A.F., Dragoni, D., Didan, K., Barreto-Munoz, A. & Hutabarat, J.A. (2013). Detecting Large Scale Conversion of Mangrove to Aquaculture with Change

- Point and Mixed-Pixel Analyses of High-Fidelity MODIS Data. *Remote Sensing of Environment*, 130, 96-107.
- Ramachandra, T.V. & Kumar, U. (2004). Geographic Resources Decision Support Systems for Land use, Land cover Dynamics Analysis. In proceedings of the FOSS/GRASS users Conference-Bangkok, Thailand, pp. 12–14.
- Rashid, S. M. A., Khan, A. & Akonda, A. W. (1994). Fauna in Mangrove of the Sundarbans Volume Two: Bangladesh, IUCN, Bangkok, Thailand, 115-132.
- Rasolofoharino, M., Blasco, F., Bellan, M.F., Aizpuru, M., Gauquelin, T. & Denis, J. (1998). A Remote Sensing Based Methodology for Mangrove Studies in Madagascar. *International Journal of Remote Sensing*, 19, 1873-1886.
- Ray, T. W. (1994). A FAQ on Vegetation in Remote Sensing. California: Div. of Geological and Planetary Sciences California Institute of Technology.
- Razali, S.M. & Nuruddin, A.A. (2012). A Method of Mapping Forest Fuel Types in Peat Swamp Forest. *African Journal of Agricultural Research*, 7 (12), 1901-1909.
- Richards, J. A. (1999). Remote Sensing Digital Image Analysis: Springer-Verlag, Berlin, Germany, pp. 240.
- Rivera, S., Lowry, J.H, Hernandez, J.A., Ramsey, D., Lezama, R. & Velasquez, M.A. (2012). A Comparison between Cluster Busting Technique and Classification Tree Algorithm of a Moderate Resolution Imaging Spectrometer (MODIS) Land Cover Map of Honduras. *Geocarto International*, 27, 17-29.
- Robertson, A. I. & Duke, N. C. (1987). Mangrove as Nursery sites: Comparisons of the Abundance and Species Composition of Fish and Crustaceans in Mangrove and Other Nearshore Habitat in Tropical Australia. *Journal of Marine Biology*, 96, 193-205.
- Roy, D.P., Ju, J., Kline, K., Scaramuzza, P.L., Kovalsky, V. & Hansen, M. (2010). Web enabled Landsat data (WELD): Landsat ETM+ Compositing Mosaics of the Conterminous United States. *Remote Sensing Environment*, 114, 35-49.
- Ruiz-Luna, A. & Berlanga-Robles, C.A. (1999). Modifications in Coverage Patterns and Land Use Around the Huizache-Caimanero Lagoon System, Sinaloa, Mexico: A multi-temporal analysis using Landsat images. *Estuarine Coastal Shelf Science*, 49, 37-44.

- Sabah Forestry Department. (2012). Mangrove Forest Management & Restoration. *Annual Report, 23*, 223-226.
- Sabah Forestry Department. (2010). *Annual Report 2009*. Sabah, Malaysia.
- Sabah Department of Fisheries. (2012). *Annual Fisheries Statistics, Volume 1*. Kota Kinabalu: Department of Fisheries, Malaysia.
- Sabah Fisheries Department. (2010). *Annual Fisheries Statistics*. Kota Kinabalu: Department of Fisheries, Malaysia.
- Saito, H., Bellan, M.F., Al-Habshi, A., Aizpuru, & M., Blasco, F. (2003). Mangrove Research and Coastal Ecosystem Studies with SPOT-4 HRVIR and TERRA ASTER in Arabian Gulf. *International Journal Remote Sensing, 24*, 4073-4092.
- Selvam V., Ravichandran K.K., Gnanappazham L. & Navamuniyammal, M. (2003). Assessment of Community based Restoration of Pichavaram Mangrove Wetland using Remote sensing data. *Current Science, 85*, 794-798.
- Seto, K.C. & Fragkias, M. (2007). Mangrove Conversion and Aquaculture Development in Vietnam: A Remote Sensing-Based Approach for Evaluating the Ramsar Convention on Wetlands. *Global Environmental Change, 17*, 486-500.
- Setiawan, Y. & Yoshino, K. (2012). Change Detection in Land-Use and Land-Cover Dynamics at a Regional Scale from MODIS Time-Series Imagery. *ISPRS Annals of the Photogrammetry, Remote Sensing and Spatial Information Sciences, 1-7, XXIII, ISPRS Congress, 25 August -01 September*, Melbourne, Australia.
- Setiawan, Y., Yoshino, K. & Philpot, W. (2011). Characterizing temporal vegetation dynamics of land use in regional scale of Java Island, Indonesia. *Journal of Land Use Science*, doi:10.1080/1747423X.2011.605178.
- Shafri, H.Z.M & Ramle, F.S.H. (2009). A Comparison of Support Vector Machine and Decision Tree Classification using Satellite Data of Langkawi Island. *Information Technology Journal, 8* (1), 64-70.
- Singh, A.K. & Sharma, S. (2010). Assessment of SLC-off Landsat 7 ETM+ Images for Land Use Mapping in Lower Tapi Basin, India. *GRID-Annual Convention of ISRS & National Symposium on GIS and Remote Sensing In Infrastructure Development*, December 1-3, Lonavala India.

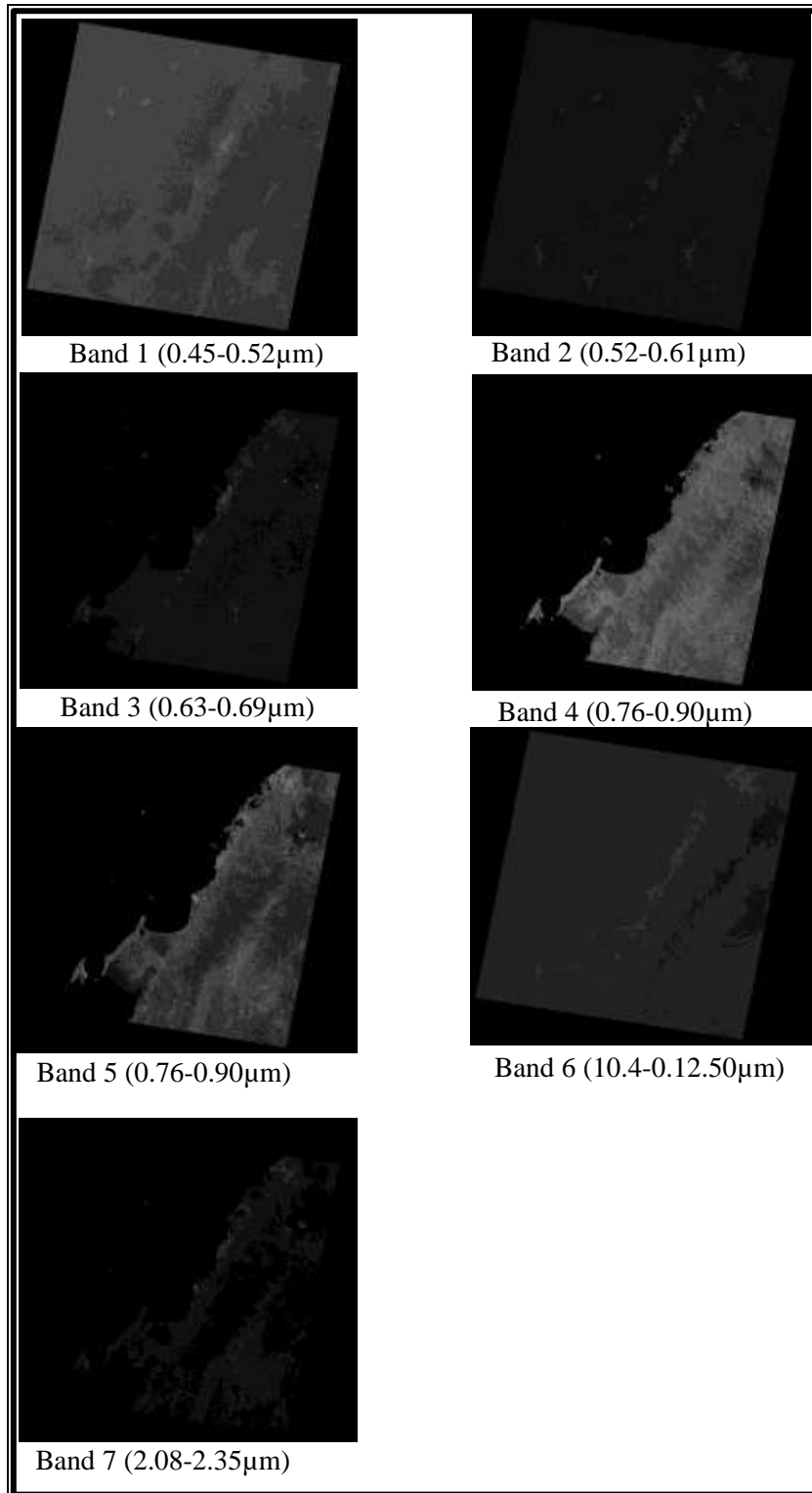
- Sirikulchayanon, P., Sun, W. & Oyana, T. J. (2008). Assessing the Impact of the 2004 Tsunami on Mangroves using Remote Sensing and GIS Techniques. *International Journal Remote Sensing*, 29, 3553-3576.
- Sivakumar, R. (2002). Image Interpretation of Remote Sensing Data. Available <http://www.gisdevelopment.net/magazine/index.htm>. (Accessed Date 21 March, 2008).
- Sulong, I., Mohd-Lokman, H., Mohd-Tarmizi, K. & Ismail, A. (2002). Mangrove Mapping Using Landsat Imagery and Aerial Photographs: Kemaman District Terengganu, Malaysia. *Environment Development and Sustainability*, 4, 135-152.
- Sulong, I. & Veddin, I. (1999). Mapping in the Coastal Area of Sabak Bernam, Kuala Selangor and Klang District with Emphasis on Mangrove forest using Remote sensing and Geographical Information Systems, in S. Lokman, M.S. Noor Azhar, S. Mohd Nasir and M.A. Borowitzka (eds.), Assessment and Monitoring of Marine Systems, Universiti Putra Malaysia Terengganu (in press).
- Sulong, I. & Ismail, H. (1990). Classification of Mangrove Forest using 1: 40 000 Scale Aerial Photographs. *Forest Ecological Management*, 33, 583-592.
- Swain, P. H. & H. Hauska. (1977). The Decision Tree Classifier: Design and Potential. *IEEE Transactions on Geoscience and Remote Sensing*, 37 (9), 69-77.
- Syed Abu, M.D., Hussin, Y.A. & Weir, M. (2001). Detecting Fragmented Mangroves in the Sundbarns, Bangladesh using Optical Radar Satellite Images. *22nd Asian Conference on Remote sensing*, 5-9 November, Singapore.
- Tarmizi, M.K., Sulong, I., Mohd-Lokman, H. & Anuar, Z.S. (1998). Classification of Mangrove Forest by using Large Scale Aerial Photographs, in Malaysian Science and Technology Congress '98, Symposium B: Agriculture, Biology, Marine, Medical and Social Sciences, Primula Pakroyal Hotel, Kuala Terengganu, 7-9 November 1998, II, pp. 198-204.
- Taylor, W. (2000a). Change-Point Analysis: A Powerful New Tool for Detecting Changes. Taylor Enterprises, Libertyville, Illinois. Web: <http://www.variation.com/cpa>.
- Taylor, W. (2000b), Change-Point Analyzer 2.0 shareware program, Taylor Enterprises, Libertyville, Illinois. Web: <http://www.variation.com/cpa>
- Terhune, J.M., Burton, H. & Green, K. (1993). Classification of diverse call types using cluster analysis techniques. *Bioacoustics*, 4, 245-258.

- Thi, V.T., Xuang, A.T.T., Nguyen, H.P., Dahdouh-Guebas, F. & Koedam, N. (2014). Application of Remote sensing and GIS for Detection of Long-Term Mangrove Shoreline Changes in Mui Cau Mau, Vietnam. *Biogeosciences*, *11*, 3781-3795.
- Thomas, V., Treitz P, McCaughey J, Noland, T. & Rich, L. (2008). Canopy Chlorophyll Concentration Estimation using Hyperspectral and LIDAR Data for a Boreal Mixed Wood Forest in Northern Ontario, Canada. *International Journal of Remote Sensing*, *29*, 1029-1052.
- Thu, P.M. & Populus, J. (2007). Status and Changes of Mangrove Forest in Mekong Delta: Case study in Tra Vinh, Vietnam. *Estuarine Coastal Shelf Science*, *71*, 98-109.
- Tomlinson, P. B. (1986). *The Botany of Mangroves*. Cambridge Cambridgeshire; New York: Cambridge University Press.
- Tong, P.H., Auda, Y., Populus, J., Aizpura, M., Habshi, A.A. & Blasco, F. (2004). Assessment from Space of Mangroves Evolution in the Mekong Delta; in Relation to Extensive Shrimp Farming. *International Journal Remote Sensing*, *25*, 4795-4812.
- USGS (United State Geological Survey). 2013. Landsat A Global Land-Imaging Mission. <http://pubs.usgs.gov/fs/2012/3072/fs2012-3072.pdf>.
- USGS (2004) Phase 2 gap-fill algorithms: SLC-off gap-filled product gap-fill algorithm methodology. Available online at Landsat.usgs.gov/documents/L7SLCGapfilledMethod.pdf. Accessed 28 Nov.2010.
- Vaiphasa, C., Ongsomwang, S., Vaiphasa, T. & Skidmore, A.K. (2005). Tropical Mangrove Species Discrimination using Hyperspectral Data: A Laboratory Study. *Estuarine Coastal and Shelf Science*, *65*, 371-379.
- Vasconcelos, M.J., Mussá Biai, J.C., Araújo, A. & Diniz, M.A. (2002). Land Covers Change in Two Protected Areas of Guinea-Bissau (1956-1998). *Applied Geographic*, *22*, 139-156.
- Vo, Q.T., Oppelt, N., Leinenkugel, P. & Kuenzer, C. (2013). Remote sensing in Mapping Mangrove Ecosystems -An Object-based Approach. *Remote sensing*, *5*, 183-201.
- Walters, B.B, Rönnbäck, P., Kovacs, J. M., Crona, B., Hussain, S.A., Badola, R., Primavera, J.H., Barbier, E. & Guebas, F.D. (2008). Ethnobiology, Socio-

- economics and Management of Mangrove Forests: A Review. *Aquatic Botany*, 89, 220-236.
- Wang, L., Mu, M., Li, X., Lin, P. & Wang, W. (2010). Differentiation between True Mangroves and Mangrove Associates Based on Leaf Traits and Salt Contents. *Plant Ecology*, 4 (4), 292-301.
- Wang, L. & Sousa, W. (2009). Distinguish Mangrove Species with Laboratory Measurement of Hyperhyperspectral Leaf Reflectance. *International Journal of Remote Sensing*, 30, 1267-1281.
- Wang, L., Sousa, W.P. & Gong, P. (2004). Integration of Object-based and Pixel-based Classification for Mapping Mangroves with IKONOS Imagery. *International Journal of Remote Sensing*, 25 (24), 5655-5668.
- Wang, Y., Bonyng, G., Nugranad, J., Traber, M., Ngusaru, A., Tobey, J., Hale, L., Bowen, R. & Makota, V. (2003). Remote Sensing of Mangrove Change Along the Tanzania Coast. *Marine Geodesy*, 26, 35-48.
- Wardlow, B.D., Egbert, S.T. & Kastens, J.H. (2007). Analysis of Time-Series MODIS 250 m Vegetation Index Data for Crop Classification in the U.S. Central Great Plains. *Remote Sensing of Environment*, 18, 290-310.
- Wasserman, J. C. & Freitas-Pinto, A. P. (2000). Mercury Concentrations in Sediment Profiles of Degraded Tropical Coastal Environment. *Environmental Technology*, 21 (3), 297- 305.
- Wessels, K. J., DeFries, R. S., Dempewolf, J., Anderson, L. O., Hansen, A. J., Powell, S. L. & Moran, E. F. (2004). Mapping Regional Land Cover with MODIS Data for Biological Conservation: Examples from the Greater Yellowstone Ecosystem, USA and Pará State, Brazil. *Remote Sensing of Environment*, 92, 67-83.
- Wijedasa, L.S., Sloan, S., Michelakis D.G. & Clements, G.R. (2012). Overcoming Limitations with Landsat Imagery for Mapping Peat Swamp Forest in Sundaland. *Remote Sensing*, 4, 2595-2618.
- Wooster, M. (2007). Remote sensing: Sensors and systems. *Progress in Physical Geography*, 31, 95-100.
- Xiang, Y., Hong-Bo, S., Xiang-Hua, L. & Dong-Zhi, Z. (2010). Applying Neural Network Classification to Obtain Mangrove Landscape Characteristics for

- Monitoring the Travel Environment Quality on the Beihai Coast of Guangxi, P. R. China. *Clean-Soil, Air, Water*, 38 (3), 289-295.
- Xiao, X.M., Braswell, B., Zhang, Q.Y., Boles, S. & Frohking, S. (2003). Sensitivity of Vegetation Indices to Atmospheric Aerosols: Continental-scale Observations in Northern Asia. *Remote Sensing of Environment*, 84, 385-392.
- Xie, Y., Zhao, X., Li, L. & Wang, H. (2010). Calculating NDVI for Landsat7-ETM Data after Atmospheric Correction using 6S model: A Case Study in Zhangye City, China, in *Proc. Geoinformatics*, pp.1-4.
- Zeng, C., Shen, H. & Zhang, L. (2013). Recovering Missing Pixels for Landsat ETM+ SLC-off Imagery using Multi-Temporal Regression Analysis and Regularization Method. *Remote sensing Environment*, 131, 182-194.
- Zhang, Q. (2004). Bio-Geomorphologic Coral Reefs and Mangroves Level Control Coastal Zonation and Tide. *Journal of Coastal Research*, 45, 202-211.
- Zhan, X., Sohlberg, R. A., Townshend, J. R. G, DiMiceli, C., Carroll, M. L. & Eastman, J. C. (2002). Detection of Land Cover Changes using MODIS 250 m data, *Remote Sensing of Environment*, 83, 336-350.
- Zhang, Z., Su, Z., Shen, A., & Qiaoying, Z. (2003). The Current Status of World Protection for Mangrove. *Chinese Journal and Limnology*, 21 (3), 261-269.
- Zhang, X.H. (2011). Identification of Mangrove using Decision Tree Method. Fourth International Conference on Information and Computing. Pp 130-132.
- Zhang, G., Li, W., Travis, D. (2007). Gaps-fill of SLC-off Landsat ETM+ Satellite Image using a Geostatistical Approach. *Int Remote Sens.*, 28, 5103–5122
- Zhu, Z. & Woodcock, C.E. (2014). Automated Cloud, Cloud Shadow a Detection in Multitemporal Landsat Data: An Algorithm Designed Specifically for monitoring Land Cover Change. *Remote Sensing Environment*, 152, 217-234.
- Zhang, C., Kovacs, J.M., Wachowiak, M.P. & Flores-Verdugo, F. (2013). Relationship between hyperspectral measurement and mangrove leaf nitrogen concentration. *Remote Sensing* 5, 891-908.

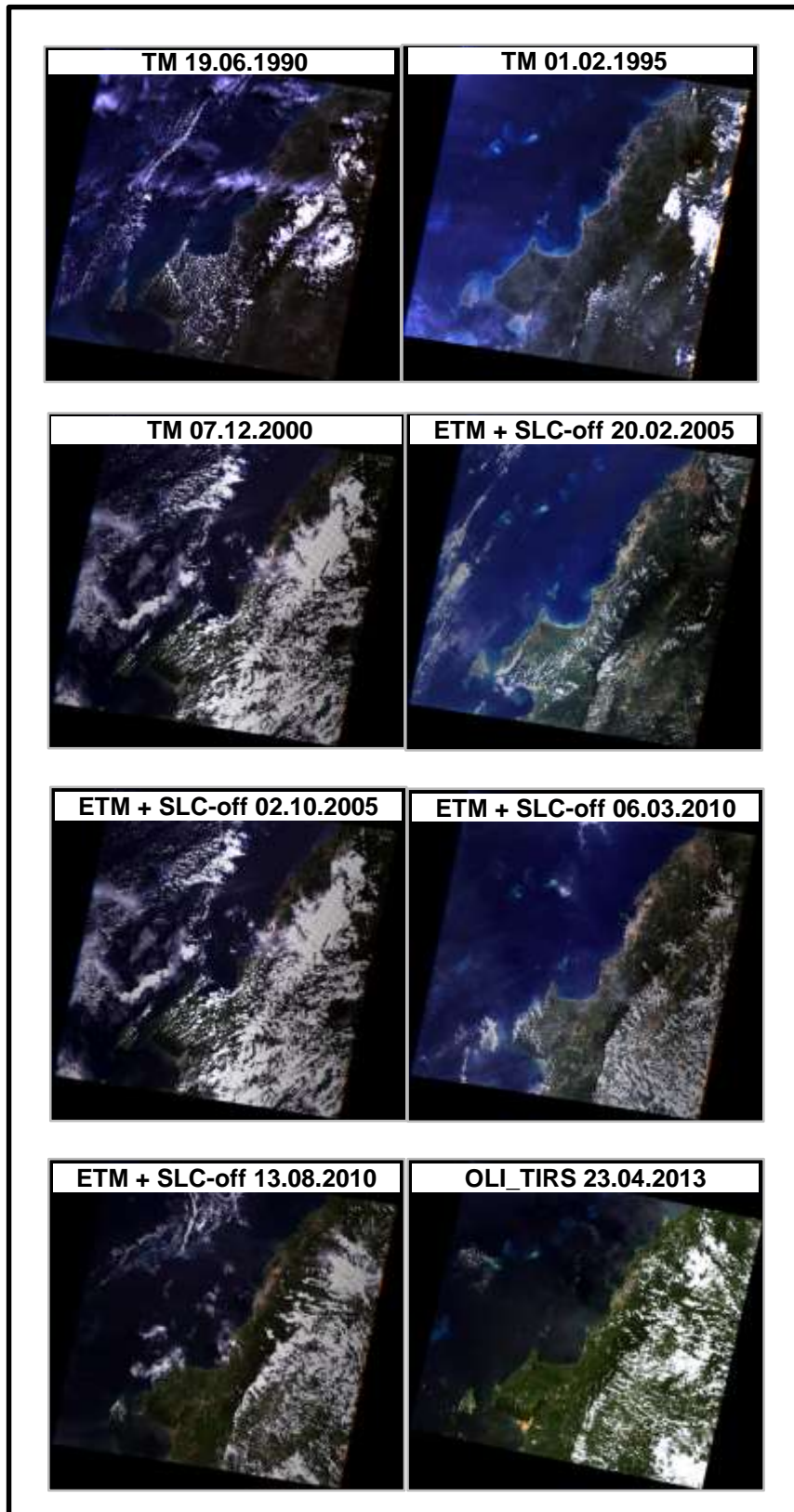
Appendix I (A) Sample of Landsat level 1T data set (1990)



Appendix I (B) Sample of metadata Landsat data set

Data Set Attribute	Attribute Value
Landsat Scene Identifier	LT41180561990170XXX03
Spacecraft Identifier	LANDSAT_4
Day/Night	DAY
WRS Path	118
WRS Row	56
WRS Type	2
Date Acquired	19061990
Start Time	1990:170:02:01:54.52494
Stop Time	1990:170:02:02:21.13500
Acquisition Quality	7
Quality Band 1	7
Quality Band 2	7
Quality Band 3	7
Quality Band 4	7
Quality Band 5	7
Quality Band 6	7
Quality Band 7	7
Cloud Cover	20
Cloud Cover Quad Upper Left	0
Cloud Cover Quad Upper Right	10
Cloud Cover Quad Lower Left	0
Cloud Cover Quad Lower Right	10
Sun Elevation	52.92207187
Sun Azimuth	58.09587356
Data Type Level 1	TM L1T
Output Format	GEOTIFF
Reflective Lines	6901
Reflective Samples	7721
Thermal Lines	6901
Thermal Samples	7721
Map Projection Level 1	UTM
Datum	WGS84
Ellipsoid	WGS84
UTM Zone	50
Grid Cell Size Reflective	30
Grid Cell Size Thermal	30
Orientation	NORTH_UP
Resampling Option	CUBIC_CONVOLUTION
Center Latitude	5°47'43.58"N
Center Longitude	115°50'06.07"E

Appendix I (C) Sample of multispectral Landsat data series

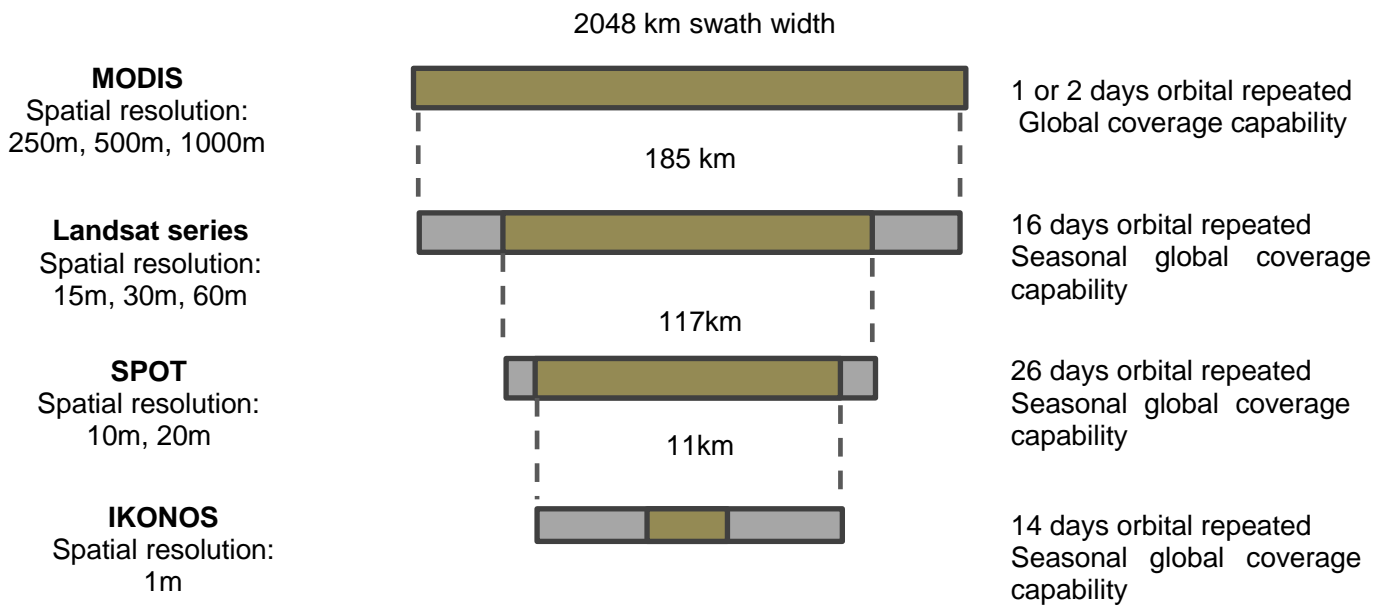


Appendix I (D) Multispectral bands of Landsat data series

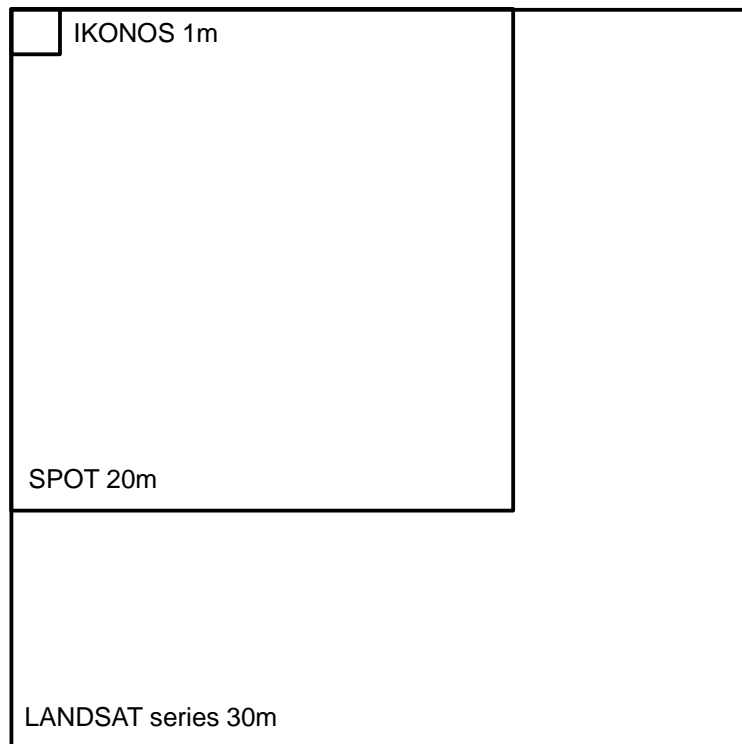
Thematic Mapper (TM) & Enhanced Thematic Mapper Plus (ETM+)	Landsat 4, 5 and 7	Wavelength (µm)	Resolutions (m)
	Band 1-Blue	0.45-0.52	30m
	Band 2-Green	0.52-0.60	30m
	Band 3-Red	0.63-0.69	30m
	Band 4-NearInfrared	0.76-0.90	30m
	Band 5-Short wave Infrared 1	1.55-1.75	30m
	Band 6-Thermal Infrared	10.40	60m
	Band 7-Short Infrared 2	2.09-2.35	30m
	Band 8-Panchromatic (Landsat 7 only)	0.52-0.90	15m

Operation Land Imager_Thermal Infrared (OLI_TIRS)	Landsat 8	Wavelength (µm)	Resolutions (m)
	Band 1-Coastal aerosol	0.43-0.45	30m
	Band 2-Blue	0.45-0.51	30m
	Band 3-Green	0.53-0.59	30m
	Band 4-Red	0.64-0.67	30m
	Band 5-NearInfrared	0.85-0.88	30m
	Band 6-Short wave Infrared 1	1.57-1.65	30m
	Band 7-Short wave Infrared	2.11-2.29	30m
	Band 8-Panchromatic	0.50-0.68	15m
	Band 9-Cirrus	1.36-1.38	30m
	Band 10-Thermal infrared 1	10.60-11.19	100m
Band 11-Thermal infrared 2	11.50-12.51	100m	

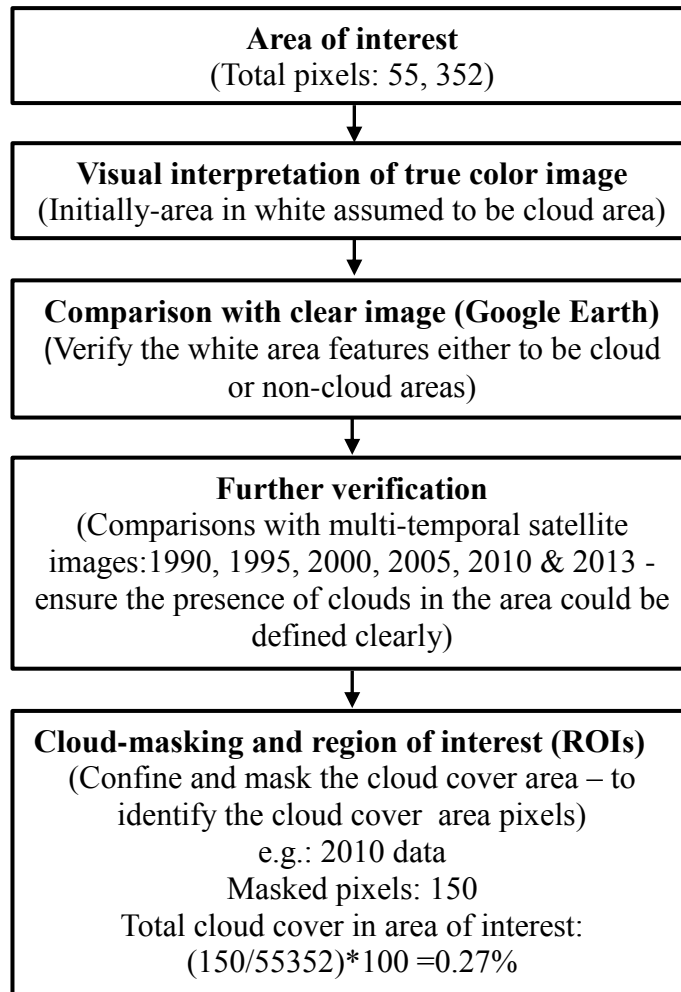
Appendix I (E) Spatial resolution and coverage area of satellite images



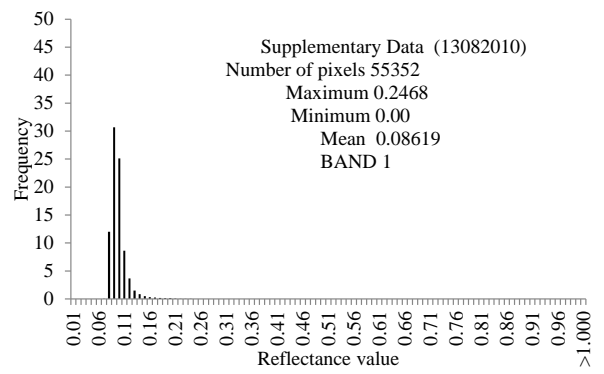
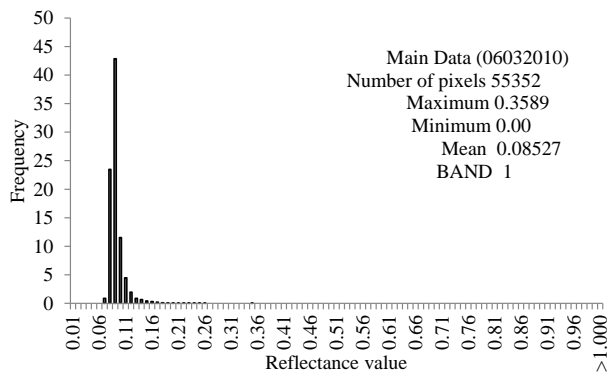
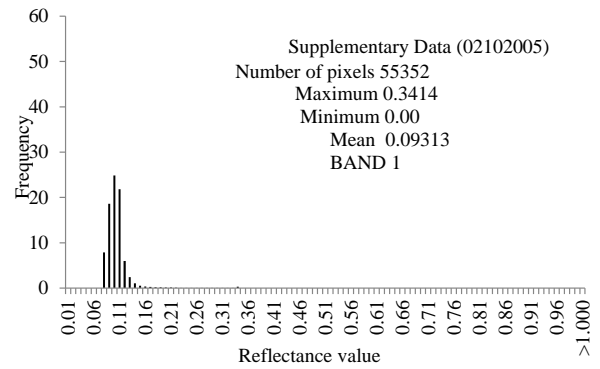
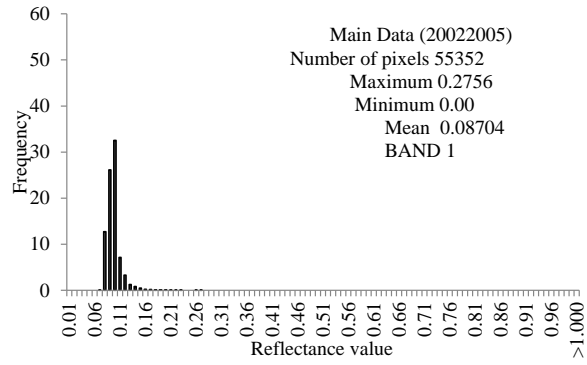
Spatial resolution of satellite images



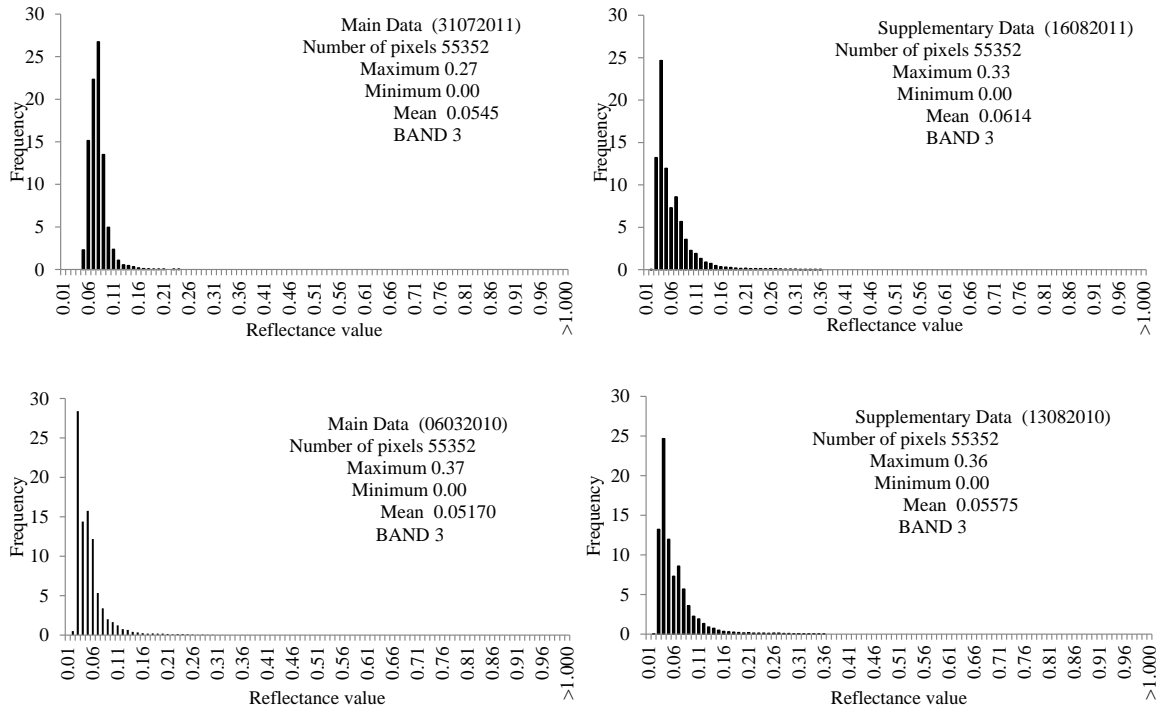
Appendix I (F) Cloud-Masking Protocol



Appendix II (A) Histogram band 1 of main and supplementary ETM+ SLC-off data



Appendix II(B) Histogram of band 3 for main and supplementary of ETM+ SLC-off data



Appendix III(A) Field Survey Schedule

Date of Survey	Activity	Remarks
4 Nov-24 Dec, 2011 (2 months)	<ul style="list-style-type: none"> • Site visit • Mangrove species inventory • Ground truthing data collection • Secondary data collections <ul style="list-style-type: none"> - Topography map - Aquaculture activity data - Vegetation map 	Department involved: 1. Kota Kinabalu Wetland Centre (KKWC) 2. Sabah Fisheries Department 3. University Malaysia Sabah 4. Sabah Forestry Department 5. Sabah Lands & Survey Department
13-30 September, 2013 (3 weeks)	<ul style="list-style-type: none"> • Ground truthing data collection • Mangrove replanting • Secondary data collection <ul style="list-style-type: none"> - Aquaculture activity data 	Department involved: 1. Sabah Fisheries Department 2. University Malaysia Sabah 3. Sabah Forestry Department

Appendix III(B) Pictures of Field Survey



Photo 1: Site identification



Photo 2: Mangrove sp. inventory



Photo 3: Shrimp pond in mangrove area



Photo 4: Mangrove seedlings for replanting project



Photo 5: *Rhizophora apiculata* sp.



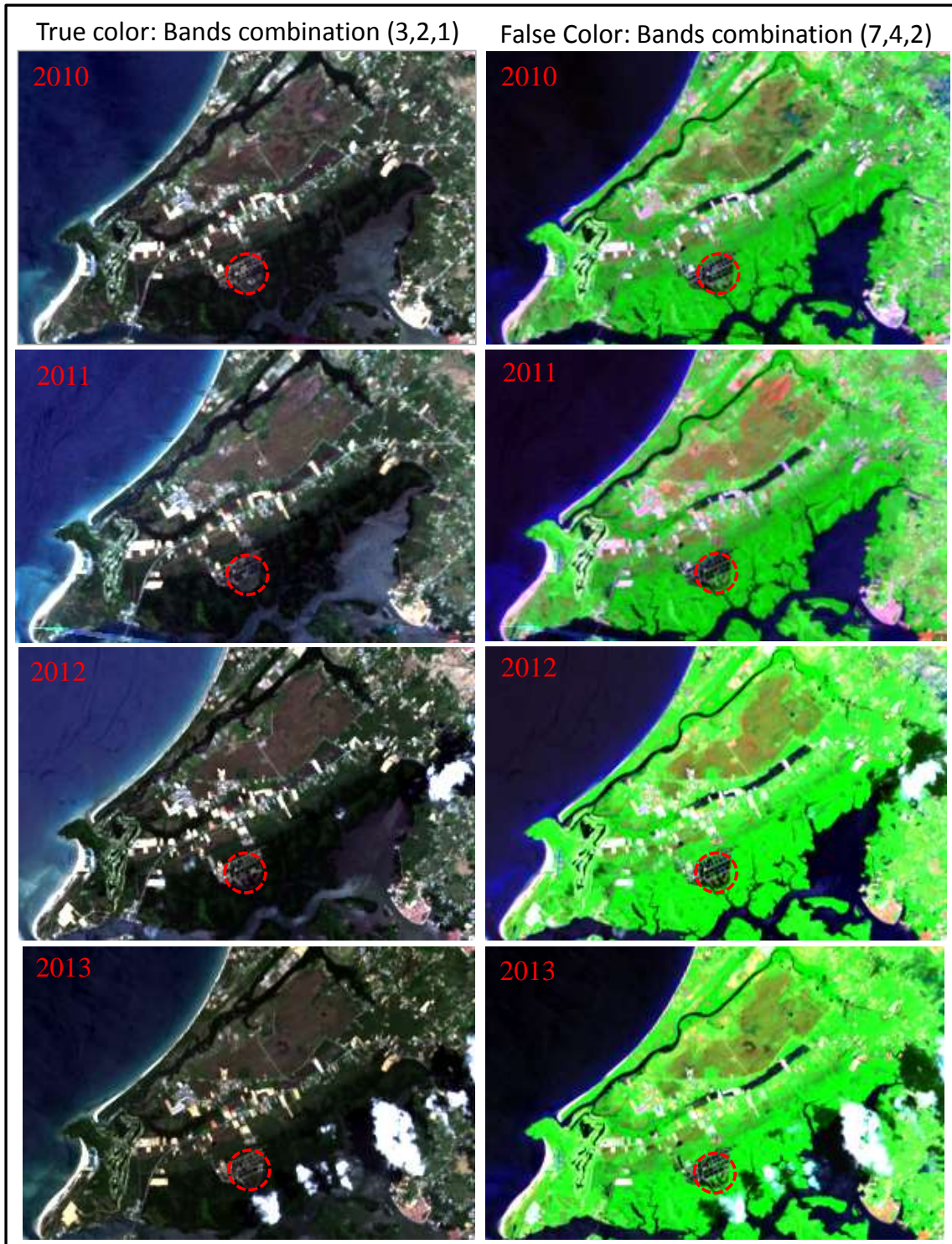
Photo 6: Mangrove replanting activity

Appendix III(C) Sample Topographic Map of Study Area

Restricted Topographic Map (1: 50,000) of Mengkabong area



Appendix IV(A) Multi-temporal of Satellite Data with Mangrove Replanting Area



Note: Red circle shows the replanting of mangrove area

Appendix IV(B) Field Photo of Mangrove Replanting Area

